

Muscle weakness in *TPM3*-myopathy is due to reduced Ca^{2+} -sensitivity and impaired acto-myosin cross-bridge cycling in slow fibres

Journal:	<i>Human Molecular Genetics</i>
Manuscript ID:	HMG-2015-W-00595.R1
Manuscript Type:	1 General Article - US Office
Date Submitted by the Author:	20-Jul-2015
Complete List of Authors:	<p>Yuen, Michaela; The Children's Hospital at Westmead, Institute for Neuroscience and Muscle Research; University of Sydney, Discipline of Paediatrics and Child Health</p> <p>Cooper, Sandra; The Children's Hospital at Westmead, Institute for Neuroscience and Muscle Research; University of Sydney, Discipline of Paediatrics and Child Health</p> <p>Marston, Steve; Imperial College London, The National Heart and Lung Institute</p> <p>Nowak, Kristen; University of Western Australia, Harry Perkins Institute of Medical Research and the Centre for Medical Research</p> <p>McNamara, Elyshia; University of Western Australia, Harry Perkins Institute of Medical Research and the Centre for Medical Research</p> <p>Mokbel, Nancy; The University of Balamand, Faculty of Health Sciences, St.George Health Complex; The Children's Hospital at Westmead, Institute for Neuroscience and Muscle Research; University of Sydney, Discipline of Paediatrics and Child Health</p> <p>Ilkovski, Biljana; The Children's Hospital at Westmead, Institute for Neuroscience and Muscle Research</p> <p>Ravenscroft, Gina; University of Western Australia, Harry Perkins Institute of Medical Research and the Centre for Medical Research</p> <p>Rendu, John; Centre Hospitalier Universitaire de Grenoble, Département de Biochimie Toxicologie et Pharmacologie, Département de Biochimie Génétique et Moléculaire</p> <p>de Winter, Josine; VU University Medical Center, Department of Physiology, Institute for Cardiovascular Research</p> <p>Klinge, Lars; University Medical Center Göttingen, Department of Pediatrics and Pediatric Neurology</p> <p>Beggs, Alan; Boston Children's Hospital, Division of Genetics and Genomics, The Manton Center for Orphan Disease Research; Harvard Medical School, Pediatrics</p> <p>North, Kathryn; The Royal Children's Hospital, Murdoch Childrens Research Institute; University of Melbourne, Australia, Department of Paediatrics</p> <p>Ottenheijm, Coen; VU University Medical Center, Department of Physiology, Institute for Cardiovascular Research</p> <p>Clarke, Nigel; The Children's Hospital at Westmead, Institute for Neuroscience and Muscle Research; University of Sydney, Discipline of</p>

1
2
3
4
5
6
7
8
9
10
11
12
13
14
15
16
17
18
19
20
21
22
23
24
25
26
27
28
29
30
31
32
33
34
35
36
37
38
39
40
41
42
43
44
45
46
47
48
49
50
51
52
53
54
55
56
57
58
59
60

	Paediatrics and Child Health
Key Words:	tropomyosin, congenital myopathy, TPM3, congenital fiber-type disproportion, muscle weakness

SCHOLARONE™
Manuscripts

For Peer Review

1
2
3 **Muscle weakness in *TPM3*-myopathy is due to reduced Ca²⁺-sensitivity and**
4 **impaired acto-myosin cross-bridge cycling in slow fibres.**
5
6

7 Michaela Yuen^{1,2}, Sandra T. Cooper^{1,2}, Steve B. Marston³, Kristen J. Nowak⁴, Elyshia
8 McNamara⁴, Nancy Mokbel^{1,5}, Biljana Ilkovski¹, Gianina Ravenscroft⁴, John Rendu⁶, Josine
9 M. de Winter⁷, Lars Klinge⁸, Alan H. Beggs⁹, Kathryn N. North^{1, 2, 10,11}, Coen A. C.
10 Ottenheijm^{7*}, Nigel F. Clarke^{1,2*}
11
12
13

- 14
15 1. Institute for Neuroscience and Muscle Research, The Children's Hospital at Westmead,
16 Westmead, Australia
17
18 2. Discipline of Paediatrics and Child Health, University of Sydney, Sydney, Australia
19
20 3. National Heart and Lung Institute, Imperial College London, London, UK
21
22 4. Harry Perkins Institute of Medical Research and the Centre for Medical Research,
23 University of Western Australia, Nedlands, Australia
24
25 5. Faculty of Health Sciences, St.George Health Complex, The University of Balamand,
26 Beirut, Lebanon
27
28 6. Département de Biochimie Toxicologie et Pharmacologie, Département de Biochimie
29 Génétique et Moléculaire, Centre Hospitalier Universitaire de Grenoble, Grenoble, France
30
31 7. Department of Physiology, Institute for Cardiovascular Research, VU University Medical
32 Center, Amsterdam, The Netherlands
33
34 8. Department of Pediatrics and Adolescent Medicine, Division of Pediatric Neurology,
35 Faculty of Medicine, Georg August University, Göttingen, Germany
36
37 9. Division of Genetics and Genomics, The Manton Center for Orphan Disease Research,
38 Boston Children's Hospital, Harvard Medical School, Boston, USA
39
40 10. Murdoch Children's Research Institute, the Royal Children's Hospital, Parkville, Australia
41
42 11. Department of Paediatrics, University of Melbourne, Melbourne, Australia
43
44

45 * The authors wish it to be known that, in their opinion, the last two authors should be
46 regarded as joint last authors
47
48

49 **Correspondence to**

50 Michaela Yuen, Institute for Neuroscience and Muscle Research, The Children's Hospital at
51 Westmead, Locked Bag 4001, Westmead, NSW 2145, Australia,
52 email: michaela.kreissl@sydney.edu.au, phone: +61 2 9845 1495, fax: +61 2 9845 3489
53
54
55
56
57
58
59
60

Abstract

Dominant mutations in *TPM3*, encoding α -tropomyosin_{slow}, cause a congenital myopathy characterised by generalised muscle weakness. Here, we used a multidisciplinary approach to investigate the mechanism of muscle dysfunction in twelve *TPM3*-myopathy patients.

We confirm that slow myofibre hypotrophy is a diagnostic hallmark of *TPM3*-myopathy, and is commonly accompanied by skewing of fibre-type ratios (either slow or fast fibre predominance). Patient muscle contained normal ratios of the three tropomyosin isoforms and normal fibre-type expression of myosins and troponins. Using 2D-PAGE, we demonstrate that mutant α -tropomyosin_{slow} was expressed, suggesting muscle dysfunction is due to a dominant-negative effect of mutant protein on muscle contraction. Molecular modelling suggested mutant α -tropomyosin_{slow} likely impacts actin-tropomyosin interactions and, indeed, co-sedimentation assays showed reduced binding of mutant α -tropomyosin_{slow} (R168C) to filamentous actin.

Single fibre contractility studies of patient myofibres revealed marked slow myofibre specific abnormalities. At saturating $[Ca^{2+}]$ (pCa 4.5), patient slow fibres produced only 63% of the contractile force produced in control slow fibres and had reduced acto-myosin cross-bridge cycling kinetics. Importantly, due to reduced Ca^{2+} -sensitivity, at sub-saturating $[Ca^{2+}]$ (pCa 6, levels typically released during in vivo contraction) patient slow fibres produced only 26% of the force generated by control slow fibres.

Thus, weakness in *TPM3*-myopathy patients can be directly attributed to reduced slow fibre force at physiological $[Ca^{2+}]$, and impaired acto-myosin cross-bridge cycling kinetics. Fast myofibres are spared; however, they appear to be unable to compensate for slow fibre dysfunction. Abnormal Ca^{2+} -sensitivity in *TPM3*-myopathy patients suggests Ca^{2+} -sensitising drugs may represent a useful treatment for this condition.

Introduction

Dominant mutations in the *TPM3* gene, encoding α -tropomyosin_{slow} (α -TPM_{slow}), cause a congenital myopathy characterised by mild to moderate early onset, non-progressive generalised muscle weakness (1-3). Axial and respiratory muscles are commonly involved and many patients require night-time ventilatory support (1, 2). Recessive mutations, causing loss of protein, are rare with only four instances reported to date in patients with relatively severe clinical presentations (4-7). In contrast, more than 40 families with dominant *TPM3* missense mutations have been identified involving 19 different residues (1, 3, 7-13), Supplementary Tab. 1). Histologically, many *TPM3* patients present with slow skeletal myofibre hypotrophy in the absence of additional pathological features, resulting in a clinical diagnosis of congenital fibre-type disproportion (CFTD) (3). Some patients also exhibit nemaline bodies or cores in myofibres and are classified as nemaline myopathy (8) or core myopathy (1, 11, 14), respectively. The same mutation in *TPM3* can cause a variety of histological phenotypes (Supplementary Tab. 1) (1, 3, 7, 14).

Three tropomyosin isoforms are present in the skeletal muscle sarcomere (15). *TPM1* and *TPM3* encode the two α -tropomyosins expressed exclusively in fast fibres (*TPM1*; α -TPM_{fast}, Tpm1.st) or slow fibres (*TPM3*; α -TPM_{slow}, Tpm3.12st), respectively. *TPM2* encodes β -tropomyosin (β -TPM, Tpm2.2st) and is expressed in both fibre types (16, 17). Tropomyosin forms alpha-helical coiled-coil heterodimers between one α - and one β -chain. These dimers polymerise head-to-tail into a continuous filament that associates along the entire length of the actin thin filament and interacts with the troponin complex to regulate Ca²⁺-mediated actin-myosin cross-bridge cycling during muscle contraction. The structure of tropomyosin is conferred by a seven residue repeat motive [*a-b-c-d-e-f-g*] (Fig. 1A and B) (18). Residues at positions *a* and *d* in the repeat are typically hydrophobic, creating a hydrophobic pocket between two tropomyosin chains facilitating dimerisation (blue). Charged residues at positions *g* and *e* (green) stabilise the dimer through inter-helical salt bridges. Positions *b*, *c* and *f* (yellow) localise to the surface of tropomyosin dimers and likely modulate interactions with proteins such as actin and troponin.

Many dominant *TPM3* mutations (11/19) affect positions *b*, *c* or *f* on the outer surface of the dimer (Fig. 1C, yellow). Only five mutations affect positions *a* and *d* in the hydrophobic pocket (Fig. 1C, blue) and three mutations affect positions *g* and *e* constituting the inter-

1
2
3 helical salt bridges (Fig. 1C, green). All mutations fall within, or very close to, one of the
4 seven actin binding regions of tropomyosin (Fig. 1C, purple shaded area of the molecule)
5 (19). In particular, there is a striking concentration of mutations within the fifth actin-binding
6 region of α -TPM_{slow} (R168H, R168G, R168C, K169E, E174A) some of which are recurrent
7 in several unrelated families (e.g. R168 residue is mutated in 20 different families).
8
9

10
11 Although the structure and function of tropomyosin is well established, the mechanism(s) by
12 which mutations in *TPM3* cause muscle weakness remains poorly understood. Two recent
13 studies showed that four patients with dominant *TPM3* mutations had abnormal cross-bridge
14 cycling kinetics and Ca²⁺-sensitivity of contraction in single skeletal myofibres isolated from
15 patient biopsies [n=3 (20), n=1 (21)]. However, these studies were limited by small sample
16 sizes, and separate assessment of the properties of slow versus fast myofibres was only
17 possible to a limited extent. In this study, we aimed to unravel the mechanism of muscle
18 weakness in a cohort of 12 patients with dominant *TPM3* mutations. We performed thorough
19 histological characterisation, assessed thin filament protein expression and quantified the
20 contractile properties of single myofibres isolated from patient muscle specimens (10/12
21 patients, Tab. 1).
22
23
24
25
26
27
28
29
30
31
32
33
34
35
36
37
38
39
40
41
42
43
44
45
46
47
48
49
50
51
52
53
54
55
56
57
58
59
60

Results

TPM3-myopathy patients have slow fibre hypotrophy and deregulation of slow and fast muscle fibre proportions

The main histological characteristic in all patients with *TPM3* mutations is selective hypotrophy of slow-twitch type-1 fibres, compared to fast-twitch type-2 fibres (1, 3, 7) (Fig. 2A, ATPase pH 4.6, slow myofibres appear dark; see Supplementary Tab. 2 for measurements). On average, fast fibres were between 1.7 and 5.2 times larger in diameter than slow fibres (Fig. 2B), corresponding to a %FSD of 41 % - 78.3 % (Fig. 2C). The selective hypotrophy of slow fibres in *TPM3* patients is consistent with the slow-fibre specific expression of α -TPM_{slow}.

Additionally, fibre-typing was skewed in patient biopsies, either towards fast fibre predominance (five patients, less than 30 % slow fibre area) or slow fibre predominance (six patients, more than 60 % slow fibre area), compared to age-matched control biopsies where the CSA occupied by either fibre-type is approximately 50:50 [this study and (22, 23)] (Fig. 2D). Only one patient biopsy showed normal slow-fast fibre distribution (between 40-60 % slow fibre area).

Tropomyosin isoform ratios are not commonly altered in TPM3-myopathy patients

In normal muscle, the ratio of α/β tropomyosin molecules is approximately 50:50 β -TPM/ α -TPM_{fast} in fast fibres and 50:50 β -TPM/ α -TPM_{slow} in slow fibres (24). A patient and transgenic mouse model carrying the *TPM3* M9R mutation, the first mutation associated with nemaline myopathy, showed an imbalance of this ratio, with a dramatic excess of α -TPM_{slow} relative to β -TPM in skeletal muscle (25) (Fig. 3Ai, Lane 5). This disruption in tropomyosin stoichiometry was proposed as a potential mechanism of muscle weakness (25). In contrast, in this cohort of 12 *TPM3*-myopathy patients, we observed normal ratios of α/β tropomyosin, similar to controls (Fig. 3Ai). The scatter plots in Fig. 3Aii-iiii show the relative levels of each tropomyosin isoform relative to the type-1 fibre CSA, as determined by ATPase staining. β -TPM is present at equal amounts in slow and fast myofibres in all samples (~50 % of total tropomyosin, Fig. 3Aii). The relative expression of α -TPM_{slow} and α -TPM_{fast} correlates well with type-1 fibre CSA (positive correlation for α -TPM_{slow} and negative correlation for α -TPM_{fast}, Fig. 3Aiii and 3Aiiii). The linear regression slope fitted to the data was not significantly different between patients and controls, demonstrating a normal ratio of α/β tropomyosin isoforms in fast and slow fibres.

Mutant α -TPM_{slow} is expressed in muscle of TPM3-myopathy patients

The autosomal dominant inheritance of *TPM3* mutations within our cohort is consistent with the hypothesis that mutant α -TPM_{slow} is expressed in slow skeletal myofibres and causes disease via a dominant-negative effect on thin filament function. To confirm mutant α -TPM_{slow} is present in patient muscle, we isolated the filamentous fractions (representing proteins incorporated in high-molecular weight structures such as sarcomeres) and performed 2D-SDS-PAGE. Five patients in our cohort from whom skeletal muscle samples were available, had a mutation that resulted in an amino-acid substitutions affecting a charged residue leading to a predicted alteration in the isoelectric point (pI) of α -TPM_{slow}. Thus, isoelectric focusing allowed us to separate the mutant from the wild-type protein on the basis of charge in these patients, and the second dimension urea-SDS gel separated the three tropomyosin isoforms from each other. The mutant α -TPM_{slow} protein could then be observed as a left-sided (Fig. 3B; R186G, R91P, K169E, R168C) or right-sided shift (Fig. 3B, E241K) from the wild-type α -TPM_{slow} and was present in all patient muscles. The total pool of α -TPM_{slow} (both wild-type and mutant isoforms) correlated with the slow fibre CSA (% type-1 fibre area annotated above each blot, see Supplementary Tab. 2 for measurements). However, mutant α -TPM_{slow} was less abundant compared to wild-type, ranging from 27 to 45 % of total α -TPM_{slow} (% mutant α -TPM_{slow} annotated on each blot).

The actin-binding properties of K169E and R168C mutant α -TPM_{slow} proteins are altered

The position of many *TPM3* mutations within or close to actin binding sites suggest most mutations may influence interactions between α -TPM_{slow} and actin filaments. Therefore, we performed actin-tropomyosin co-sedimentation assays with two recombinant mutant α -TPM_{slow} proteins (R168C and K169E) and compared their actin binding properties to wild-type α -TPM_{slow}. These mutations were chosen because they are both located in the fifth actin binding domain, the area that harbours a hotspot for myopathy causing mutations, and affect amino acids predicted to be involved in actin interactions. We co-sedimented incremental amounts of each of the three α -TPM_{slow} proteins with 100 nM filamentous skeletal actin. Fig. 4A shows a representative SDS-PAGE of the filamentous fraction isolated following ultracentrifugation, demonstrating dose-dependent binding of wild-type α -TPM_{slow} to actin filaments. Densitometry data of the bound fraction versus the total amount of α -TPM_{slow} added to the reaction was fitted to a Hill equation, to determine the binding constant K_d and

1
2
3 the Hill coefficient (h) for all three α -TPM_{slow} proteins (Fig. 4B). The α -TPM_{slow} R168C
4 protein showed reduced actin binding affinity compared to wild-type or the α -TPM_{slow} K169E
5 protein ($K_d = 771.4 \pm 188.6$ nM for R168C, 180.2 ± 37.6 nM for wild-type and 164.0 ± 110.6 nM
6 for K169E, range represents 95% confidence interval). The Hill coefficient was similar in all
7 three mutations ($h =$ wild-type 4.471 ± 3.0 , R168C 3.308 ± 2.4 , K169E 1.602 ± 1.3). These
8 results suggest actin binding may be the mechanism by which the *TPM3* R168C mutation
9 alters contractile function and causes muscle weakness.
10
11
12
13
14
15

16 ***Fast fibre specific α -actinin-3 is ectopically expressed in slow fibres of patients with*** 17 ***R168H/G TPM3 mutations*** 18

19 As many *TPM3* patient biopsies displayed a skewing to either slow- or fast- fibre
20 predominance by ATPase stain, we stained serial muscle sections with antibodies recognizing
21 fibre-type specific isoforms of MHC, troponin and α -actinin to investigate whether the
22 expression of several fibre-type-specific proteins was normal (Fig. 5A, Supplementary Fig.
23 1). Three patients (Patients 4, 6a and 6b, each with R168 substitutions), showed elevated
24 levels of hybrid fibres expressing both slow and fast myosin isoforms. All other patients
25 showed normal fibre profiling of myosin and troponin. Curiously, when further
26 characterizing the expression profile of hybrid fibres in Patients 4, 6a, 6b and 10, we
27 observed ectopic expression of α -actinin-3 in dedicated slow fibres as determined by the
28 expression of myosin and troponin (Fig. 5A, Supplementary Fig. 1). α -Actinin-3 is a
29 component of the Z-disc normally present in fast myofibres and has been found to be
30 important for muscle performance (strength and speed) (26, 27). Our results suggest that the
31 restricted fibre-type expression profiles of α -actinin-2 and -3 is differently regulated to
32 myosin, troponin and tropomyosin in patients with *TPM3* mutations compared to age-
33 matched controls.
34
35
36
37
38
39
40
41
42
43
44
45

46 ***Phosphorylation of tropomyosin is increased in patients with mutations in TPM3*** 47

48 In normal skeletal muscle, a proportion of both α - and β -TPM is phosphorylated at residue
49 S283 (28, 29)(Fig. 5Bi). The effect of tropomyosin phosphorylation in skeletal muscle is
50 poorly understood, but studies suggest it is important for tropomyosin function by enhancing
51 head-to-tail interactions and increasing the cooperative activation of myosin resulting in
52 enhanced force production (30). We investigated whether phosphorylation at S283 was
53 altered in *TPM3* patients (as a possible contributor to muscle dysfunction) by Western blot
54
55
56
57
58
59
60

1
2
3 analysis using an anti-phosphor-S283 specific antibody (Fig. 5Bii shows a representative
4 Western blot). Phosphorylation of tropomyosin (all three isoforms were analysed in
5 combination) was increased in 6/8 of patients with samples available for analysis, compared
6 to five age-matched controls (Fig. 5Biii). However, elevated levels of S283 phosphorylation
7 were also observed in patients with mutations in *TPM2*, *ACTA1*, *DNM2*, *DMD* and *DYSF*
8 (Fig. 5Biiii).

9
10
11
12
13
14 Mutations in *DMD* (causing Duchenne and Becker muscular dystrophy) and *DYSF* (causing
15 limb girdle muscular dystrophy type-2B) cause muscle fibre breakdown and regeneration. It
16 is well documented that tropomyosin phosphorylation is higher during development in
17 animals (29), and thus we explored whether increased phosphor-S283 in dystrophic muscle
18 was related to fibre re-generation. Using IHC analysis, we established that phospho-S283
19 tropomyosin levels did not correlate with fibre-type or with fibre re-generation in control or
20 patient biopsies (Supplementary Fig. 2B-C). In *TPM3* patients however, levels of phospho-
21 S283 tropomyosin were specifically elevated in small, slow-twitch myofibres (Supplementary
22 Fig. 2A). This suggests that increased phosphorylation of tropomyosin is not specific to
23 *TPM3* disease, but may be a compensatory response to muscle dysfunction due to a variety of
24 mechanisms.

25
26
27
28
29
30
31
32
33
34
35 ***Slow myofibres of TPM3-myopathy patients have reduced maximal force, likely due***
36 ***to altered cross-bridge cycling***

37
38 In order to understand how muscle weakness develops in *TPM3* patients we performed
39 contractile studies on single, chemically-permeabilised patient myofibres or small fibre
40 bundles by immersing them in Ca^{2+} -containing solutions (see methods regarding details for
41 analysis of bundles). This induces activation of the contractile filaments allowing
42 measurement of isometric force production.

43
44
45
46
47
48 First, fibres and fibre bundles were activated at saturating $[\text{Ca}^{2+}]$ of pCa 4.5 ($\sim 31.6 \mu\text{M}$) to
49 induce maximal isometric contraction (F_{max} , Fig. 6A). A small but significant force deficit
50 was observed in slow myofibres and fibre bundles from seven of 10 *TPM3*-myopathy patients
51 compared to pooled control samples (F_{max} in all *TPM3* patients ranges from 52.17 – 116
52 mN/mm^2 compared to $143.1 \pm 31.8 \text{ mN}/\text{mm}^2$ in controls, $*p < 0.01$ one-way ANOVA, Fig. 6C
53 and D). This force deficit was present despite normalization to the smaller CSA in slow fibres
54
55
56
57
58
59
60

1
2
3 of *TPM3* patients. Fmax in type-2 fibres was not different from control fibres (106.7-186.7
4 mN/mm² in patient fibres and 147.7±29.34 mN/mm² in control fibres) (Fig. 6B). In bundles,
5 Fmax was lower in bundles with higher slow MHC content in two of three patients
6 (Supplementary Fig. 3).
7
8
9

10
11 During muscle contraction, a cyclic interaction between the myosin heads and thin filaments,
12 followed by a conformational change in myosin, allows the filaments to slide past each other.
13 Correct positioning of tropomyosin on actin filaments during the various stages of myosin-
14 actin interactions is crucial for efficient cross-bridge cycling. To determine if the force deficit
15 in slow myofibres of *TPM3* patients can be attributed to changes in cross-bridge cycling
16 kinetics we measured the rate of tension re-development (K_{tr}) during maximal activation,
17 after a short period of unloaded shortening following by re-stretch (a typical length and force
18 trace are presented in Fig. 7Ai). The speed of cross-bridge cycling is physiologically faster in
19 type-2 (fast-twitch) fibres compared to type-1 (slow-twitch) fibres (see controls in Fig. 7Aii-
20 iii). Slow fibres from eight of 10 *TPM3* patient biopsies displayed a significant reduction in
21 K_{tr} compared to controls (K_{tr} in all *TPM3* patients ranges from 0.758-1.217 s⁻¹ compared to
22 1.493±0.25 s⁻¹ in controls, *** p<0.0001, * p<0.01, one-way ANOVA, Fig. 7Aii), whereas
23 fast myofibres were not different from control myofibres (Fig. 7Aiii). These results suggest
24 that myosin cross-bridge cycling kinetics are altered in slow fibres of *TPM3* patients,
25 contributing to muscle weakness by reducing the fraction of strongly bound cross-bridges
26 during activation.
27
28
29
30
31
32
33
34
35
36
37
38
39

40 Fmax is proportional to the force generated by a single strongly bound actin-myosin cross-
41 bridge and the fraction of myosin heads attached to actin. We assessed active stiffness in
42 *TPM3* biopsies, a measure proportional to the number of myosin heads strongly attached to
43 actin during an isometric contraction (31), to study whether this contributes to muscle
44 weakness. We measured active stiffness by performing fast length changes in isometrically
45 contracted single myofibres (typical length/force traces are presented in Supplementary Fig. 4
46 and a typical patient and control plot of the length change (ΔL) versus force change (ΔF) is
47 presented in Fig. 7Bi and ii, respectively)(32). We observed a trend towards reduced absolute
48 active stiffness in type-1 fibres and bundles/hybrid fibres of most *TPM3* patients (Fig. 7Biii
49 and iiiii), which was not present in type-2 fibres (Fig. 7Bv). The change in active stiffness was
50 proportional to Fmax, as the difference was not present when stiffness was normalised to
51 Fmax (Fig. 7Bvi-viii). Since stiffness is proportional to the number of strongly attached
52
53
54
55
56
57
58
59
60

1
2
3 myosin cross-bridges, a reduction of active stiffness proportional to force reduction suggests
4 that forces per cross-bridge were normal, but, in line with the reduced K_{tr} , the number of
5 strongly attached cross-bridges may be reduced in slow fibres of *TPM3* patients, likely
6 contributing to muscle weakness.
7
8
9

10
11 ***Ca²⁺-sensitivity of contraction and maximal contractile force are decreased in***
12 ***patients with TPM3 mutations***
13

14 Tropomyosin and the troponin complex are pivotal in regulating Ca^{2+} -induced cross-bridge
15 cycling during muscle contraction. We assessed the sensitivity to Ca^{2+} of permeabilised
16 fibres, by bathing preparations in incrementally increasing $[Ca^{2+}]$ (pCa 6.2-4.5) and
17 measuring the generated contractile force. In slow myofibres and fibre bundles/hybrid fibres
18 of all patients, the force-pCa curves were shifted to the right compared to controls (Fig. 8Ai-
19 ii). As a result, the pCa_{50} , representing the negative logarithm of the $[Ca^{2+}]$ at which
20 preparations produce 50 % of their F_{max} , was significantly reduced in type-1 fibres and
21 bundles/hybrid fibres from all patients compared to controls (pCa_{50} type-1: 5.96 ± 0.06
22 controls, 5.69 ± 0.04 patients; pCa_{50} bundles/hybrid: 5.99 ± 0.09 controls, 5.67 ± 0.05 patient,
23 Fig. 8Bi-ii). This result indicates that more Ca^{2+} was required in patient biopsies than control
24 biopsies to achieve the same relative force. In contrast, fast fibres from patients and controls
25 showed normal Ca^{2+} -activated force production (Fig. 8Aiii, Fig. 8Biii).
26
27
28
29
30
31
32
33
34
35

36 Our data demonstrates that slow fibres and in bundles/hybrid fibres from patients with *TPM3*
37 mutations produce on average ~ 63 % of the force produced by control fibres at saturating
38 $[Ca^{2+}]$ (pCa 4.5). During a maximal contraction the intracellular $[Ca^{2+}]$ can rise from resting
39 levels of ~0.1 μM (pCa 7) to ~10 μM (pCa 5) (33). However, myofibres *in vivo* rarely
40 undergo maximal stimulation and mostly operate at sub-maximal levels, typically resulting in
41 $[Ca^{2+}]$ of around 1-5 μM in type-1 fibres (yellow area in Fig. 8A) (34-36). At these
42 physiological Ca^{2+} levels (pCa 6.0), slow fibres and bundles/hybrid fibres from *TPM3*
43 patients produce on average only 26 % of the force produced by control slow fibres and
44 bundles/hybrid fibres (Fig. 8Ci-ii), whereas patient fast fibres produce forces similar to
45 controls (Fig. 8Ciii). Thus, our results suggest reduced Ca^{2+} -sensitivity is a significant basis
46 for muscle weakness in *TPM3*-myopathy.
47
48
49
50
51
52
53
54
55
56
57
58
59
60

1
2
3 ***Ectopic α -actinin-3 expression in slow myofibres does not correlate with increased***
4 ***maximal force***
5

6
7 Four patients with *TPM3* mutations at R168 displayed ectopic expression of α -actinin-3 in
8 slow myofibres. Since α -actinin-3 expression is associated with increased muscle strength
9 and speed (26, 27) we determined whether α -actinin-3 in slow fibres may influence
10 contractile properties. We tested if α -actinin-3 expression was more commonly observed in
11 fibres with higher Fmax in eight fibres from two patients. However, we found no correlation
12 between ectopic α -actinin-3 and force production in these patient fibres (Supplementary Fig.
13 5).
14
15
16
17
18
19
20
21
22
23
24
25
26
27
28
29
30
31
32
33
34
35
36
37
38
39
40
41
42
43
44
45
46
47
48
49
50
51
52
53
54
55
56
57
58
59
60

For Peer Review

Discussion

Mutations in *TPM3* cause a range of histopathological patterns and are associated with generalised muscle weakness. To date, the cause of muscle dysfunction is not well understood in these patients, hindering the development of evidence-based treatments for *TPM3*-myopathies. Thus, we performed extensive phenotypical and functional characterization of a large cohort of *TPM3*-myopathy patients to understand the molecular mechanism(s) of their muscle weakness.

The main histological feature of *TPM3*-myopathy patients in this cohort, and other published cohorts (1-3), was a selective hypotrophy of slow myofibres, while other histological features such as nemaline rods and caps were rarely present (four of 15 patients). The selective hypotrophy and contractile dysfunction of slow myofibres is consistent with the restricted slow-fibre expression of α -TPM_{slow}, the main protein expressed from *TPM3* in skeletal muscle. We confirmed the presence of mutant α -TPM_{slow} in the filamentous fraction of patient skeletal muscle via 2D-SDS-PAGE for patients possessing a *TPM3* mutation resulting in a charge change. In patients with protein aggregates (e.g. nemaline bodies), it has been uncertain whether mutant protein is actually incorporated into the sarcomere, or partitions into protein aggregates within the muscle fibre. In our study, protein aggregates were not observed in biopsies analysed by 2D-SDS-PAGE, suggesting that α -TPM_{slow} mutant protein is likely incorporated into sarcomeres causing muscle weakness via a dominant negative effect on contractile function.

Muscle contraction and force production rely on efficient interactions between tropomyosin polymers and major binding partners, the troponins and the actin filament, in response to Ca²⁺-influx. In this series of twelve muscle biopsies from *TPM3*-myopathy patients, we showed normal fibre-type expression of the major contractile proteins myosin, actin, troponin and tropomyosin. Furthermore, we confirmed normal ratios of the three skeletal muscle tropomyosin isoforms according to fibre-type composition for all patients. Our data suggest the higher relative abundance of α -TPM_{slow} previously reported in a patient bearing a M9R substitution in *TPM3* (25, 37) may be a specific property of this mutation, perhaps related to its position within the dimerisation domain. In a small number of patients, we observed ectopic expression of the fast fibre Z-disc protein α -actinin-3 in slow myofibres. The consequence of slow-fibre expression of the fast-fibre α -actinin-3 is not clear, and may relate

1
2
3 to both metabolic and structural roles of α -actinin-3, though we excluded an overt effect on
4 contractile force of single myofibres.
5

6
7 We investigated tropomyosin phosphorylation at residue S283 in our cohort. Tropomyosin
8 phosphorylation has mainly been studied in the context of cardiac function (38-41) and to the
9 best of our knowledge has not been investigated in skeletal myopathy patients. *In vitro*
10 studies suggest phosphorylation strongly affects tropomyosin properties [e.g. stronger head-
11 to-tail interaction, enhanced troponin binding, higher myosin ATPase activity and long-range
12 cooperative activation of myosin-thin filament binding (30, 42, 43)]. We showed
13 tropomyosin phosphorylation was commonly increased in a wide range of genetic muscle
14 disorders including *TPM3*-myopathy. However, the cause of this up-regulation and the effect
15 on skeletal muscle contractility is unclear. The p38-MAPK (mitogene-activated protein
16 kinase) and ERK (extracellular signal-related kinase) signalling pathways are likely involved
17 in tropomyosin phosphorylation of cardiac muscle and non-muscle cells, respectively (44-
18 46). In skeletal muscle, these pathways regulate exercise-induced adaptive responses on gene
19 expression (reviewed in 47), suggesting tropomyosin phosphorylation may be involved in
20 remodelling or adaptation to cellular stress.
21

22
23 Most reported *TPM3* substitutions lie within or near actin-binding domains, with several
24 substitutions believed to influence direct electrostatic interactions with actin in the “off” state
25 [when tropomyosin blocks myosin binding sites on the actin filament e.g. R91, R168, R245
26 directly interact with actin D25 (48-50)]. Our data and previous studies have shown that
27 many tropomyosin substitutions indeed affect binding to actin-filaments (51-54). Thus,
28 altered actin-binding likely represents a common mechanism by which tropomyosin mutants
29 alter sarcomeric function, perhaps related to the Ca^{2+} -activated movement of tropomyosin
30 between the “on” and “off” position during cross-bridge cycling (50, discussed in 55).
31

32
33 Recent studies have attempted to predict the effect of mutations on actin-tropomyosin
34 interactions and the resulting contractile abnormality, classifying them as “gain-of-function”
35 changes (hyper-contractile phenotype, shift towards “on” state) and “loss-of-function”
36 changes (hypo-contractile phenotype, stabilizing the “off” state) (49, 56, 57). Most mutations
37 in our cohort are predicted to cause a “loss-of-function” (e.g. decreased Ca^{2+} -sensitivity and a
38 hypocontractile phenotype). The only exception is *TPM3* K169E, predicted to favour the
39 “on” position and enhance myosin-actin binding (49, 56)]. This phenotype was confirmed in
40 reconstituted thin filaments *in vitro* (49). However, isolated slow myofibres and fibre bundles
41
42
43
44
45
46
47
48
49
50
51
52
53
54
55
56
57
58
59
60

1
2
3 of all *TPM3* patients (including Patient 1 carrying the K169E mutation), showed reduced
4 Ca^{2+} -sensitivity of contraction. Our data are consistent with the patient phenotype described
5 in (1) and do not support the hyper-contractile phenotype of the K169E mutation present in *in*
6 *vitro* assessment of isolated filaments (49). This discrepancy may be explained by the greater
7 complexity of single-fibre contractility studies, a setting that evaluates the combined
8 contributions of actin, tropomyosin and troponin binding and regulatory proteins within a
9 mature myofibre, which may also have undergone adaptive responses to disease. These may
10 not be mirrored by *in vitro* actin motility studies or predictions via molecular modelling.
11 Additional factors, such as interactions with other sarcomeric proteins like the troponin
12 complex (58), may also contribute. Additionally, a recurrent mutation in *TPM3*, R168H, was
13 found to reduce [current study and (21)] or increase Ca^{2+} -sensitivity (20) in different patients
14 with the same mutation. The cause for this patient to patient variability remains to be
15 established.

16
17
18
19
20
21
22
23
24
25
26 In our study, we identified two major abnormalities in contractile performance that we
27 believe directly underpins weakness in *TPM3*-myopathy. Firstly, all patients exhibited
28 reduced Ca^{2+} -sensitivity of contraction in slow myofibres, likely resulting in a significant
29 reduction in the contractile force generated at physiological, sub-maximal activation of
30 muscle. Secondly, slow myofibres demonstrated a significant reduction in cross-bridge
31 cycling kinetics and a small reduction in active stiffness (assesses the number of strongly
32 bound myosin-actin cross-bridges) – meaning that myosin less effectively and less stably
33 transits along actin filaments during contraction. Collectively, these two abnormalities likely
34 cause insufficient force production during a normal action potential resulting in slow fibre
35 weakness.

36
37
38
39
40
41
42
43 The selective dysfunction of slow myofibres in our cohort demonstrates the importance of
44 assessing the two fibre types separately, and raises the question as to why fast myofibres are
45 not able to compensate for dysfunctional slow myofibres. Inherent differences exist between
46 the two fibre types. Slow myofibres are less fatigable than fast myofibres, probably due at
47 least in part to larger numbers of mitochondria and a greater capacity for oxidative
48 metabolism (59, 60). Additionally, fast myofibres have a higher ATP consumption. Particular
49 muscle groups, such as respiratory muscles, rely on slow fibres to produce sustained, low
50 intensity contractions. Substantial weakness of respiratory muscles is common in *TPM3*
51 patients, and effective treatments that specifically target slow muscle fibre dysfunction may
52 ameliorate respiratory insufficiency.

1
2
3 In summary, contractile function was commonly impaired in *TPM3*-myopathy patients. In
4 particular, we showed reduced force generation caused by altered cross-bridge cycling
5 kinetics and reduced Ca^{2+} -sensitivity of muscle contraction. The identification of abnormal
6 Ca^{2+} -sensitivity suggests the use of Ca^{2+} -sensitisers may present a viable therapeutic
7 approach for TPM-related myopathies. To date, a number of agents are known to be effective
8 at improving Ca^{2+} -sensitivity in isolated skeletal myofibres from various species including
9 bovine, human, mouse and rabbit (21, 61-64). Additionally, Ca^{2+} -sensitisers were able to
10 ameliorate muscle dysfunction in a rat model of myasthenia gravis (61) and isolated skeletal
11 myofibres from congenital myopathy patients with mutations in *TPM3*, *TPM2* and *NEB* (21,
12 62). This therapeutic approach appears to be promising; however, most of these agents target
13 the fast troponin isoforms and are unlikely to ameliorate slow fibre dysfunction. A Ca^{2+} -
14 sensitiser acting on slow skeletal/cardiac troponin-C did not improve Ca^{2+} -sensitivity in
15 skeletal myofibres in a recent study, suggesting that new compounds targeting slow myofibre
16 dysfunction have yet to be developed (65). Also, it appears that *TPM2* and *TPM3* mutations
17 can either increase or decrease Ca^{2+} -sensitivity in a patient and mutation-specific manner
18 (overview in Supplementary Tab. 4), thus Ca^{2+} -sensitisers will only be useful in a subset of
19 patients. Patients with increased Ca^{2+} -sensitivity display a hyper-contractile clinical
20 phenotype (21, 53), suggesting treatment with Ca^{2+} -sensitisers must be tightly regulated to
21 ensure appropriate muscle function and avoid side effects.
22
23
24
25
26
27
28
29
30
31
32
33
34

35 **Materials and Methods**

36 ***Study approval***

37
38 This study was approved by the human ethics committees of the Stollery Children's Hospital,
39 Edmonton, Canada (ID: 5856), Royal Children's Hospital, Melbourne, Australia (ID:
40 21102A), Children's Hospital at Westmead, Sydney, Australia (ID: 2000/068, 10.CHW.45),
41 University of Sydney, Australia (ID: 01/11/50) and Boston Children's Hospital Institutional
42 Review Board (03-08-128R). Informed consent was obtained from all individuals.
43
44
45
46
47
48

49 ***Molecular modelling***

50 Molecular modelling was based on the 7 Ångstroms resolution crystal structure of an α -
51 TPM_{fast} dimer isolated from adult porcine ventricles (RCSB Protein Data Bank 1C1G,
52 Whitby and Phillips (23)). Molecular graphics were created with Swiss-PDB Viewer v4.1.0
53 (66).
54
55
56
57
58
59
60

Antibodies

1
2
3
4
5
6
7
8
9
10
11
12
13
14
15
16
17
18
19
20
21
22
23
24
25
26
27
28
29
30
31
32
33
34
35
36
37
38
39
40
41
42
43
44
45
46
47
48
49
50
51
52
53
54
55
56
57
58
59
60

Mouse anti-sarcomeric actin (**5C5**, 1:100 for immunohistochemistry [IHC] and 1:10000 for Western blot), fast myosin [**MY32**, 1:800 for IHC, tropomyosin (**TM311**, 1:20,000 for Western blot and 1:800 for IHC), troponin-T_{fast} (**TNNT3**, 1:30 for IHC and 1:1000 for Western blot) were obtained from Sigma Aldrich. S283-phosphorylated tropomyosin was detected using the rabbit **anti-Tm-pS283-050** (1:500 for Western blot and 1:30 for IHC, 21st Century Biochemicals) and slow myosin antibodies were obtained from Chemicon (1:800 for IHC and 1:7000 for Western blot). Polyclonal α -actinin-3 antibodies were produced in-house (antibody **5B3** diluted 1:50 for IHC and antibody **5A2** 1:1500 for Western blot) (67). Troponin-I_{slow} (**MYNT-S**, diluted 1:10 for IHC) and fast (**MYNT-F**, diluted 1:150) antibodies were kindly supplied by Takeshi Nakamura, Japan. Troponin-T_{slow} antibodies (**CT3**) were obtained from the Developmental Studies Hybridoma Bank, University of Iowa (diluted 1:50 for IHC). Cardiac actin and neonatal myosin heavy chain (MHC) antibodies were obtained from American Research Products Inc, USA and Novocastra Laboratories Ltd, UK, respectively.

IHC and Zenon labelling

IHC was performed as described previously (68). Sections were either fixed as described in (37) (**MYNT-S**) or for 10 min in 3% PFA (**MYNT-F**, **CT3** and **TNNT3**) or used unfixed (other antibodies). A Zenon mouse IgG labelling kit (Molecular Probes) was used to directly label primary antibodies with different fluorophores for co-staining with two mouse antibodies as per manufacturer's instructions (either MHC type-2A and type-1 [Fig. 5] or neonatal MHC and cardiac actin [Supplementary Fig. 2C]). Staining was imaged using standard fluorescence microscopy.

Fibre morphometry

Fibre morphometry was performed on cryo-sections stained for myosin ATPase (69)] or following IHC for MHC isoforms. At least 200 fibres, visible in two distant fields of the same section were analysed using ImagePro Plus 4 software (Media Cybernetics). The greatest distance between opposite sides of the narrowest aspect, the MinFerret diameter, was measured to obtain the fibre diameter from a cross sectional cut. The percentage fibre-size disproportion (%FSD) was calculated as described in (1) and slow fibre area was calculated assuming circular shape of myofibres.

Western blot and 2D-polyacrylamide gel electrophoresis (2D-SDS-PAGE)

Western blot methods were based on (70) and tropomyosin isoforms were resolved as described in (53). Extraction of the filamentous protein pool from skeletal muscle sections and 2D-SDS-PAGE to determine mutant tropomyosin expression were performed as described previously (14, 71).

Protein sources and actin-tropomyosin co-sedimentation

We employed site-directed mutagenesis to produce wild-type and mutant (R168C, K169E) α -TPM_{slow} baculoviruses to infect *Sf9* insect cells using the baculovirus expression method as described previously (72, 73).

Filamentous actin was prepared from actin-acetone powder isolated from rabbit muscle (74) and a 1 μ M stock with 1 μ M phalloidin and 0.1 mM ATP was used for experiments.

All protein stocks were prepared in and dialyzed against a buffer containing 100 mM KCl, 50 mM Imidazole, 8 mM MgCl₂, 2 mM EDTA, 10 mM DTT and 0.5 mg/mL ultrapure bovine serum albumin (BSA, Sigma). Ten μ M tropomyosin stocks were cleared of aggregates by ultracentrifugation at 603,180 x g (Sorvall M120-SE centrifuge, S100AT6-0199 rotor) for 20 min at 4 °C. Ten nM actin were co-sedimented with incremental amounts of tropomyosin (50-1000 nM) in 1 mL reaction volume at 51,427 x g for 1.5 hr at 25 °C (Sorvall Evolution RC centrifuge, F20-Micro rotor) in siliconised polypropylene tubes. The pelleted fractions were solubilised in loading buffer and loaded on 4-15 % Criterion TGX gels (Biorad). Densitometry analysis on actin and tropomyosin bands was performed using GeneTools 4.0 software (Synoptics Ltd). Values were corrected for sedimentation in the absence of actin and plotted as the ratio tropomyosin/actin vs. total [tropomyosin] added. Data were fitted to a Hill equation to determine the binding constant K_d and Hill's coefficient h using GraphPad, Prism (Version 5.01).

Contractile measurement of myofibres isolated from frozen human muscle biopsies

Small fractions of frozen muscle biopsies were thawed as described previously (62) in a solution containing 50 % glycerol and 50 % Ca²⁺-free relaxing-solution (100 mM BES, 6.97 mM EGTA, 6.48 mM MgCl₂, 6 mM Na₂ATP, 1 mM DTT, 40.76 mM K-propionate, 14.5 mM creatine phosphate, 0.5 mM PMSF, 10 μ M E64, 40 μ M leupeptin, pH 7.1 and pCa 9 at 15 °C).

1
2
3 For contractile measurements, single fibres or small fibre bundles [$\sim 0.07 \text{ mm}^2$ cross sectional
4 area (CSA) and $\sim 0.5 \text{ mm}$ length] were dissected in glycerinating solution at $4 \text{ }^\circ\text{C}$. Fibre
5 bundles were prepared if the fibre CSA was too small for reliable force measurements.
6 Aluminium T-clips were attached to both ends of the preparation followed by chemical
7 skinning in glycerinating solution containing 1 % TritonX-100 for 10 min (single fibres) or
8 30 min (bundles) at $4 \text{ }^\circ\text{C}$. The preparations were then stored at $4 \text{ }^\circ\text{C}$ in glycerinating solution
9 until mounting onto a permeabilised fibre apparatus between a length motor and a force
10 transducer (ASI 802D, ASI 403A, ASI 315C-I, respectively, Aurora Scientific Inc., Canada)
11 in relaxing-solution. All force measurements were performed at sarcomere lengths of $2.5 \mu\text{m}$
12 [optimal myofilament overlap, (75)] and at a temperature of $20 \text{ }^\circ\text{C}$ (bath temperature
13 controller ASI 825A, Aurora Scientific). The sarcomere length was set and the CSA was
14 measured as described in (62).
15
16
17
18
19
20
21
22
23

24 Prior to $[\text{Ca}^{2+}]$ -induced activations preparations were pre-activated for 1 min in 100 mM
25 BES, 0.1mM EGTA, 6.42 mM MgCl_2 , 6 mM Na_2ATP , 41.14 mM K-propionate, 14.5 mM
26 creatine phosphate, 6.9 mM HDTA (pH 7.1 and pCa 9 at $15 \text{ }^\circ\text{C}$). Maximal isometric
27 contraction (F_{max}) was measured by bathing fibres in saturating $[\text{Ca}^{2+}]$ buffer (100 mM BES,
28 7 mM CaEGTA, 6.28 mM MgCl_2 , 6 mM Na_2ATP , 40.64 mM K-propionate, 14.5 mM
29 creatine phosphate, pH 7.1 and pCa 4.5 at $15 \text{ }^\circ\text{C}$) until a force plateau was achieved. The
30 maximal specific force (F_{max} at pCa 4.5 normalised to the CSA) is presented in this study.
31 Force/pCa curves and pCa 50 were measured as described in (20). The rate constant of
32 tension re-development (K_{tr}) was measured by allowing the preparations to shorten to 70% of
33 the initial length for 30 ms followed by re-stretch to 100 % and fitting the data to a mono-
34 exponential function using Labview (National Instruments, USA) as described in (20). Active
35 stiffness was measured immediately after the K_{tr} protocol as described previously (32, 76). In
36 brief, we measured the force response (FI) to six 2 s length changes (ΔL : +0.3 %, +0.6 %, +0.9 %, -0.3 %, -0.6 %, -0.9 %; Supplementary Fig. 4). ΔL was plotted against the force
37 changes (ΔF) and a linear regression was fitted to obtain the slope using Graph Pad, Prism
38 (Version 5.01).
39
40
41
42
43
44
45
46
47
48
49
50
51
52

53 The MHC content of measured fibres was determined as described previously (62) and the
54 proportion of each MHC was determined by densitometry. Single myofibres/fibre bundles
55 containing exclusively slow MHC (>90 % type-1), exclusively fast MHC (>90 % type-2A or
56 2X) or a mixture of both (11–90 % type-1 or type-2A/2X) were grouped for analysis. The
57
58
59
60

1
2
3 contractile properties of bundles and hybrid fibres containing a mix of type-1 and type-2A/2X
4 MHC represent the average properties of both fibre types. The K_{tr} in bundles/hybrid fibres is
5 highly variable due to the physiologically difference in type-1 or type-2A/2X fibres and was
6 therefore not presented. Preparations were excluded from the analysis if the Fmax decreased
7 >15 % during the protocol. Single myofibres from eight control biopsies (age 6-54 y) and
8 bundles from two control biopsies (aged 0.6 and 6 y) were pooled for statistical analysis.
9
10
11
12

13 14 15 16 **Acknowledgements**

17 The authors would like to thank the study patients and their families for their participation.
18 Additionally, we are thankful to Dr. Nicole Monnier and Dr. Isabelle Pennison-Besnier (CHU
19 Angers, Département de Neurologie, Angers, France) for supply patient tissue for this study.
20 This work was supported by the National Health and Medical Research Council of Australia
21 [APP571287 to N.F.C., K.N.N. and B.I.; APP1022707 to N.F.C. and K.N.N.; APP1048816 to
22 S.T.C.; APP1035955 to G.R.] and by the National Institutes of Health (USA) [R01
23 HD075802 from the National Institute of Child Health and Human Development to A.H.B.].
24 M.Y. is supported by a University of Sydney Australian Postgraduate Award, an International
25 Postgraduate Research Scholarship and a Boehringer Ingelheim Fonds Travel Grant. K.J.N. is
26 supported by an Australian Resource Council Future Fellowship [FT100100734].
27
28
29
30
31
32
33
34
35
36

37 **Conflict of interest**

38 The authors declare that they have no conflict of interest.
39
40
41
42
43
44
45
46
47
48
49
50
51
52
53
54
55
56
57
58
59
60

References

- 1 Clarke, N.F., Kolski, H., Dye, D.E., Lim, E., Smith, R.L., Patel, R., Fahey, M.C., Bellance, R., Romero, N.B., Johnson, E.S. *et al.* (2008) Mutations in TPM3 are a common cause of congenital fiber type disproportion. *Annals of neurology*, **63**, 329-337.
- 2 Lawlor, M.W., Dechene, E.T., Roumm, E., Geggel, A.S., Moghadaszadeh, B. and Beggs, A.H. (2009) Mutations of tropomyosin 3 (TPM3) are common and associated with type 1 myofiber hypotrophy in congenital fiber type disproportion. *Hum Mutat*.
- 3 Marttila, M., Lehtokari, V.L., Marston, S., Nyman, T.A., Barnerias, C., Beggs, A.H., Bertini, E., Ceyhan-Birsoy, O., Cintas, P., Gerard, M. *et al.* (2014) Mutation update and genotype-phenotype correlations of novel and previously described mutations in TPM2 and TPM3 causing congenital myopathies. *Hum Mutat*, **35**, 779-790.
- 4 Tan, P., Briner, J., Boltshauser, E., Davis, M.R., Wilton, S.D., North, K., Wallgren-Pettersson, C. and Laing, N.G. (1999) Homozygosity for a nonsense mutation in the alpha-tropomyosin slow gene TPM3 in a patient with severe infantile nemaline myopathy. *Neuromuscul Disord*, **9**, 573-579.
- 5 Wattanasirichaigoon, D., Swoboda, K.J., Takada, F., Tong, H.Q., Lip, V., Iannaccone, S.T., Wallgren-Pettersson, C., Laing, N.G. and Beggs, A.H. (2002) Mutations of the slow muscle alpha-tropomyosin gene, TPM3, are a rare cause of nemaline myopathy. *Neurology*, **59**, 613-617.
- 6 Lehtokari, V.-L., Pelin, K., Donner, K., Voit, T., Rudnik-Schöneborn, S., Stoetter, M., Talim, B., Topaloglu, H., Laing, N.G. and Wallgren-Pettersson, C. (2008) Identification of a founder mutation in TPM3 in nemaline myopathy patients of Turkish origin. *European Journal of Human Genetics*, **16**, 1055-1061.
- 7 Lawlor, M.W., Dechene, E.T., Roumm, E., Geggel, A.S., Moghadaszadeh, B. and Beggs, A.H. (2010) Mutations of tropomyosin 3 (TPM3) are common and associated with type 1 myofiber hypotrophy in congenital fiber type disproportion. *Hum Mutat*, **31**, 176-183.
- 8 Laing, N.G., Wilton, S.D., Akkari, P.A., Dorosz, S., Boundy, K., Kneebone, C., Blumbergs, P., White, S., Watkins, H., Love, D.R. *et al.* (1995) A mutation in the alpha tropomyosin gene TPM3 associated with autosomal dominant nemaline myopathy. *Nat Genet*, **9**, 75-79.
- 9 Schreckenbach, T., Schroder, J.M., Voit, T., Abicht, A., Neuen-Jacob, E., Roos, A., Bulst, S., Kuhl, C., Schulz, J.B., Weis, J. *et al.* (2014) Novel TPM3 mutation in a family with cap myopathy and review of the literature. *Neuromuscul Disord*, **24**, 117-124.
- 10 Kiphuth, I.C., Krause, S., Huttner, H.B., Dekomien, G., Struffert, T. and Schroder, R. (2010) Autosomal dominant nemaline myopathy caused by a novel alpha-tropomyosin 3 mutation. *J Neurol*, **257**, 658-660.
- 11 Ohlsson, M., Fidzianska, A., Tajsharghi, H. and Oldfors, A. (2009) TPM3 mutation in one of the original cases of cap disease. *Neurology*, **72**, 1961-1963.
- 12 De Paula, A.M., Franques, J., Fernandez, C., Monnier, N., Lunardi, J., Pellissier, J.F., Figarella-Branger, D. and Pouget, J. (2009) A TPM3 mutation causing cap myopathy. *Neuromuscul Disord*, **19**, 685-688.
- 13 Penisson-Besnier, I., Monnier, N., Toutain, A., Dubas, F. and Laing, N. (2007) A second pedigree with autosomal dominant nemaline myopathy caused by TPM3 mutation: a clinical and pathological study. *Neuromuscul Disord*, **17**, 330-337.
- 14 Waddell, L.B., Kreissl, M., Kornberg, A., Kennedy, P., McLean, C., Labarre-Vila, A., Monnier, N., North, K.N. and Clarke, N.F. (2010) Evidence for a dominant negative disease mechanism in cap myopathy due to TPM3. *Neuromuscul Disord*, **20**, 464-466.
- 15 Geeves, M.A., Hitchcock-DeGregori, S.E. and Gunning, P.W. (2015) A systematic nomenclature for mammalian tropomyosin isoforms. *J Muscle Res Cell Motil*, **36**, 147-153.
- 16 Billeter, R., Heizmann, C.W., Reist, U., Howald, H. and Jenny, E. (1981) alpha- and beta-tropomyosin in typed single fibers of human skeletal muscle. *FEBS letters*, **132**, 133-136.
- 17 Pieples, K. and Wicczorek, D.F. (2000) Tropomyosin 3 increases striated muscle isoform diversity. *Biochemistry*, **39**, 8291-8297.

- 1
2
3 18 McLachlan, A.D. and Stewart, M. (1975) Tropomyosin coiled-coil interactions: evidence for
4 an unstaggered structure. *J Mol Biol*, **98**, 293-304.
- 5 19 McLachlan, A.D. and Stewart, M. (1976) The 14-fold periodicity in alpha-tropomyosin and
6 the interaction with actin. *J Mol Biol*, **103**, 271-298.
- 7 20 Ottenheijm, C.A., Lawlor, M.W., Stienen, G.J., Granzier, H. and Beggs, A.H. (2011) Changes in
8 cross-bridge cycling underlie muscle weakness in patients with tropomyosin 3-based myopathy. *Hum*
9 *Mol Genet*, **20**, 2015-2025.
- 10 21 Ochala, J., Gokhin, D.S., Penisson-Besnier, I., Quijano-Roy, S., Monnier, N., Lunardi, J.,
11 Romero, N.B. and Fowler, V.M. (2012) Congenital myopathy-causing tropomyosin mutations induce
12 thin filament dysfunction via distinct physiological mechanisms. *Hum Mol Genet*, **21**, 4473-4485.
- 13 22 Johnson, M.A., Polgar, J., Weightman, D. and Appleton, D. (1973) Data on the distribution of
14 fibre types in thirty-six human muscles. An autopsy study. *J Neurol Sci*, **18**, 111-129.
- 15 23 Polgar, J., Johnson, M.A., Weightman, D. and Appleton, D. (1973) Data on fibre size in thirty-
16 six human muscles. An autopsy study. *J Neurol Sci*, **19**, 307-318.
- 17 24 Billeter, R., Heizmann, C.W., Reist, U., Howald, H. and Jenny, E. (1982) Two-dimensional
18 peptide analysis of myosin heavy chains and actin from single-typed human skeletal muscle fibers.
19 *FEBS Lett*, **139**, 45-48.
- 20 25 Corbett, M.A., Akkari, P.A., Domazetovska, A., Cooper, S.T., North, K.N., Laing, N.G., Gunning,
21 P.W. and Hardeman, E.C. (2005) An alphaTropomyosin mutation alters dimer preference in nemaline
22 myopathy. *Annals of neurology*, **57**, 42-49.
- 23 26 Clarkson, P.M., Devaney, J.M., Gordish-Dressman, H., Thompson, P.D., Hubal, M.J., Urso, M.,
24 Price, T.B., Angelopoulos, T.J., Gordon, P.M., Moyna, N.M. *et al.* (2005) ACTN3 genotype is
25 associated with increases in muscle strength in response to resistance training in women. *Journal of*
26 *applied physiology*, **99**, 154-163.
- 27 27 Eynon, N., Hanson, E.D., Lucia, A., Houweling, P.J., Garton, F., North, K.N. and Bishop, D.J.
28 (2013) Genes for elite power and sprint performance: ACTN3 leads the way. *Sports Med*, **43**, 803-
29 817.
- 30 28 Mak, A., Smillie, L.B. and Barany, M. (1978) Specific phosphorylation at serine-283 of alpha
31 tropomyosin from frog skeletal and rabbit skeletal and cardiac muscle. *Proc Natl Acad Sci U S A*, **75**,
32 3588-3592.
- 33 29 Montarras, D., Fiszman, M.Y. and Gros, F. (1981) Characterization of the tropomyosin
34 present in various chick embryo muscle types and in muscle cells differentiated in vitro. *J Biol Chem*,
35 **256**, 4081-4086.
- 36 30 Rao, V.S., Marongelli, E.N. and Guilford, W.H. (2009) Phosphorylation of tropomyosin
37 extends cooperative binding of myosin beyond a single regulatory unit. *Cell Motil Cytoskeleton*, **66**,
38 10-23.
- 39 31 Linari, M., Caremani, M., Piperio, C., Brandt, P. and Lombardi, V. (2007) Stiffness and fraction
40 of Myosin motors responsible for active force in permeabilized muscle fibers from rabbit psoas.
41 *Biophys J*, **92**, 2476-2490.
- 42 32 Chandra, M., Mamidi, R., Ford, S., Hidalgo, C., Witt, C., Ottenheijm, C., Labeit, S. and
43 Granzier, H. (2009) Nebulin alters cross-bridge cycling kinetics and increases thin filament activation:
44 a novel mechanism for increasing tension and reducing tension cost. *J Biol Chem*, **284**, 30889-30896.
- 45 33 Baylor, S.M. and Hollingworth, S. (2012) Intracellular calcium movements during excitation-
46 contraction coupling in mammalian slow-twitch and fast-twitch muscle fibers. *J Gen Physiol*, **139**,
47 261-272.
- 48 34 Westerblad, H. and Allen, D.G. (1991) Changes of myoplasmic calcium concentration during
49 fatigue in single mouse muscle fibers. *J Gen Physiol*, **98**, 615-635.
- 50 35 Allen, D.G., Lamb, G.D. and Westerblad, H. (2008) Skeletal muscle fatigue: cellular
51 mechanisms. *Physiol Rev*, **88**, 287-332.
- 52
53
54
55
56
57
58
59
60

- 1
2
3 36 Launikonis, B.S., Stephenson, D.G. and Friedrich, O. (2009) Rapid Ca²⁺ flux through the
4 transverse tubular membrane, activated by individual action potentials in mammalian skeletal
5 muscle. *J Physiol*, **587**, 2299-2312.
- 6 37 Ilkovski, B., Mokbel, N., Lewis, R.A., Walker, K., Nowak, K.J., Domazetovska, A., Laing, N.G.,
7 Fowler, V.M., North, K.N. and Cooper, S.T. (2008) Disease severity and thin filament regulation in
8 M9R TPM3 nemaline myopathy. *J Neuropathol Exp Neurol*, **67**, 867-877.
- 9 38 Marston, S.B., Copeland, O., Messer, A.E., MacNamara, E., Nowak, K., Zampronio, C.G. and
10 Ward, D.G. (2013) Tropomyosin isoform expression and phosphorylation in the human heart in
11 health and disease. *J Muscle Res Cell Motil*, **34**, 189-197.
- 12 39 Schulz, E.M., Wilder, T., Chowdhury, S.A., Sheikh, H.N., Wolska, B.M., Solaro, R.J. and
13 Wieczorek, D.F. (2013) Decreasing tropomyosin phosphorylation rescues tropomyosin-induced
14 familial hypertrophic cardiomyopathy. *J Biol Chem*, **288**, 28925-28935.
- 15 40 Schulz, E.M. and Wieczorek, D.F. (2013) Tropomyosin de-phosphorylation in the heart: what
16 are the consequences? *J Muscle Res Cell Motil*, **34**, 239-246.
- 17 41 Warren, C.M., Arteaga, G.M., Rajan, S., Ahmed, R.P., Wieczorek, D.F. and Solaro, R.J. (2008)
18 Use of 2-D DIGE analysis reveals altered phosphorylation in a tropomyosin mutant (Glu54Lys) linked
19 to dilated cardiomyopathy. *Proteomics*, **8**, 100-105.
- 20 42 Heeley, D.H. (2013) Phosphorylation of tropomyosin in striated muscle. *J Muscle Res Cell
21 Motil*, **34**, 233-237.
- 22 43 Lehman, W., Medlock, G., Li, X.E., Suphamungmee, W., Tu, A.Y., Schmidtman, A., Ujfalusi,
23 Z., Fischer, S., Moore, J.R., Geeves, M.A. *et al.* (2015) Phosphorylation of Ser283 enhances the
24 stiffness of the tropomyosin head-to-tail overlap domain. *Arch Biochem Biophys*, **571**, 10-15.
- 25 44 Vahebi, S., Ota, A., Li, M., Warren, C.M., de Tombe, P.P., Wang, Y. and Solaro, R.J. (2007)
26 p38-MAPK induced dephosphorylation of alpha-tropomyosin is associated with depression of
27 myocardial sarcomeric tension and ATPase activity. *Circ Res*, **100**, 408-415.
- 28 45 Houle, F., Poirier, A., Dumaresq, J. and Huot, J. (2007) DAP kinase mediates the
29 phosphorylation of tropomyosin-1 downstream of the ERK pathway, which regulates the formation
30 of stress fibers in response to oxidative stress. *J Cell Sci*, **120**, 3666-3677.
- 31 46 Houle, F., Rousseau, S., Morrice, N., Luc, M., Mongrain, S., Turner, C.E., Tanaka, S., Moreau,
32 P. and Huot, J. (2003) Extracellular signal-regulated kinase mediates phosphorylation of
33 tropomyosin-1 to promote cytoskeleton remodeling in response to oxidative stress: impact on
34 membrane blebbing. *Mol Biol Cell*, **14**, 1418-1432.
- 35 47 Widegren, U., Ryder, J.W. and Zierath, J.R. (2001) Mitogen-activated protein kinase signal
36 transduction in skeletal muscle: effects of exercise and muscle contraction. *Acta Physiol Scand*, **172**,
37 227-238.
- 38 48 Li, X.E., Tobacman, L.S., Mun, J.Y., Craig, R., Fischer, S. and Lehman, W. (2011) Tropomyosin
39 position on F-actin revealed by EM reconstruction and computational chemistry. *Biophys J*, **100**,
40 1005-1013.
- 41 49 Marston, S., Memo, M., Messer, A., Papadaki, M., Nowak, K., McNamara, E., Ong, R., El-
42 Mezgueldi, M., Li, X. and Lehman, W. (2013) Mutations in repeating structural motifs of tropomyosin
43 cause gain of function in skeletal muscle myopathy patients. *Hum Mol Genet*, **22**, 4978-4987.
- 44 50 Orzechowski, M., Moore, J.R., Fischer, S. and Lehman, W. (2014) Tropomyosin movement on
45 F-actin during muscle activation explained by energy landscapes. *Arch Biochem Biophys*, **545**, 63-68.
- 46 51 Robaszkiewicz, K., Dudek, E., Kasprzak, A.A. and Moraczewska, J. (2012) Functional effects of
47 congenital myopathy-related mutations in gamma-tropomyosin gene. *Biochim Biophys Acta*, **1822**,
48 1562-1569.
- 49 52 Moraczewska, J., Greenfield, N.J., Liu, Y. and Hitchcock-DeGregori, S.E. (2000) Alteration of
50 tropomyosin function and folding by a nemaline myopathy-causing mutation. *Biophys J*, **79**, 3217-
51 3225.
- 52
53
54
55
56
57
58
59
60

- 1
2
3 53 Mokbel, N., Ilkovski, B., Kreissl, M., Memo, M., Jeffries, C.M., Marttila, M., Lehtokari, V.L.,
4 Lemola, E., Gronholm, M., Yang, N. *et al.* (2013) K7del is a common TPM2 gene mutation associated
5 with nemaline myopathy and raised myofibre calcium sensitivity. *Brain*, **136**, 494-507.
6 54 Akkari, P.A., Song, Y., Hitchcock-DeGregori, S., Blechynden, L. and Laing, N. (2002) Expression
7 and biological activity of Baculovirus generated wild-type human slow alpha tropomyosin and the
8 Met9Arg mutant responsible for a dominant form of nemaline myopathy. *Biochem Biophys Res*
9 *Commun*, **296**, 300-304.
10 55 Ochala, J. (2008) Thin filament proteins mutations associated with skeletal myopathies:
11 Defective regulation of muscle contraction. *Journal of Molecular Medicine*, **86**, 1197-1204.
12 56 Memo, M. and Marston, S. (2013) Skeletal muscle myopathy mutations at the actin
13 tropomyosin interface that cause gain- or loss-of-function. *J Muscle Res Cell Motil*, **34**, 165-169.
14 57 Orzechowski, M., Fischer, S., Moore, J.R., Lehman, W. and Farman, G.P. (2014) Energy
15 landscapes reveal the myopathic effects of tropomyosin mutations. *Arch Biochem Biophys*, **564**, 89-
16 99.
17 58 Robaszekiewicz, K., Ostrowska, Z., Cyranka-Czaja, A. and Moraczewska, J. (2015) Impaired
18 tropomyosin-troponin interactions reduce activation of the actin thin filament. *Biochimica et*
19 *biophysica acta*, **1854**, 381-390.
20 59 Schwerzmann, K., Hoppeler, H., Kayar, S.R. and Weibel, E.R. (1989) Oxidative capacity of
21 muscle and mitochondria: correlation of physiological, biochemical, and morphometric
22 characteristics. *Proc Natl Acad Sci U S A*, **86**, 1583-1587.
23 60 Jackman, M.R. and Willis, W.T. (1996) Characteristics of mitochondria isolated from type I
24 and type IIb skeletal muscle. *Am J Physiol*, **270**, C673-678.
25 61 Russell, A.J., Hartman, J.J., Hinken, A.C., Muci, A.R., Kawas, R., Driscoll, L., Godinez, G., Lee,
26 K.H., Marquez, D., Browne, W.F.t. *et al.* (2012) Activation of fast skeletal muscle troponin as a
27 potential therapeutic approach for treating neuromuscular diseases. *Nat Med*, **18**, 452-455.
28 62 de Winter, J.M., Buck, D., Hidalgo, C., Jasper, J.R., Malik, F.I., Clarke, N.F., Stienen, G.J.,
29 Lawlor, M.W., Beggs, A.H., Ottenheijm, C.A. *et al.* (2013) Troponin activator augments muscle force
30 in nemaline myopathy patients with nebulin mutations. *J Med Genet*, **50**, 383-392.
31 63 Lee, E.J., De Winter, J.M., Buck, D., Jasper, J.R., Malik, F.I., Labeit, S., Ottenheijm, C.A. and
32 Granzier, H. (2013) Fast skeletal muscle troponin activation increases force of mouse fast skeletal
33 muscle and ameliorates weakness due to nebulin-deficiency. *PLoS One*, **8**, e55861.
34 64 Hooijman, P.E., Beishuizen, A., de Waard, M.C., de Man, F.S., Vermeijden, J.W., Steenvoorde,
35 P., Bouwman, R.A., Lommen, W., van Hees, H.W., Heunks, L.M. *et al.* (2014) Diaphragm fiber
36 strength is reduced in critically ill patients and restored by a troponin activator. *Am J Respir Crit Care*
37 *Med*, **189**, 863-865.
38 65 de Winter, J.M., Joureau, B., Sequeira, V., Clarke, N.F., van der Velden, J., Stienen, G.J.,
39 Granzier, H., Beggs, A.H. and Ottenheijm, C.A. (2015) Effect of levosimendan on the contractility of
40 muscle fibers from nemaline myopathy patients with mutations in the nebulin gene. *Skelet Muscle*,
41 **5**, 12.
42 66 Guex, N. and Peitsch, M.C. (1997) SWISS-MODEL and the Swiss-PdbViewer: an environment
43 for comparative protein modeling. *Electrophoresis*, **18**, 2714-2723.
44 67 Chan, Y., Tong, H.Q., Beggs, A.H. and Kunkel, L.M. (1998) Human skeletal muscle-specific
45 alpha-actinin-2 and -3 isoforms form homodimers and heterodimers in vitro and in vivo. *Biochem*
46 *Biophys Res Commun*, **248**, 134-139.
47 68 Lo, H.P., Cooper, S.T., Evesson, F.J., Seto, J.T., Chiotis, M., Tay, V., Compton, A.G., Cairns,
48 A.G., Corbett, A., MacArthur, D.G. *et al.* (2008) Limb-girdle muscular dystrophy: diagnostic
49 evaluation, frequency and clues to pathogenesis. *Neuromuscul Disord*, **18**, 34-44.
50 69 Brooke, M.H. and Kaiser, K.K. (1970) Muscle fiber types: how many and what kind? *Arch*
51 *Neurol*, **23**, 369-379.
52 70 Cooper, S.T., Lo, H.P. and North, K.N. (2003) Single section Western blot: improving the
53 molecular diagnosis of the muscular dystrophies. *Neurology*, **61**, 93-97.
54
55
56
57
58
59
60

- 1
2
3 71 Ilkovski, B., Nowak, K.J., Domazetovska, A., Maxwell, A.L., Clement, S., Davies, K.E., Laing,
4 N.G., North, K.N. and Cooper, S.T. (2004) Evidence for a dominant-negative effect in ACTA1 nemaline
5 myopathy caused by abnormal folding, aggregation and altered polymerization of mutant actin
6 isoforms. *Hum Mol Genet*, **13**, 1727-1743.
- 7 72 Akkari, P.A., Song, Y., Hitchcock-DeGregori, S., Blechynden, L. and Laing, N. (2002) Expression
8 and biological activity of Baculovirus generated wild-type human slow alpha tropomyosin and the
9 Met9Arg mutant responsible for a dominant form of nemaline myopathy. *Biochemical and
10 biophysical research communications*, **296**, 300-304.
- 11 73 Marttila, M., Lemola, E., Wallefeld, W., Memo, M., Donner, K., Laing, N.G., Marston, S.,
12 Gronholm, M. and Wallgren-Pettersson, C. (2012) Abnormal actin binding of aberrant beta-
13 tropomyosins is a molecular cause of muscle weakness in TPM2-related nemaline and cap
14 myopathy. *The Biochemical journal*, **442**, 231-239.
- 15 74 Bing, W., Fraser, I.D. and Marston, S.B. (1997) Troponin I and troponin T interact with
16 troponin C to produce different Ca²⁺-dependent effects on actin-tropomyosin filament motility.
17 *Biochem J*, **327 (Pt 2)**, 335-340.
- 18 75 Ottenheijm, C.A., Witt, C.C., Stienen, G.J., Labeit, S., Beggs, A.H. and Granzier, H. (2009) Thin
19 filament length dysregulation contributes to muscle weakness in nemaline myopathy patients with
20 nebulin deficiency. *Hum Mol Genet*, **18**, 2359-2369.
- 21 76 Manders, E., Bogaard, H.J., Handoko, M.L., van de Veerdonk, M.C., Keogh, A., Westerhof, N.,
22 Stienen, G.J., Dos Remedios, C.G., Humbert, M., Dorfmueller, P. *et al.* (2014) Contractile dysfunction
23 of left ventricular cardiomyocytes in patients with pulmonary arterial hypertension. *J Am Coll
24 Cardiol*, **64**, 28-37.
25
26
27
28
29
30
31
32
33
34
35
36
37
38
39
40
41
42
43
44
45
46
47
48
49
50
51
52
53
54
55
56
57
58
59
60

Figures:

Fig. 1: Dominant mutations in *TPM3* affect amino acids located within or close to actin binding domains

Tropomyosins form α -helical coiled-coil dimers via a seven residue repeat motive in their amino acid sequence [*a-b-c-d-e-f-g*] as illustrated in (A-B). Positions *a* and *d* (blue) are usually hydrophobic and create a hydrophobic pocket between two tropomyosin chains facilitating dimerisation in a “knobs-into-holes” fashion. Positions *g* and *e* (green) are occupied by charged amino acids that further stabilise the dimer through inter-helical salt bridges. Positions *b*, *c* and *f* (yellow) localise to the surface of the TM dimer and likely modulate interactions with protein binding partners such as actin and troponin. (C) A ribbon model of a whole tropomyosin dimer with the actin binding domains marked in pink on one strand. The residues affected by dominant mutations in *TPM3* are shown. All affected residues are located in or close to actin binding domains. Eight mutations affect residues in the *b*, *c* or *f* positions of the repeat (yellow). Three mutations affect residues in the *a* and *d* position (blue) and two affect residues in the *g* and *e* position (green). RCSB Protein Data Bank access code for protein structure model is 1C1G [tropomyosin dimer, Whitby and Phillips (23)]. Swiss-PDB Viewer v4.1.0 was used to create molecular graphics (66).

Fig. 2: *TPM3*-myopathy patients have slow fibre hypotrophy and a deregulation of slow and fast muscle fibre proportions

(A) ATPase pH 4.6 stained muscle cross section of one control and four patients with mutations at residue R168, of α -*TPM*_{slow} demonstrating a selective hypotrophy of slow type-1 myofibres. Fast type-2 fibres are between 1.7 and 5.2 times larger in size than type-1 fibres, whereas age-matched controls (age between 0.8 -57 y) showed roughly equally sized fibres (B). This corresponds to a fibre-size disproportion (FSD) between 41 % and 78.3 % (C). Patients with *TPM3* mutations show an abnormal fibre type distribution ranging from complete type-1 fibre predominance (A: Patient 10) to type-2 fibre predominance (A: Patient 8). (D) In the majority of control biopsies between 40-60 % of the CSA is composed of type-1 fibres. *TPM3*-myopathy patients have either below 40 % or above 60 % type-1 fibre area. Fibre type measurements were performed twice at different times from the same biopsy in Patients 2, 3c, 6b and 8 (also see Supplementary Tab. 2) and the plotted values represent the average of both measurements. All images were taken at 100x magnification. Fibre size

1
2
3 measurements and further information on patient and control biopsies are summarised in
4 Supplementary Tab. 2.
5
6
7

8
9 **Fig. 3: Tropomyosin isoform ratios are not commonly altered and mutant α -TPM_{slow} is**
10 **expressed in *TPM3*-myopathy patient muscle**

11 (Ai) A representative Western blot of *TPM3*-myopathy patient and control muscle tissue
12 showing the three skeletal muscle tropomyosin isoforms (β -TPM, α -TPM_{fast} and α -TPM_{slow}). In
13 normal muscle, type-1 fibres contain about 50:50 α -TPM_{slow}/ β -TPM and type-2 fibres contain
14 about 50:50 α -TPM_{fast}/ β -TPM. Most sample had β -TPM and α -TPM_{fast/slow} levels consistent
15 with the relative proportion of type-1 and type-2 fibres present in the sample (% type-1 fibre
16 area was determined from ATPase staining, see Supplementary Tab. 2). Only one patient
17 (*TPM3* M9R mutation, lane 5) had reduced β -TPM levels and increased expression of α -
18 TPM_{slow} relative to other tropomyosin isoforms and the fibre type proportion in the biopsy as
19 described previously (25). (Aii-iiiii) Densitometry analysis of Western blots from 10 patients
20 with mutations L100M (n=3), R168C (n=1), R168G (n=1), R168H (n=3), K169E (n=1),
21 R245G (n=1) was performed to quantify the proportion of each tropomyosin isoform as a
22 percentage of total TPM. The relative abundance of each isoform was plotted against the %
23 type-1 fibre area (measurements from *TPM3* M9R patient are not included). (Aii) β -TPM
24 levels are about 50 % of total tropomyosin in patients and controls. (Aiii-iiiii) About 50 % of
25 tropomyosin is α -TPM_{fast/slow}, but the amount of these fibre-type specific isoforms correlates
26 closely with the % type-1 fibre area in both patients and controls (positive correlation for α -
27 TPM_{slow}, negative correlation for α -TPM_{fast}). Linear regression analysis showed that slopes of
28 patient and controls were not significantly different for any of the three isoforms (p=0.4997,
29 0.9538 and 0.4595 for α -TPM_{slow}, α -TPM_{fast} and β -TPM, respectively). (B) Isoelectric
30 focusing of patient and control muscle lysates shows three spots (corresponding to β -TPM, α -
31 TPM_{fast}, α -TPM_{slow}). An additional spot (marked by an arrow) consistent with the predicted
32 isoelectric point (pI) of each mutation (as annotated, wild-type α -TPM_{slow} is 4.69) is present
33 in patient biopsies. Mutant α -TPM_{slow} accounted for 27-45% of total α -TPM_{slow} in different
34 patient biopsies (annotated in the blot, the proportion of each tropomyosin in patient slow
35 fibres is given in Supplementary Tab. 3). Note the ratio of expression of α -TPM_{fast/slow}
36 depends on the percentage of slow and fast myofibres in the biopsy (e.g. Patient 8 (R168C)
37 mainly contains fast myofibres). Picture 3 from the left in (B) is reprinted from Neuromuscul
38
39
40
41
42
43
44
45
46
47
48
49
50
51
52
53
54
55
56
57
58
59
60

Disord, 20/7 Waddell et al., Evidence for a dominant negative disease mechanism in cap myopathy due to TPM3, 464-466, Copyright (2010), with permission from Elsevier.

Fig. 4: Mutant α -TPM_{slow} R168C proteins has a reduced affinity to filamentous actin

Phalloidin stabilised actin filaments were co-sedimented with incremental amounts of tropomyosin and the pelleted fractions were analysed by SDS-PAGE. (A) A representative SDS-PAGE of wild-type α -TPM_{slow} protein as was used for densitometry analysis. (B) The ratio of TPM/actin was plotted vs. total [TPM] added and a Hill's equation was fitted. The K_d was increased in α -TPM_{slow} R168C compared to α -TPM_{slow} wild-type and K169E suggesting weaker binding affinity to actin (771.4 \pm 188.6 nM, 180.2 \pm 37.6 nM, 164.0 \pm 110.6 nM for α -TPM_{slow} R168C, wild-type and K169E, respectively). The Hill's coefficient h and maximal binding (Bmax) was similar in all three proteins (h = wild-type 4.471 \pm 3.0, R168C 3.308 \pm 2.4, K169E 1.602 \pm 1.3; Bmax wild-type 0.489 \pm 0.055, R168C 0.431 \pm 0.078 and K169E 0.443 \pm 0.156). Values are best-fit values \pm 95% confidence interval.

Fig. 5: TPM3 patients show increased phosphorylation of tropomyosin and ectopic expression of fast fibre specific α -actinin-3 in slow myofibres

(A) Consecutive sections were labelled with type-1 and type-2a MHC (blue and green, co-labelled respectively), type-2 MHC (red), α -actinin-3 (green) and troponin-T_{fast} (green) (the same fibre in multiple stains is indicated by a white arrow). Troponin-T_{fast} is only expressed in fast fibres as expected. Abnormal expression of α -actinin-3, a fast fibre specific Z-disc protein, was observed in type-1 myofibres of Patients 10, 4 and 6a (yellow stars). The biopsy of Patient 6b showed similar abnormalities but is not shown in this panel. Other patients had normal expression of α -actinin-3. Staining of Patient 1 and 8 are representative for these patients. (Bi) S283 is conserved and can be phosphorylated in all three sarcomeric tropomyosin proteins. (Bii) We assessed the level of S283 phosphorylation (pTPM) and total tropomyosin protein levels by duplicate Western blot and equal loading was confirmed by using sarcomeric actin (s Actin) (representative Western blot shown). The phosphorylation status of all three tropomyosin isoforms was determined by densitometry and normalised to the total tropomyosin levels. The graph shows phosphorylation levels normalised to the control average in (Biii) TPM3 patients and (Biiii) patients with congenital myopathies and muscular dystrophies due to mutations in TPM3, TPM2, ACTA1, DNM2, DMD and DYSF. Horizontal lines and error bars represent mean and standard deviation. Phosphorylation was commonly increased in both TPM3 patients and patients with other genetic causes of muscle

disease. Statistical analysis was only performed on patients with the R168H mutation due to insufficient data points for other groups. Phosphorylation was significantly higher in patients with the R168H mutation compared to controls ($*p < 0.05$, Mann-Whitney U test).

Fig. 6: The force generation at saturating $[Ca^{2+}]$ is decreased in *TPM3*-myopathy patients

Maximal force generation (F_{max}) measured at pCa 4.5 and sarcomere length of 2.5 μm , normalised to fibre CSA. **(A)** A typical force trace from a patient (Patient 6) and control type-1 fibre. Most *TPM3* patients showed a significant force deficit in type-1 myofibres **(C)** whereas type-2 fibres produced similar maximal force compared to controls **(B)**. In hybrid fibres and fibre bundles all patients had a slightly lower force average, however only Patient 1 showed a significant force deficit **(D)**. C_{slow} = Control type-1 fibres (pooled from eight biopsies aged: 11-54 y), C_{fast} = Control type-2 fibres (pooled from eight biopsies aged: 6-54 y), $C_{h/b}$ = Control hybrid fibres (contain a mix of type-1 and type-2 MHC, age 11-54 y) and small fibre bundles (bundles were taken from two biopsies of 0.9 y and 6 y old controls). $P =$ Patient. The black line in **(B-D)** indicates the average. $*** p < 0.0001$, $* p < 0.01$, one-way ANOVA.

Fig. 7: The force deficit in *TPM3*-myopathy patients is likely due to abnormal cross-bridge cycling

We assessed the rate of tension re-development (K_{tr}) **(A)** and active stiffness **(B)** in *TPM3*-myopathy patients to investigate if the force deficit in patient type-1 fibres was due to altered cross-bridge cycling. A typical K_{tr} trace of a patient (Patient 6) and a control are shown in **(Ai)**. The K_{tr} in single myofibres from *TPM3* patient biopsies and control biopsies are shown in **(Aii)** (type-1) and **(Aiii)** (type-2). Note that due to different MHC-ATPase properties the K_{tr} is physiologically higher in type-2 than in type-1 fibres. **(Aii)** The type-1 fibres of most *TPM3* patients showed a significant decrease in K_{tr} compared to control type-1 fibres (exceptions: Patient 1, 2 and 3a ($*** p < 0.0001$, $* p < 0.01$, one-way ANOVA) **(Aiii)** The type-2 fibres were not different to control type-2 fibres, with the exception of Patient 6 which showed a small decrease in K_{tr} . **(B)** Active stiffness was analysed by plotting the length changes (ΔL) against the force changes (ΔF) and fitting a linear regression to the data. A representative graph of type-1 fibres from Patient 4 and from controls is shown in **(Bi)**: absolute length change) and **(Bii)**: length change/ F_{max}). Graphs from other all other samples

are presented in Supplementary Fig. 6. Error bars represent standard deviation. **(Biii-v)** The slope of the linear regression was not significantly different from controls in all fibre-types in most patients with the exception of type-1 fibres or bundles/hybrid fibres of Patient 1, 2 and 7 where stiffness was reduced (* $p < 0.01$, ** $p < 0.001$, *** $p < 0.0001$, one-way ANOVA). However, a trend towards a small reduction was present in type-1 fibres and bundles/hybrid fibres of most patients **(Biii-iii)**. **(vi-vii)** When ΔF was normalised to F_{max} the slope was not significantly different from controls with the exception of P3c, which showed an increase in the slope (I, *** $p < 0.0001$, one-way ANOVA). Error bars represent standard deviation. C_{slow} and C_{fast} = Control type-1 and type-2 fibres (pooled from eight biopsies aged: 11 - 54 y), $C_{h/b}$ = Control hybrid fibres (contain a mix of type-1 and type-2 MHC, age 6 - 54 y) and small fibre bundles (bundles were taken from two biopsies of 0.9 y and 6 y old controls). The black line in all scatter plots indicates the average.

Fig. 8: Ca^{2+} -sensitivity is decreased in *TPM3*-myopathy patients resulting in reduced specific force generation at physiological $[Ca^{2+}]$

(A) Specific force generation at incremental $[Ca^{2+}]$ in skinned type-1 fibres **(i)**, hybrid fibres or bundles **(ii)** and type-2 fibres **(C)** shown as percent of F_{max} fitted to a variable slope log (dose) response curve. Note the rightward shift of the force/pCa curve in type-1 fibres, hybrid fibres/bundles in *TPM3* patients, whereas type-2 fibres were not different to controls. The dotted lines indicate the pCa50 ($[Ca^{2+}]$ required to achieve 50 % of maximal force) and the yellow area indicates physiological cytoplasmic $[Ca^{2+}]$ during muscle contraction (between 1 - 5 μM) **(B)** The pCa 50 was significantly higher in type-1 fibres, hybrid fibres/ bundles of *TPM3* patients compared to controls and type-2 fibres of *TPM3* patients. **(C)** Specific force generation measured at pCa 6.0 (1 μM , physiological calcium). The force was significantly lower in **(i)** type-1 fibres and **(ii)** hybrid fibres/bundles of all *TPM3* patients, but was not different from controls in **(iii)** type-2 fibres. C_{slow} and C_{fast} = Control type-1 and type-2 fibres (pooled from eight biopsies aged: 11-54 y), $C_{h/b}$ = Control hybrid fibres (contain a mix of type-1 and type-2 MHC, age 6-54 y) and small fibre bundles (bundles were taken from two biopsies of 0.9 y and 6 y old controls). The black line in the scatter plot indicates the average and error bars in force/pCa curves are standard deviations. *** $p < 0.0001$, * $p < 0.01$, one-way ANOVA. P=Patient, C= control.

Table 1: Patient cohort with dominant TPM3 mutations

P	Mutation in <i>TPM3</i>	Disease	Muscle type	Sex	Age at biopsy	Clinical classification	Publication	Contractile studies
1	K169E	CFTD	Q	M	16 m	moderate	(1): P 2	Y
2	R245G	CFTD	Q	M	20 m	moderate	(1): P 1	Y
3a	L100M	CFTD	Q	F	3 y	mild	(1): P 5	Y
3b	L100M	CFTD	B	M	30 y	mild	(1): P 7	Y
3c	L100M	CFTD	B	M	36 y	mild	(1): P 8	Y
4	R168G	CFTD	Q	M	10 y	mild	(1): P 3	Y
5	R168H	CFTD	Q	F	40 y	mild	unpublished	Y
6a	R168H	NM	D	F	20 y	mild	(1): P 10	N
6b	R168H	CFTD	?	M	56 y	mild	(1): P 11	Y
7	R168C	Cap	?	M	3 y	mild	(14): P 1	Y
8	R168C	CFTD	Q	F	19 y	moderate	(1): P 9	Y
9	M9R	NM	Q	F	21 y	mild	(8); (37): P 1	N
10	R168H	NM	D	M	53 y	mild	(13): P III-4	N
11	E241K	CFTD	Q	F	0.5y	moderate	(2): P 311-1	N
12	R91P	CFTD	Q	F	0.5y	severe	(2): P 913-1	N

Q=Quadriceps, B = Biceps, D = Deltoid, P = Patient

Abbreviations

α -tropomyosin _{slow}	α -TPM _{slow}
α -tropomyosin _{fast}	α -TPM _{fast}
bovine serum albumin	BSA
β -tropomyosin	β -TPM
congenital fibre-type disproportion	CFTD
cross sectional area	CSA
immunohistochemistry	IHC
$-\log$ of molar free $[Ca^{2+}]$	pCa
maximal isometric contraction	Fmax
myosin heavy chain	MHC
percentage fibre-size disproportion	% FSD
phosphate buffered saline	PBS
two-dimensional SDS polyacrylamide gel electrophoresis	2D-SDS-PAGE

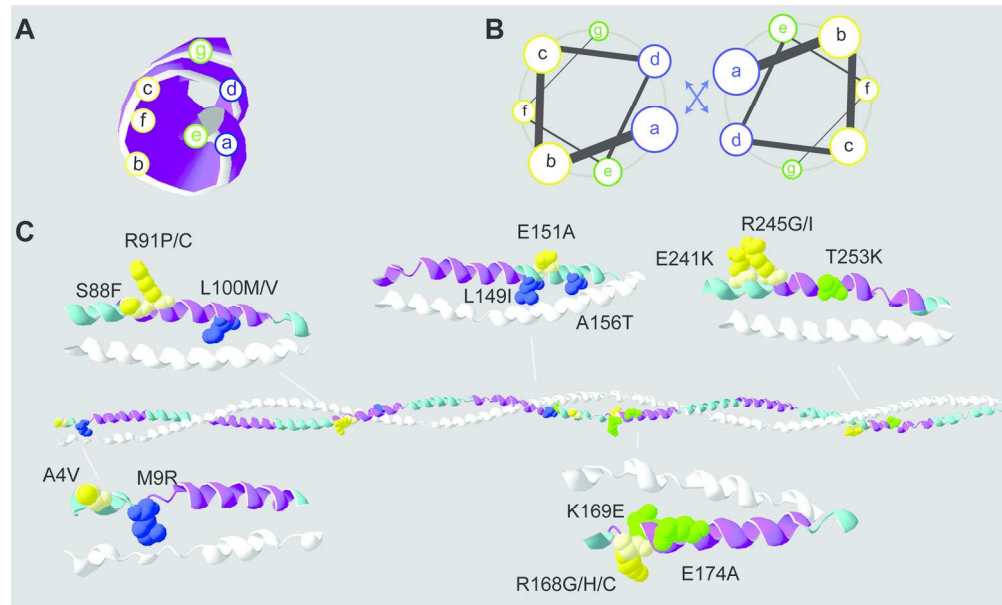


Fig. 1: Dominant mutations in TPM3 affect amino acids located within or close to actin binding domains
 Tropomyosins form α -helical coiled-coil dimers via a seven residue repeat motive in their amino acid sequence [a-b-c-d-e-f-g] as illustrated in (A-B). Positions a and d (blue) are usually hydrophobic and create a hydrophobic pocket between two tropomyosin chains facilitating dimerisation in a “knobs-into-holes” fashion. Positions g and e (green) are occupied by charged amino acids that further stabilise the dimer through inter-helical salt bridges. Positions b, c and f (yellow) localise to the surface of the TM dimer and likely modulate interactions with protein binding partners such as actin and troponin. (C) A ribbon model of a whole tropomyosin dimer with the actin binding domains marked in pink on one strand. The residues affected by dominant mutations in TPM3 are shown. All affected residues are located in or close to actin binding domains. Eight mutations affect residues in the b, c or f positions of the repeat (yellow). Three mutations affect residues in the a and d position (blue) and two affect residues in the g and e position (green). RCSB Protein Data Bank access code for protein structure model is 1C1G [tropomyosin dimer, Whitby and Phillips (23)]. Swiss-PDB Viewer v4.1.0 was used to create molecular graphics (66).
 177x107mm (300 x 300 DPI)

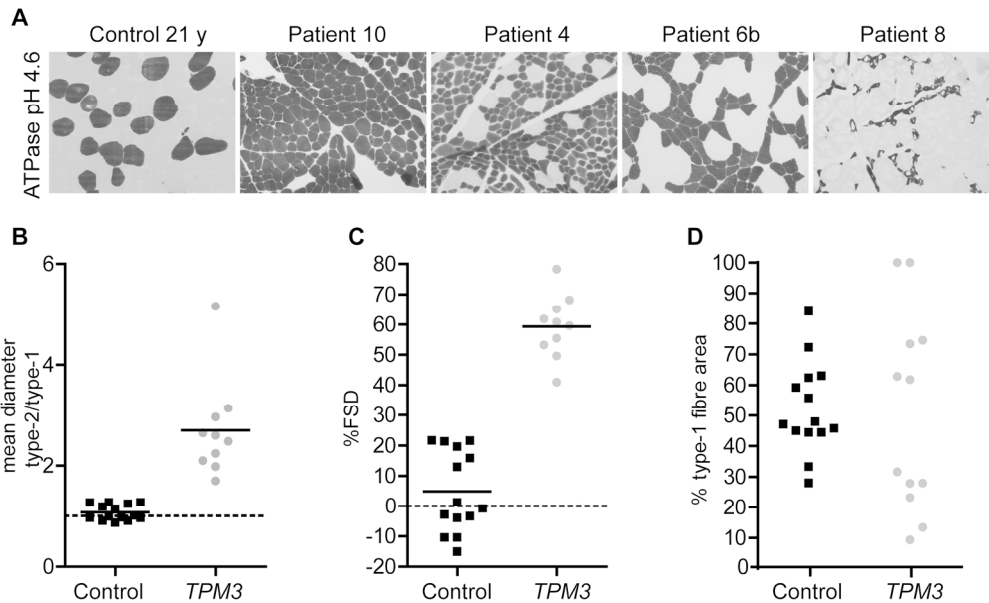


Fig. 2: TPM3-myopathy patients have slow fibre hypotrophy and a deregulation of slow and fast muscle fibre proportions

(A) ATPase pH 4.6 stained muscle cross section of one control and four patients with mutations at residue R168, of α -TPMslow demonstrating a selective hypotrophy of slow type-1 myofibres. Fast type-2 fibres are between 1.7 and 5.2 times larger in size than type-1 fibres, whereas age-matched controls (age between 0.8 -57 y) showed roughly equally sized fibres (B). This corresponds to a fibre-size disproportion (FSD) between 41 % and 78.3 % (C). Patients with TPM3 mutations show an abnormal fibre type distribution ranging from complete type-1 fibre predominance (A: Patient 10) to type-2 fibre predominance (A: Patient 8). (D) In the majority of control biopsies between 40-60 % of the CSA is composed of type-1 fibres. TPM3-myopathy patients have either below 40 % or above 60 % type-1 fibre area. Fibre type measurements were performed twice at different times from the same biopsy in Patients 2, 3c, 6b and 8 (also see Supplementary Tab. 2) and the plotted values represent the average of both measurements. All images were taken at 100x magnification. Fibre size measurements and further information on patient and control biopsies are summarised in Supplementary Tab. 2.

177x106mm (300 x 300 DPI)

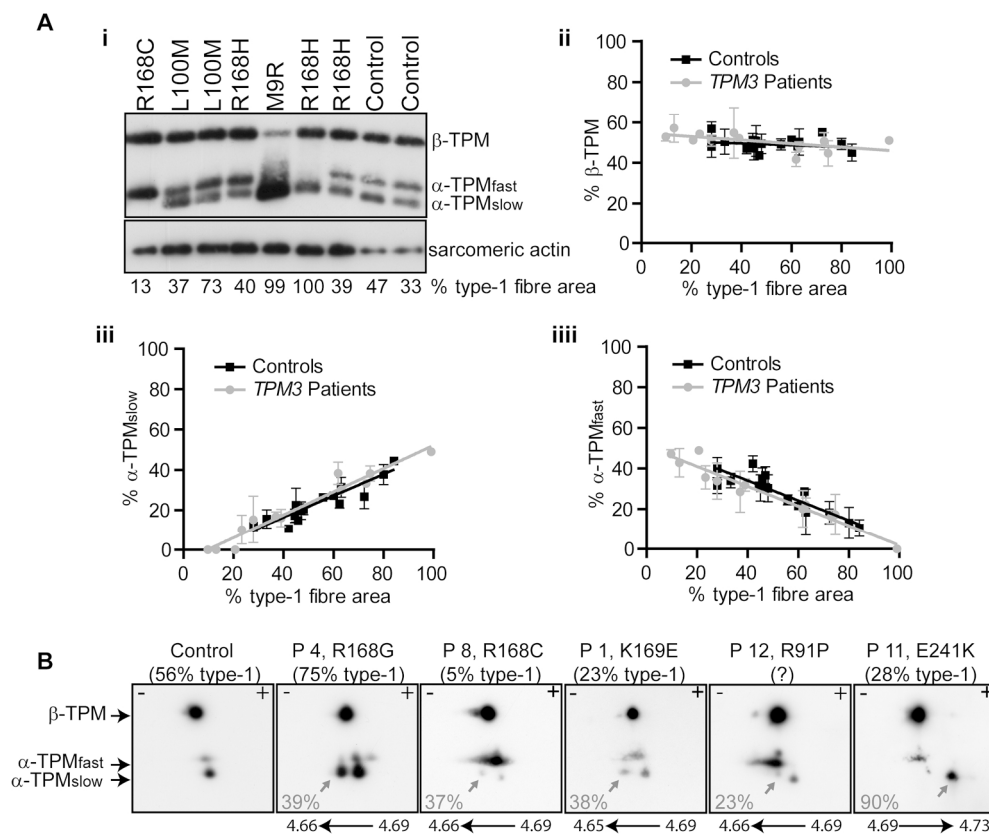


Fig. 3: Tropomyosin isoform ratios are not commonly altered and mutant α -TPMslow is expressed in TPM3-miopathy patient muscle

(Ai) A representative Western blot of TPM3-miopathy patient and control muscle tissue showing the three skeletal muscle tropomyosin isoforms (β -TPM, α -TPMfast and α -TPMslow). In normal muscle, type-1 fibres contain about 50:50 α -TPMslow/ β -TPM and type-2 fibres contain about 50:50 α -TPMfast/ β -TPM. Most sample had β -TPM and α -TPMfast/slow levels consistent with the relative proportion of type-1 and type-2 fibres present in the sample (% type-1 fibre area was determined from ATPase staining, see Supplementary Tab. 2). Only one patient (TPM3 M9R mutation, lane 5) had reduced β -TPM levels and increased expression of α -TPMslow relative to other tropomyosin isoforms and the fibre type proportion in the biopsy as described previously (25). (Aii-iiii) Densitometry analysis of Western blots from 10 patients with mutations L100M (n=3), R168C (n=1), R168G (n=1), R168H (n=3), K169E (n=1), R245G (n=1) was performed to quantify the proportion of each tropomyosin isoform as a percentage of total TPM. The relative abundance of each isoform was plotted against the % type-1 fibre area (measurements from TPM3 M9R patient are not included). (Aii) β -TPM levels are about 50 % of total tropomyosin in patients and controls. (Aiii-iiii) About 50 % of tropomyosin is α -TPMfast/slow, but the amount of these fibre-type specific isoforms correlates closely with the % type-1 fibre area in both patients and controls (positive correlation for α -TPMslow, negative correlation for α -TPMfast). Linear regression analysis showed that slopes of patient and controls were not significantly different for any of the three isoforms ($p=0.4997$, 0.9538 and 0.4595 for α -TPMslow, α -TPMfast and β -TPM, respectively). (B) Isoelectric focusing of patient and control muscle lysates shows three spots (corresponding to β -TPM, α -TPMfast, α -TPMslow). An additional spot (marked by an arrow) consistent with the predicted isoelectric point (pI) of each mutation (as annotated, wild-type α -TPMslow is 4.69) is present in patient biopsies. Mutant α -TPMslow accounted for 27-45% of total α -TPMslow in different patient biopsies (annotated in the blot, the proportion of each tropomyosin in patient slow fibres is given in Supplementary Tab. 3). Note the ratio of expression of α -TPMfast/slow depends on the percentage of slow and fast myofibres in the biopsy (e.g. Patient 8 (R168C) mainly contains fast myofibres). Picture 3 from the left in (B) is reprinted from *Neuromuscul Disord*, 20/7 Waddell et al., Evidence for a dominant negative disease

1
2
3
4
5
6
7
8
9
10
11
12
13
14
15
16
17
18
19
20
21
22
23
24
25
26
27
28
29
30
31
32
33
34
35
36
37
38
39
40
41
42
43
44
45
46
47
48
49
50
51
52
53
54
55
56
57
58
59
60

mechanism in cap myopathy due to TPM3, 464-466, Copyright (2010), with permission from Elsevier.

180x150mm (300 x 300 DPI)

For Peer Review

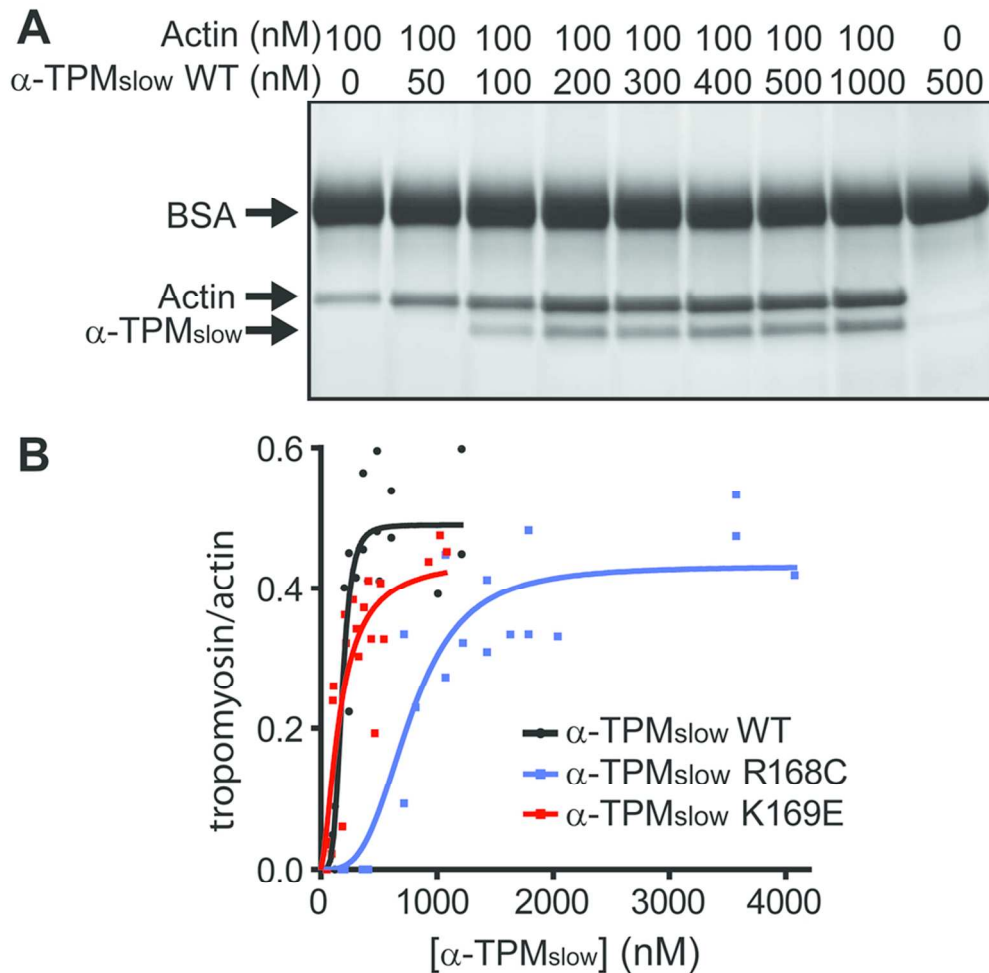


Fig. 4: Mutant α -TPM_{slow} R168C proteins has a reduced affinity to filamentous actin
Phalloidin stabilised actin filaments were co-sedimented with incremental amounts of tropomyosin and the pelleted fractions were analysed by SDS-PAGE. (A) A representative SDS-PAGE of wild-type α -TPM_{slow} protein as was used for densitometry analysis. (B) The ratio of TPM/actin was plotted vs. total [TPM] added and a Hill's equation was fitted. The K_d was increased in α -TPM_{slow} R168C compared to α -TPM_{slow} wild-type and K169E suggesting weaker binding affinity to actin (771.4 ± 188.6 nM, 180.2 ± 37.6 nM, 164.0 ± 110.6 nM for α -TPM_{slow} R168C, wild-type and K169E, respectively). The Hill's coefficient h and maximal binding (B_{max}) was similar in all three proteins (h = wild-type 4.471 ± 3.0 , R168C 3.308 ± 2.4 , K169E 1.602 ± 1.3 ; B_{max} wild-type 0.489 ± 0.055 , R168C 0.431 ± 0.078 and K169E 0.443 ± 0.156). Values are best-fit values \pm 95% confidence interval.
90x87mm (300 x 300 DPI)

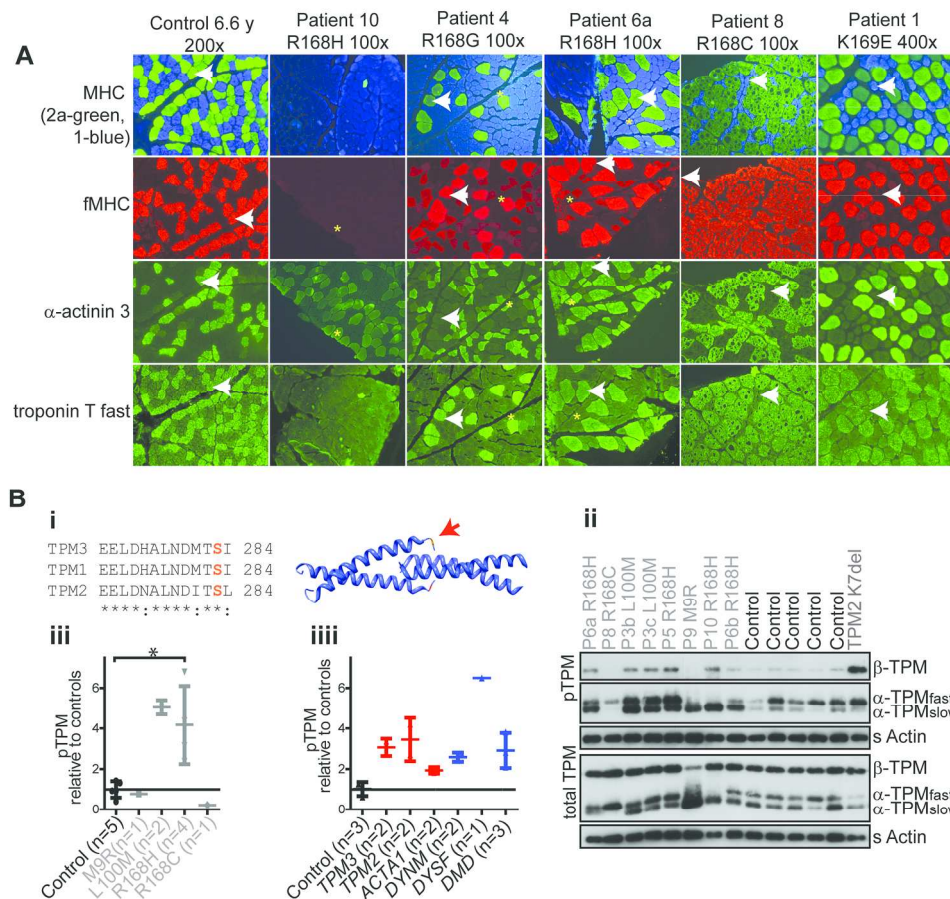


Fig. 5: TPM3 patients show increased phosphorylation of tropomyosin and ectopic expression of fast fibre specific α -actinin-3 in slow myofibres

(A) Consecutive sections were labelled with type-1 and type-2a MHC (blue and green, co-labelled respectively), type-2 MHC (red), α -actinin-3 (green) and troponin-Tfast (green) (the same fibre in multiple stains is indicated by a white arrow). Troponin-Tfast is only expressed in fast fibres as expected. Abnormal expression of α -actinin-3, a fast fibre specific Z-disc protein, was observed in type-1 myofibres of Patients 10, 4 and 6a (yellow stars). The biopsy of Patient 6b showed similar abnormalities but is not shown in this panel. Other patients had normal expression of α -actinin-3. Staining of Patient 1 and 8 are representative for these patients. (Bi) S283 is conserved and can be phosphorylated in all three sarcomeric tropomyosin proteins. (Bii) We assessed the level of S283 phosphorylation (pTPM) and total tropomyosin protein levels by duplicate Western blot and equal loading was confirmed by using sarcomeric actin (s Actin) (representative Western blot shown). The phosphorylation status of all three tropomyosin isoforms was determined by densitometry and normalised to the total tropomyosin levels. The graph shows phosphorylation levels normalised to the control average in (Biii) TPM3 patients and (Biiii) patients with congenital myopathies and muscular dystrophies due to mutations in TPM3, TPM2, ACTA1, DNM2, DMD and DYSF. Horizontal lines and error bars represent mean and standard deviation. Phosphorylation was commonly increased in both TPM3 patients and patients with other genetic causes of muscle disease. Statistical analysis was only performed on patients with the R168H mutation due to insufficient data points for other groups. Phosphorylation was significantly higher in patients with the R168H mutation compared to controls (* $p < 0.05$, Mann-Whitney U test).

192x180mm (300 x 300 DPI)

1
2
3
4
5
6
7
8
9
10
11
12
13
14
15
16
17
18
19
20
21
22
23
24
25
26
27
28
29
30
31
32
33
34
35
36
37
38
39
40
41
42
43
44
45
46
47
48
49
50
51
52
53
54
55
56
57
58
59
60

For Peer Review

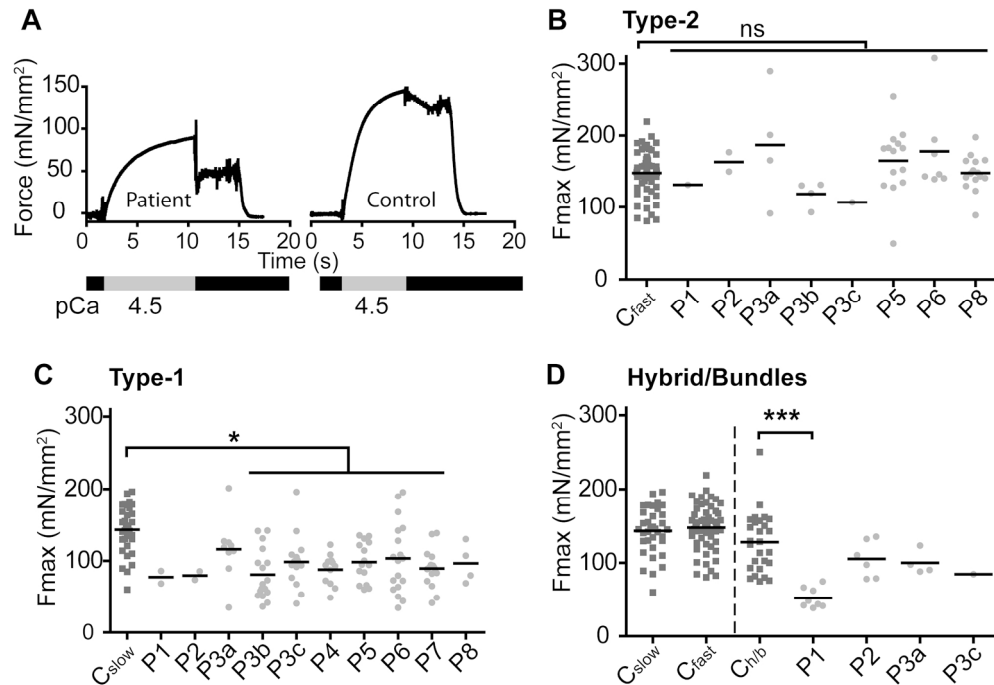


Fig. 6: The force generation at saturating [Ca²⁺] is decreased in TPM3-myopathy patients. Maximal force generation (F_{max}) measured at pCa 4.5 and sarcomere length of 2.5 μm, normalised to fibre CSA. (A) A typical force trace from a patient (Patient 6) and control type-1 fibre. Most TPM3 patients showed a significant force deficit in type-1 myofibres (C) whereas type-2 fibres produced similar maximal force compared to controls (B). In hybrid fibres and fibre bundles all patients had a slightly lower force average, however only Patient 1 showed a significant force deficit (D). C_{slow} = Control type-1 fibres (pooled from eight biopsies aged: 11-54 y), C_{fast} = Control type-2 fibres (pooled from eight biopsies aged: 6-54 y), C_{h/b} = Control hybrid fibres (contain a mix of type-1 and type-2 MHC, age 11-54 y) and small fibre bundles (bundles were taken from two biopsies of 0.9 y and 6 y old controls). P = Patient. The black line in (B-D) indicates the average. *** p < 0.0001, * p < 0.01, one-way ANOVA.

172x118mm (300 x 300 DPI)

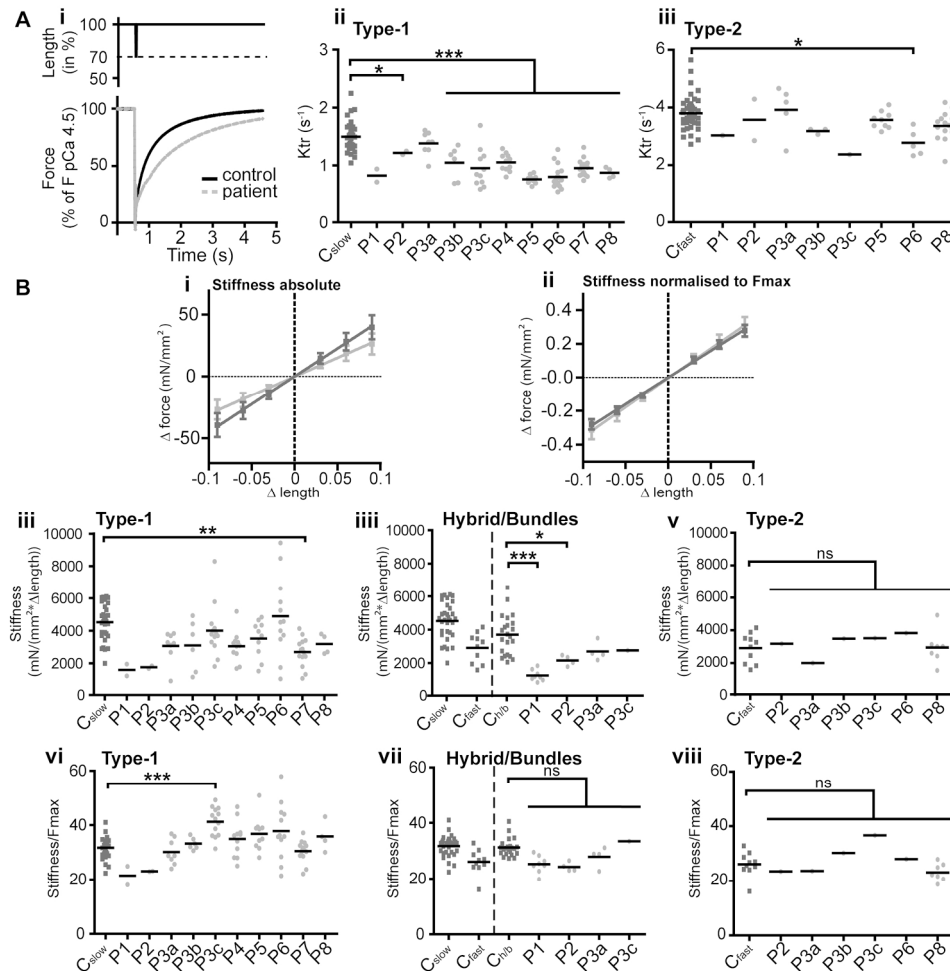


Fig. 7: The force deficit in TPM3-myopathy patients is likely due to abnormal cross-bridge cycling

We assessed the rate of tension re-development (Ktr) (A) and active stiffness (B) in TPM3-myopathy patients to investigate if the force deficit in patient type-1 fibres was due to altered cross-bridge cycling. A typical Ktr trace of a patient (Patient 6) and a control are shown in (Ai). The Ktr in single myofibres from TPM3 patient biopsies and control biopsies are shown in (Aii) (type-1) and (Aiii) (type-2). Note that due to different MHC-ATPase properties the Ktr is physiologically higher in type-2 than in type-1 fibres. (Aii) The type-1 fibres of most TPM3 patients showed a significant decrease in Ktr compared to control type-1 fibres (exceptions: Patient 1, 2 and 3a (***) $p < 0.0001$, * $p < 0.01$, one-way ANOVA) (Aiii) The type-2 fibres were not different to control type-2 fibres, with the exception of Patient 6 which showed a small decrease in Ktr. (B) Active stiffness was analysed by plotting the length changes (ΔL) against the force changes (ΔF) and fitting a linear regression to the data. A representative graph of type-1 fibres from Patient 4 and from controls is shown in (Bi: absolute length change) and (Bii: length change/ F_{max}). Graphs from other all other samples are presented in Supplementary Fig. 6. Error bars represent standard deviation. (Bii-v) The slope of the linear regression was not significantly different from controls in all fibre-types in most patients with the exception of type-1 fibres or bundles/hybrid fibres of Patient 1, 2 and 7 where stiffness was reduced (* $p < 0.01$, ** $p < 0.001$, *** $p < 0.0001$, one-way ANOVA). However, a trend towards a small reduction was present in type-1 fibres and bundles/hybrid fibres of most patients (Biii-iii). (vi-vii) When ΔF was normalised to F_{max} the slope was not significantly different from controls with the exception of P3c, which showed an increase in the slope (I, *** $p < 0.0001$, one-way ANOVA). Error bars represent standard deviation. C_{slow} and C_{fast} = Control type-1 and type-2 fibres (pooled from eight biopsies aged: 11 - 54 y), Ch/b = Control hybrid fibres (contain a mix of type-1 and type-2 MHC, age 6 - 54 y) and small fibre bundles (bundles were taken from two biopsies of 0.9 y and 6 y old controls). The black line in all scatter plots indicates the

1
2
3
4
5
6
7
8
9
10
11
12
13
14
15
16
17
18
19
20
21
22
23
24
25
26
27
28
29
30
31
32
33
34
35
36
37
38
39
40
41
42
43
44
45
46
47
48
49
50
51
52
53
54
55
56
57
58
59
60

average.
191x186mm (300 x 300 DPI)

For Peer Review

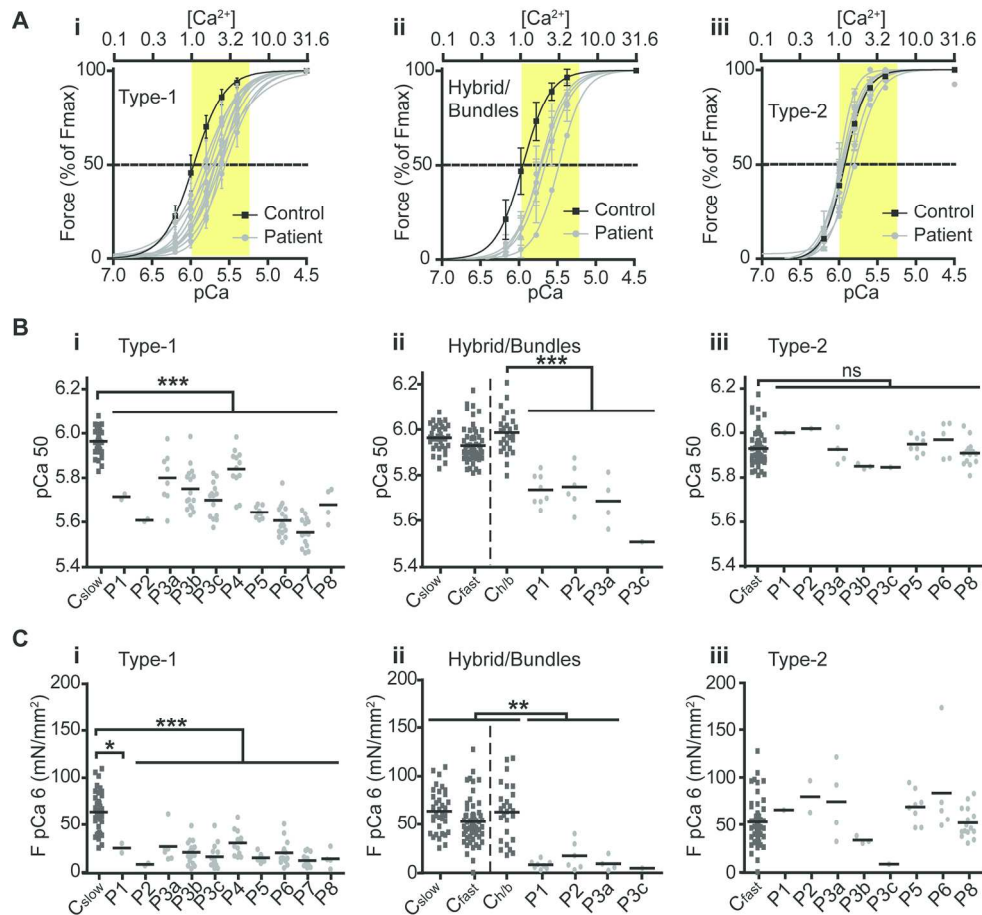


Fig. 8: Ca²⁺-sensitivity is decreased in TPM3-myopathy patients resulting in reduced specific force generation at physiological [Ca²⁺]

(A) Specific force generation at incremental [Ca²⁺] in skinned type-1 fibres (i), hybrid fibres or bundles (ii) and type-2 fibres (C) shown as percent of Fmax fitted to a variable slope log (dose) response curve. Note the rightward shift of the force/pCa curve in type-1 fibres, hybrid fibres/bundles in TPM3 patients, whereas type-2 fibres were not different to controls. The dotted lines indicate the pCa 50 ([Ca²⁺] required to achieve 50 % of maximal force) and the yellow area indicates physiological cytoplasmic [Ca²⁺] during muscle contraction (between 1 - 5 μM) (B) The pCa 50 was significantly higher in type-1 fibres, hybrid fibres/bundles of TPM3 patients compared to controls and type-2 fibres of TPM3 patients. (C) Specific force generation measured at pCa 6.0 (1 μM, physiological calcium). The force was significantly lower in (i) type-1 fibres and (ii) hybrid fibres/bundles of all TPM3 patients, but was not different from controls in (iii) type-2 fibres. Cslow and Cfast = Control type-1 and type-2 fibres (pooled from eight biopsies aged: 11-54 y), Ch/b = Control hybrid fibres (contain a mix of type-1 and type-2 MHC, age 6-54 y) and small fibre bundles (bundles were taken from two biopsies of 0.9 y and 6 y old controls). The black line in the scatter plot indicates the average and error bars in force/pCa curves are standard deviations. *** p<0.0001, * p<0.01, one-way ANOVA. P=Patient, C= control.

180x165mm (300 x 300 DPI)

1
2
3 **Muscle weakness in *TPM3*-myopathy is due to reduced Ca²⁺-sensitivity and**
4 **impaired acto-myosin cross-bridge cycling in slow fibres.**
5
6
7

8
9 Michaela Yuen^{1,2*}, Sandra T. Cooper^{1,2}, Steve B. Marston³, Kristen J. Nowak⁴, Elyshia
10 McNamara⁴, Nancy Mokbel^{1,5}, Biljana Ilkovski¹, Gianina Ravenscroft⁴, John Rendu⁶, Josine
11 M. de Winter⁷, Lars Klinge⁸, Alan H. Beggs⁹, Kathryn N. North^{1, 2, 10,11}, Coen A. C.
12 Ottenheijm⁷⁺, Nigel F. Clarke^{1,2+}
13
14
15
16
17

- 18
19 1. Institute for Neuroscience and Muscle Research, The Children's Hospital at Westmead,
20 Westmead, Australia
21
22 2. Discipline of Paediatrics and Child Health, University of Sydney, Sydney, Australia
23
24 3. National Heart and Lung Institute, Imperial College London, London, UK
25
26 4. Harry Perkins Institute of Medical Research and the Centre for Medical Research,
27 University of Western Australia, Nedlands, Australia
28
29 5. Faculty of Health Sciences, St.George Health Complex, The University of Balamand,
30 Beirut, Lebanon
31
32 6. Département de Biochimie Toxicologie et Pharmacologie, Département de Biochimie
33 Génétique et Moléculaire, Centre Hospitalier Universitaire de Grenoble, Grenoble, France
34
35 7. Department of Physiology, Institute for Cardiovascular Research, VU University Medical
36 Center, Amsterdam, The Netherlands
37
38 8. Department of Pediatrics and Adolescent Medicine, Division of Pediatric Neurology,
39 Faculty of Medicine, Georg August University, Göttingen, Germany
40
41 9. Division of Genetics and Genomics, The Manton Center for Orphan Disease Research,
42 Boston Children's Hospital, Harvard Medical School, Boston, USA
43
44 10. Murdoch Children's Research Institute, the Royal Children's Hospital, Parkville, Australia
45
46 11. Department of Paediatrics, University of Melbourne, Melbourne, Australia
47
48
49
50
51
52
53
54
55
56
57
58
59
60

1
2
3 † The authors wish it to be known that, in their opinion, the last two authors should be
4
5 regarded as joint last authors
6
7

8 **Correspondence to**

9
10 Michaela Yuen, Institute for Neuroscience and Muscle Research, The Children's Hospital at
11
12 Westmead, Locked Bag 4001, Westmead, NSW 2145, Australia,
13
14 email: michaela.kreissl@sydney.edu.au, phone: +61 2 9845 1495, fax: +61 2 9845 3489
15
16
17
18
19
20
21
22
23
24
25
26
27
28
29
30
31
32
33
34
35
36
37
38
39
40
41
42
43
44
45
46
47
48
49
50
51
52
53
54
55
56
57
58
59
60

For Peer Review

Abstract

Dominant mutations in *TPM3*, encoding α -tropomyosin_{slow}, cause a congenital myopathy characterised by generalised muscle weakness. Here, we used a multidisciplinary approach to investigate the mechanism of muscle dysfunction in twelve *TPM3*-myopathy patients.

We confirm that slow myofibre hypotrophy is a diagnostic hallmark of *TPM3*-myopathy, and is commonly accompanied by skewing of fibre-type ratios (either slow or fast fibre predominance). Patient muscle contained normal ratios of the three tropomyosin isoforms and normal fibre-type expression of myosins and troponins. Using 2D-PAGE, we demonstrate that mutant α -tropomyosin_{slow} was expressed, suggesting muscle dysfunction is due to a dominant-negative effect of mutant protein on muscle contraction. Molecular modelling suggested mutant α -tropomyosin_{slow} likely impacts actin-tropomyosin interactions and, indeed, co-sedimentation assays showed reduced binding of mutant α -tropomyosin_{slow} (R168C) to filamentous actin.

Single fibre contractility studies of patient myofibres revealed marked slow myofibre specific abnormalities. At saturating $[Ca^{2+}]$ (pCa 4.5), patient slow fibres produced only 63% of the contractile force produced in control slow fibres and had reduced acto-myosin cross-bridge cycling kinetics. Importantly, due to reduced Ca^{2+} -sensitivity, at sub-saturating $[Ca^{2+}]$ (pCa 6, levels typically released during in vivo contraction) patient slow fibres produced only 26% of the force generated by control slow fibres.

Thus, weakness in *TPM3*-myopathy patients can be directly attributed to reduced slow fibre force at physiological $[Ca^{2+}]$, and impaired acto-myosin cross-bridge cycling kinetics. Fast myofibres are spared; however, they appear to be unable to compensate for slow fibre dysfunction. Abnormal Ca^{2+} -sensitivity in *TPM3*-myopathy patients suggests Ca^{2+} -sensitising drugs may represent a useful treatment for this condition.

Introduction

Dominant mutations in the *TPM3* gene, encoding α -tropomyosin_{slow} (α -TPM_{slow}), cause a congenital myopathy characterised by mild to moderate early onset, non-progressive generalised muscle weakness (1-3). Axial and respiratory muscles are commonly involved and many patients require night-time ventilatory support (1, 2). Recessive mutations, causing loss of protein, are rare with only four instances reported to date in patients with relatively severe clinical presentations (4-7). In contrast, more than 40 families with dominant *TPM3* missense mutations have been identified involving 19 different residues (1, 3, 7-13), Supplementary Tab. 1). Histologically, many *TPM3* patients present with slow skeletal myofibre hypotrophy in the absence of additional pathological features, resulting in a clinical diagnosis of congenital fibre-type disproportion (CFTD) (3). Some patients also exhibit nemaline bodies or cores in myofibres and are classified as nemaline myopathy (8) or core myopathy (1, 11, 14), respectively. The same mutation in *TPM3* can cause a variety of histological phenotypes (Supplementary Tab. 1) (1, 3, 7, 14).

Three tropomyosin isoforms are present in the skeletal muscle sarcomere (15). *TPM1* and *TPM3* encode the two α -tropomyosins expressed exclusively in fast fibres (*TPM1*; α -TPM_{fast}, Tpm1.st) or slow fibres (*TPM3*; α -TPM_{slow}, Tpm3.12st), respectively. *TPM2* encodes β -tropomyosin (β -TPM, Tpm2.2st) and is expressed in both fibre types (15-17). Tropomyosin forms alpha-helical coiled-coil heterodimers between one α - and one β -chain. These dimers polymerise head-to-tail into a continuous filament that associates along the entire length of the actin thin filament and interacts with the troponin complex to regulate Ca²⁺-mediated actin-myosin cross-bridge cycling during muscle contraction. The structure of tropomyosin is conferred by a seven residue repeat motive [*a-b-c-d-e-f-g*] (Fig. 1A and B) (18). Residues at positions *a* and *d* in the repeat are typically hydrophobic, creating a hydrophobic pocket

1
2
3 between two tropomyosin chains facilitating dimerisation (blue). Charged residues at
4
5 positions *g* and *e* (green) stabilise the dimer through inter-helical salt bridges. Positions *b*, *c*
6
7 and *f* (yellow) localise to the surface of tropomyosin dimers and likely modulate interactions
8
9 with proteins such as actin and troponin.
10

11
12
13
14 Many dominant *TPM3* mutations (11/19) affect positions *b*, *c* or *f* on the outer surface of the
15
16 dimer (Fig. 1C, yellow). Only five mutations affect positions *a* and *d* in the hydrophobic
17
18 pocket (Fig. 1C, blue) and three mutations affect positions *g* and *e* constituting the inter-
19
20 helical salt bridges (Fig. 1C, green). All mutations fall within, or very close to, one of the
21
22 seven actin binding regions of tropomyosin (Fig. 1C, purple shaded area of the molecule)
23
24 (19). In particular, there is a striking concentration of mutations within the fifth actin-binding
25
26 region of α -TPM_{slow} (R168H, R168G, R168C, K169E, E174A) some of which are recurrent
27
28 in several unrelated families (e.g. R168 residue is mutated in 20 different families).
29
30
31

32
33 Although the structure and function of tropomyosin is well established, the mechanism(s) by
34
35 which mutations in *TPM3* cause muscle weakness remains poorly understood. Two recent
36
37 studies showed that four patients with dominant *TPM3* mutations had abnormal cross-bridge
38
39 cycling kinetics and Ca²⁺-sensitivity of contraction in single skeletal myofibres isolated from
40
41 patient biopsies [n=3 (20), n=1 (21)]. However, these studies were limited by small sample
42
43 sizes, and separate assessment of the properties of slow versus fast myofibres was only
44
45 possible to a limited extent. In this study, we aimed to unravel the mechanism of muscle
46
47 weakness in a cohort of 12 patients with dominant *TPM3* mutations. We performed thorough
48
49 histological characterisation, assessed thin filament protein expression and quantified the
50
51 contractile properties of single myofibres isolated from patient muscle specimens (10/12
52
53 patients, Tab. 1).
54
55
56
57
58
59
60

Results

TPM3-myopathy patients have slow fibre hypotrophy and deregulation of slow and fast muscle fibre proportions

The main histological characteristic in all patients with *TPM3* mutations is selective hypotrophy of slow-twitch type-1 fibres, compared to fast-twitch type-2 fibres (1, 3, 7) (Fig. 2A, ATPase pH 4.6, slow myofibres appear dark; see Supplementary Tab. 2 for measurements). On average, fast fibres were between 1.7 and 5.2 times larger in diameter than slow fibres (Fig. 2B), corresponding to a %FSD of 41 % - 78.3 % (Fig. 2C). The selective hypotrophy of slow fibres in *TPM3* patients is consistent with the slow-fibre specific expression of α -TPM_{slow}.

Additionally, fibre-typing was skewed in patient biopsies, either towards fast fibre predominance (five patients, less than 30 % slow fibre area) or slow fibre predominance (six patients, more than 60 % slow fibre area), compared to age-matched control biopsies where the CSA occupied by either fibre-type is approximately 50:50 [this study and (22, 23)] (Fig. 2D). Only one patient biopsy showed normal slow-fast fibre distribution (between 40-60 % slow fibre area).

Tropomyosin isoform ratios are not commonly altered in TPM3-myopathy patients

In normal muscle, the ratio of α/β tropomyosin molecules is approximately 50:50 β -TPM/ α -TPM_{fast} in fast fibres and 50:50 β -TPM/ α -TPM_{slow} in slow fibres (24). A patient and transgenic mouse model carrying the *TPM3* M9R mutation, the first mutation associated with nemaline myopathy, showed an imbalance of this ratio, with a dramatic excess of α -TPM_{slow} relative to β -TPM in skeletal muscle (25) (Fig. 3Ai, Lane 5). This disruption in tropomyosin stoichiometry was proposed as a potential mechanism of muscle weakness (25). In contrast, in this cohort of 12 *TPM3*-myopathy patients, we observed normal ratios of α/β tropomyosin,

1
2
3 similar to controls (Fig. 3Ai). The scatter plots in Fig. 3Aii-iiii show the relative levels of
4
5 each tropomyosin isoform relative to the type-1 fibre CSA, as determined by ATPase
6
7 staining. β -TPM is present at equal amounts in slow and fast myofibres in all samples (~50 %
8
9 of total tropomyosin, Fig. 3Aii). The relative expression of α -TPM_{slow} and α -TPM_{fast}
10
11 correlates well with type-1 fibre CSA (positive correlation for α -TPM_{slow} and negative
12
13 correlation for α -TPM_{fast}, Fig. 3Aiii and 3Aiiii). The linear regression slope fitted to the data
14
15 was not significantly different between patients and controls, demonstrating a normal ratio of
16
17 α/β tropomyosin isoforms in fast and slow fibres.
18
19

20 21 22 ***Mutant α -TPM_{slow} is expressed in muscle of TPM3-myopathy patients***

23
24 The autosomal dominant inheritance of *TPM3* mutations within our cohort is consistent with
25
26 the hypothesis that mutant α -TPM_{slow} is expressed in slow skeletal myofibres and causes
27
28 disease via a dominant-negative effect on thin filament function. To confirm mutant α -
29
30 TPM_{slow} is present in patient muscle, we isolated the filamentous fractions (representing
31
32 proteins incorporated in high-molecular weight structures such as sarcomeres) and performed
33
34 2D-SDS-PAGE. Five patients in our cohort from whom skeletal muscle samples were
35
36 available, had a mutation that resulted in an amino-acid substitutions affecting a charged
37
38 residue leading to a predicted alteration in the isoelectric point (pI) of α -TPM_{slow}. Thus,
39
40 isoelectric focusing allowed us to separate the mutant from the wild-type protein on the basis
41
42 of charge in these patients, and the second dimension urea-SDS gel separated the three
43
44 tropomyosin isoforms from each other. The mutant α -TPM_{slow} protein could then be observed
45
46 as a left-sided (Fig. 3B; R186G, R91P, K169E, R168C) or right-sided shift (Fig. 3B, E241K)
47
48 from the wild-type α -TPM_{slow} and was present in all patient muscles. The total pool of α -
49
50 TPM_{slow} (both wild-type and mutant isoforms) correlated with the slow fibre CSA (% type-1
51
52 fibre area annotated above each blot, see Supplementary Tab. 2 for measurements). However,
53
54
55
56
57
58
59
60

1
2
3 mutant α -TPM_{slow} was less abundant compared to wild-type, ranging from 27 to 45 % of total
4
5 α -TPM_{slow} (% mutant α -TPM_{slow} annotated on each blot).
6
7
8

9
10 ***The actin-binding properties of K169E and R168C mutant α -TPM_{slow} proteins are***
11
12 ***altered***
13

14 The position of many *TPM3* mutations within or close to actin binding sites suggest most
15 mutations may influence interactions between α -TPM_{slow} and actin filaments. Therefore, we
16 performed actin-tropomyosin co-sedimentation assays with two recombinant mutant α -
17 TPM_{slow} proteins (R168C and K169E) and compared their actin binding properties to wild-
18 type α -TPM_{slow}. These mutations were chosen because they are both located in the fifth actin
19 binding domain, the area that harbours a hotspot for myopathy causing mutations, and affect
20 amino acids predicted to be involved in actin interactions. We co-sedimented incremental
21 amounts of each of the three α -TPM_{slow} proteins with 100 nM filamentous skeletal actin. Fig.
22 4A shows a representative SDS-PAGE of the filamentous fraction isolated following
23 ultracentrifugation, demonstrating dose-dependent binding of wild-type α -TPM_{slow} to actin
24 filaments. Densitometry data of the bound fraction versus the total amount of α -TPM_{slow}
25 added to the reaction was fitted to a Hill equation, to determine the binding constant K_d and
26 the Hill coefficient (h) for all three α -TPM_{slow} proteins (Fig. 4B). The α -TPM_{slow} R168C
27 protein showed reduced actin binding affinity compared to wild-type or the α -TPM_{slow} K169E
28 protein ($K_d = 771.4 \pm 188.6$ nM for R168C, 180.2 ± 37.6 nM for wild-type and 164.0 ± 110.6 nM
29 for K169E, range represents 95% confidence interval). The Hill coefficient was similar in all
30 three mutations ($h =$ wild-type 4.471 ± 3.0 , R168C 3.308 ± 2.4 , K169E 1.602 ± 1.3). These
31 results suggest actin binding may be the mechanism by which the *TPM3* R168C mutation
32 alters contractile function and causes muscle weakness.
33
34
35
36
37
38
39
40
41
42
43
44
45
46
47
48
49
50
51
52
53
54
55
56
57
58
59
60

1
2
3 ***Fast fibre specific α -actinin-3 is ectopically expressed in slow fibres of patients with***
4
5 ***R168H/G TPM3 mutations***
6

7
8 As many *TPM3* patient biopsies displayed a skewing to either slow- or fast- fibre
9
10 predominance by ATPase stain, we stained serial muscle sections with antibodies recognizing
11
12 fibre-type specific isoforms of MHC, troponin and α -actinin to investigate whether the
13
14 expression of several fibre-type-specific proteins was normal (Fig. 5A, Supplementary Fig.
15
16 1). Three patients (Patients 4, 6a and 6b, each with R168 substitutions), showed elevated
17
18 levels of hybrid fibres expressing both slow and fast myosin isoforms. All other patients
19
20 showed normal fibre profiling of myosin and troponin. Curiously, when further
21
22 characterizing the expression profile of hybrid fibres in Patients 4, 6a, 6b and 10, we
23
24 observed ectopic expression of α -actinin-3 in dedicated slow fibres as determined by the
25
26 expression of myosin and troponin (Fig. 5A, Supplementary Fig. 1). α -Actinin-3 is a
27
28 component of the Z-disc normally present in fast myofibres and has been found to be
29
30 important for muscle performance (strength and speed) (26, 27). Our results suggest that the
31
32 restricted fibre-type expression profiles of α -actinin-2 and -3 is differently regulated to
33
34 myosin, troponin and tropomyosin in patients with *TPM3* mutations compared to age-
35
36 matched controls.
37
38
39
40
41
42

43 ***Phosphorylation of tropomyosin is increased in patients with mutations in TPM3***
44

45
46 In normal skeletal muscle, a proportion of both α - and β -TPM is phosphorylated at residue
47
48 S283 (28, 29)(Fig. 5Bi). The effect of tropomyosin phosphorylation in skeletal muscle is
49
50 poorly understood, but studies suggest it is important for tropomyosin function by enhancing
51
52 head-to-tail interactions and increasing the cooperative activation of myosin resulting in
53
54 enhanced force production (30). We investigated whether phosphorylation at S283 was
55
56 altered in *TPM3* patients (as a possible contributor to muscle dysfunction) by Western blot
57
58
59
60

1
2
3 analysis using an anti-phosphor-S283 specific antibody (Fig. 5Bii shows a representative
4
5 Western blot). Phosphorylation of tropomyosin (all three isoforms were analysed in
6
7 combination) was increased in 6/8 of patients with samples available for analysis, compared
8
9 to five age-matched controls (Fig. 5Biii). However, elevated levels of S283 phosphorylation
10
11 were also observed in patients with mutations in *TPM2*, *ACTA1*, *DNM2*, *DMD* and *DYSF*
12
13 (Fig. 5Biiii).

14
15
16
17
18 Mutations in *DMD* (causing Duchenne and Becker muscular dystrophy) and *DYSF* (causing
19
20 limb girdle muscular dystrophy type-2B) cause muscle fibre breakdown and regeneration. It
21
22 is well documented that tropomyosin phosphorylation is higher during development in
23
24 animals (29), and thus we explored whether increased phosphor-S283 in dystrophic muscle
25
26 was related to fibre re-generation. Using IHC analysis, we established that phospho-S283
27
28 tropomyosin levels did not correlate with fibre-type or with fibre re-generation in control or
29
30 patient biopsies (Supplementary Fig. 2B-C). In *TPM3* patients however, levels of phospho-
31
32 S283 tropomyosin were specifically elevated in small, slow-twitch myofibres (Supplementary
33
34 Fig. 2A). This suggests that increased phosphorylation of tropomyosin is not specific to
35
36 *TPM3* disease, but may be a compensatory response to muscle dysfunction due to a variety of
37
38 mechanisms.
39
40
41
42
43
44

45 ***Slow myofibres of TPM3-myopathy patients have reduced maximal force, likely due***
46
47 ***to altered cross-bridge cycling***

48
49 In order to understand how muscle weakness develops in *TPM3* patients we performed
50
51 contractile studies on single, chemically-permeabilised patient myofibres or small fibre
52
53 bundles by immersing them in Ca^{2+} -containing solutions (see methods regarding details for
54
55
56
57
58
59
60

1
2
3 analysis of bundles). This induces activation of the contractile filaments allowing
4
5 measurement of isometric force production.
6
7

8
9
10 First, fibres and fibre bundles were activated at saturating $[Ca^{2+}]$ of pCa 4.5 ($\sim 31.6 \mu M$) to
11
12 induce maximal isometric contraction (F_{max} , Fig. 6A). A small but significant force deficit
13
14 was observed in slow myofibres and fibre bundles from seven of 10 *TPM3*-myopathy patients
15
16 compared to pooled control samples (F_{max} in all *TPM3* patients ranges from 52.17 – 116
17
18 mN/mm^2 compared to $143.1 \pm 31.8 mN/mm^2$ in controls, $*p < 0.01$ one-way ANOVA, Fig. 6C
19
20 and D). This force deficit was present despite normalization to the smaller CSA in slow fibres
21
22 of *TPM3* patients. F_{max} in type-2 fibres was not different from control fibres (106.7 - 186.7
23
24 mN/mm^2 in patient fibres and $147.7 \pm 29.34 mN/mm^2$ in control fibres) (Fig. 6B). In bundles,
25
26 F_{max} was lower in bundles with higher slow MHC content in two of three patients
27
28 (Supplementary Fig. 3).
29
30
31
32
33

34 During muscle contraction, a cyclic interaction between the myosin heads and thin filaments,
35
36 followed by a conformational change in myosin, allows the filaments to slide past each other.
37
38 Correct positioning of tropomyosin on actin filaments during the various stages of myosin-
39
40 actin interactions is crucial for efficient cross-bridge cycling. To determine if the force deficit
41
42 in slow myofibres of *TPM3* patients can be attributed to changes in cross-bridge cycling
43
44 kinetics we measured the rate of tension re-development (K_{tr}) during maximal activation,
45
46 after a short period of unloaded shortening following by re-stretch (a typical length and force
47
48 trace are presented in Fig. 7Ai). The speed of cross-bridge cycling is physiologically faster in
49
50 type-2 (fast-twitch) fibres compared to type-1 (slow-twitch) fibres (see controls in Fig. 7Aii-
51
52 iii). Slow fibres from eight of 10 *TPM3* patient biopsies displayed a significant reduction in
53
54 K_{tr} compared to controls (K_{tr} in all *TPM3* patients ranges from 0.758 - $1.217 s^{-1}$ compared to
55
56
57
58
59
60

1
2
3 1.493±0.25 s⁻¹ in controls, *** p<0.0001, * p<0.01, one-way ANOVA, Fig. 7Aii), whereas
4
5 fast myofibres were not different from control myofibres (Fig. 7Aiii). These results suggest
6
7 that myosin cross-bridge cycling kinetics are altered in slow fibres of *TPM3* patients,
8
9 contributing to muscle weakness by reducing the fraction of strongly bound cross-bridges
10
11 during activation.
12
13

14
15
16 Fmax is proportional to the force generated by a single strongly bound actin-myosin cross-
17
18 bridge and the fraction of myosin heads attached to actin. We assessed active stiffness in
19
20 *TPM3* biopsies, a measure proportional to the number of myosin heads strongly attached to
21
22 actin during an isometric contraction (31), to study whether this contributes to muscle
23
24 weakness. We measured active stiffness by performing fast length changes in isometrically
25
26 contracted single myofibres (typical length/force traces are presented in Supplementary Fig. 4
27
28 and a typical patient and control plot of the length change (ΔL) versus force change (ΔF) is
29
30 presented in Fig. 7Bi and ii, respectively)(32). We observed a trend towards reduced absolute
31
32 active stiffness in type-1 fibres and bundles/hybrid fibres of most *TPM3* patients (Fig. 7Biii
33
34 and iiiii), which was not present in type-2 fibres (Fig. 7Bv). The change in active stiffness was
35
36 proportional to Fmax, as the difference was not present when stiffness was normalised to
37
38 Fmax (Fig. 7Bvi-viii). Since stiffness is proportional to the number of strongly attached
39
40 myosin cross-bridges, a reduction of active stiffness proportional to force reduction suggests
41
42 that forces per cross-bridge were normal, but, in line with the reduced Ktr, the number of
43
44 strongly attached cross-bridges may be reduced in slow fibres of *TPM3* patients, likely
45
46 contributing to muscle weakness.
47
48
49
50
51

52
53
54 ***Ca²⁺-sensitivity of contraction and maximal contractile force are decreased in***
55
56 ***patients with TPM3 mutations***
57
58
59
60

1
2
3 Tropomyosin and the troponin complex are pivotal in regulating Ca^{2+} -induced cross-bridge
4 cycling during muscle contraction. We assessed the sensitivity to Ca^{2+} of permeabilised
5 fibres, by bathing preparations in incrementally increasing $[\text{Ca}^{2+}]$ (pCa 6.2-4.5) and
6 measuring the generated contractile force. In slow myofibres and fibre bundles/hybrid fibres
7 of all patients, the force-pCa curves were shifted to the right compared to controls (Fig. 8Ai-
8 ii). As a result, the pCa_{50} , representing the negative logarithm of the $[\text{Ca}^{2+}]$ at which
9 preparations produce 50 % of their F_{max} , was significantly reduced in type-1 fibres and
10 bundles/hybrid fibres from all patients compared to controls (pCa_{50} type-1: 5.96 ± 0.06
11 controls, 5.69 ± 0.04 patients; pCa_{50} bundles/hybrid: 5.99 ± 0.09 controls, 5.67 ± 0.05 patient,
12 Fig. 8Bi-ii). This result indicates that more Ca^{2+} was required in patient biopsies than control
13 biopsies to achieve the same relative force. In contrast, fast fibres from patients and controls
14 showed normal Ca^{2+} -activated force production (Fig. 8Aiii, Fig. 8Biii).

15
16
17
18
19
20
21
22
23
24
25
26
27
28
29
30
31
32 Our data demonstrates that slow fibres and in bundles/hybrid fibres from patients with *TPM3*
33 mutations produce on average ~ 63 % of the force produced by control fibres at saturating
34 $[\text{Ca}^{2+}]$ (pCa 4.5). During a maximal contraction the intracellular $[\text{Ca}^{2+}]$ can rise from resting
35 levels of ~0.1 μM (pCa 7) to ~10 μM (pCa 5) (33). However, myofibres *in vivo* rarely
36 undergo maximal stimulation and mostly operate at sub-maximal levels, typically resulting in
37 $[\text{Ca}^{2+}]$ of around 1-5 μM in type-1 fibres (yellow area in Fig. 8A) (34-36). At these
38 physiological Ca^{2+} levels (pCa 6.0), slow fibres and bundles/hybrid fibres from *TPM3*
39 patients produce on average only 26 % of the force produced by control slow fibres and
40 bundles/hybrid fibres (Fig. 8Ci-ii), whereas patient fast fibres produce forces similar to
41 controls (Fig. 8Ciii). Thus, our results suggest reduced Ca^{2+} -sensitivity is a significant basis
42 for muscle weakness in *TPM3*-myopathy.
43
44
45
46
47
48
49
50
51
52
53
54
55
56
57
58
59
60

1
2
3 ***Ectopic α -actinin-3 expression in slow myofibres does not correlate with increased***
4
5 ***maximal force***
6

7
8 Four patients with *TPM3* mutations at R168 displayed ectopic expression of α -actinin-3 in
9
10 slow myofibres. Since α -actinin-3 expression is associated with increased muscle strength
11
12 and speed (26, 27) we determined whether α -actinin-3 in slow fibres may influence
13
14 contractile properties. We tested if α -actinin-3 expression was more commonly observed in
15
16 fibres with higher Fmax in eight fibres from two patients. However, we found no correlation
17
18 between ectopic α -actinin-3 and force production in these patient fibres (Supplementary Fig.
19
20 5).
21
22
23
24
25
26
27
28
29
30
31
32
33
34
35
36
37
38
39
40
41
42
43
44
45
46
47
48
49
50
51
52
53
54
55
56
57
58
59
60

Discussion

Mutations in *TPM3* cause a range of histopathological patterns and are associated with generalised muscle weakness. To date, the cause of muscle dysfunction is not well understood in these patients, hindering the development of evidence-based treatments for *TPM3*-myopathies. Thus, we performed extensive phenotypical and functional characterization of a large cohort of *TPM3*-myopathy patients to understand the molecular mechanism(s) of their muscle weakness.

The main histological feature of *TPM3*-myopathy patients in this cohort, and other published cohorts (1-3), was a selective hypotrophy of slow myofibres, while other histological features such as nemaline rods and caps were rarely present (four of 15 patients). The selective hypotrophy and contractile dysfunction of slow myofibres is consistent with the restricted slow-fibre expression of α -TPM_{slow}, the main protein expressed from *TPM3* in skeletal muscle. We confirmed the presence of mutant α -TPM_{slow} in the filamentous fraction of patient skeletal muscle via 2D-SDS-PAGE for patients possessing a *TPM3* mutation resulting in a charge change. In patients with protein aggregates (e.g. nemaline bodies), it has been uncertain whether mutant protein is actually incorporated into the sarcomere, or partitions into protein aggregates within the muscle fibre. In our study, protein aggregates were not observed in biopsies analysed by 2D-SDS-PAGE, suggesting that α -TPM_{slow} mutant protein is likely incorporated into sarcomeres causing muscle weakness via a dominant negative effect on contractile function. Interestingly, the amount of α -TPM_{slow} mutant protein did not correlate well with disease severity in our patient cohort. This may be explained by a number of factors influencing disease severity, such as a mutation-specific effect and varying proportions of slow fibres in different parts of the same muscle or different muscle groups.

1
2
3 Muscle contraction and force production rely on efficient interactions between tropomyosin
4
5 polymers and major binding partners, the troponins and the actin filament, in response to
6
7 Ca^{2+} -influx. In this series of twelve muscle biopsies from *TPM3*-myopathy patients, we
8
9 showed normal fibre-type expression of the major contractile proteins myosin, actin, troponin
10
11 and tropomyosin. Furthermore, we confirmed normal ratios of the three skeletal muscle
12
13 tropomyosin isoforms according to fibre-type composition for all patients. Our data suggest
14
15 the higher relative abundance of α -TPM_{slow} previously reported in a patient bearing a M9R
16
17 substitution in *TPM3* (25, 37) may be a specific property of this mutation, perhaps related to
18
19 its position within the dimerisation domain. In a small number of patients, we observed
20
21 ectopic expression of the fast fibre Z-disc protein α -actinin-3 in slow myofibres. The
22
23 consequence of slow-fibre expression of the fast-fibre α -actinin-3 is not clear, and may relate
24
25 to both metabolic and structural roles of α -actinin-3, though we excluded an overt effect on
26
27 contractile force of single myofibres. Interestingly, similar ectopic expression of α -actinin-3
28
29 was previously observed in some patients with *ACTA1* mutations (38) and is thus not specific
30
31 to *TPM3*-associated disease but could potentially be due to incomplete or abnormal fibre type
32
33 conversion present in some myopathy patients.
34
35
36
37
38

39 We investigated tropomyosin phosphorylation at residue S283 in our cohort. Tropomyosin
40
41 phosphorylation has mainly been studied in the context of cardiac function (39-42) and to the
42
43 best of our knowledge has not been investigated in skeletal myopathy patients. *In vitro*
44
45 studies suggest phosphorylation strongly affects tropomyosin properties [e.g. stronger head-
46
47 to-tail interaction, enhanced troponin binding, higher myosin ATPase activity and long-range
48
49 cooperative activation of myosin-thin filament binding (30, 43, 44)]. We showed
50
51 tropomyosin phosphorylation was commonly increased in a wide range of genetic muscle
52
53 disorders including *TPM3*-myopathy. However, the cause of this up-regulation and the effect
54
55 on skeletal muscle contractility is unclear. The p38-MAPK (mitogene-activated protein
56
57
58
59
60

1
2
3 kinase) and ERK (extracellular signal-related kinase) signalling pathways are likely involved
4
5 in tropomyosin phosphorylation of cardiac muscle and non-muscle cells, respectively (45-
6
7 47). In skeletal muscle, these pathways regulate exercise-induced adaptive responses on gene
8
9 expression (reviewed in 48), suggesting tropomyosin phosphorylation may be involved in
10
11 remodelling or adaptation to cellular stress.
12

13
14 Most reported *TPM3* substitutions lie within or near actin-binding domains, with several
15
16 substitutions believed to influence direct electrostatic interactions with actin in the “off” state
17
18 [when tropomyosin blocks myosin binding sites on the actin filament e.g. R91, R168, R245
19
20 directly interact with actin D25 (49-51)]. Our data and previous studies have shown that
21
22 many tropomyosin substitutions indeed affect binding to actin-filaments (52-55). Thus,
23
24 altered actin-binding likely represents a common mechanism by which tropomyosin mutants
25
26 alter sarcomeric function, perhaps related to the Ca^{2+} -activated movement of tropomyosin
27
28 between the “on” and “off” position during cross-bridge cycling (51, discussed in 56).
29
30
31
32
33
34

35 Recent studies have attempted to predict the effect of mutations on actin-tropomyosin
36
37 interactions and the resulting contractile abnormality, classifying them as “gain-of-function”
38
39 changes (hyper-contractile phenotype, shift towards “on” state) and “loss-of-function”
40
41 changes (hypo-contractile phenotype, stabilizing the “off” state) (50, 57, 58). Most mutations
42
43 in our cohort are predicted to cause a “loss-of-function” (e.g. decreased Ca^{2+} -sensitivity and a
44
45 hypocontractile phenotype). The only exception is *TPM3* K169E, predicted to favour the
46
47 “on” position and enhance myosin-actin binding (50, 57)]. This phenotype was confirmed in
48
49 reconstituted thin filaments *in vitro* (50). However, isolated slow myofibres and fibre bundles
50
51 of all *TPM3* patients (including Patient 1 carrying the K169E mutation), showed reduced
52
53 Ca^{2+} -sensitivity of contraction. Our data are consistent with the patient phenotype described
54
55 in (1) and do not support the hyper-contractile phenotype of the K169E mutation present in *in*
56
57
58
59
60

1
2
3 *in vitro* assessment of isolated filaments (50). This discrepancy may be explained by the greater
4 complexity of single-fibre contractility studies, a setting that evaluates the combined
5 contributions of actin, tropomyosin and troponin binding and regulatory proteins within a
6 mature myofibre, which may also have undergone adaptive responses to disease. These may
7 not be mirrored by *in vitro* actin motility studies or predictions via molecular modelling.
8 Additional factors, such as interactions with other sarcomeric proteins like the troponin
9 complex (59), may also contribute. Additionally, a recurrent mutation in *TPM3*, R168H, was
10 found to reduce [current study and (21)] or increase Ca^{2+} -sensitivity (20) in different patients
11 with the same mutation. The cause for this patient to patient variability remains to be
12 established.
13
14
15
16
17
18
19
20
21
22
23
24

25
26 In our study, we identified two major abnormalities in contractile performance that we
27 believe directly underpins weakness in *TPM3*-myopathy. Firstly, all patients exhibited
28 reduced Ca^{2+} -sensitivity of contraction in slow myofibres, likely resulting in a significant
29 reduction in the contractile force generated at physiological, sub-maximal activation of
30 muscle. Secondly, slow myofibres demonstrated a significant reduction in cross-bridge
31 cycling kinetics and a small reduction in active stiffness (assesses the number of strongly
32 bound myosin-actin cross-bridges) – meaning that myosin less effectively and less stably
33 transits along actin filaments during contraction. Collectively, these two abnormalities likely
34 cause insufficient force production during a normal action potential resulting in slow fibre
35 weakness.
36
37
38
39
40
41
42
43
44
45
46
47
48

49 The selective dysfunction of slow myofibres in our cohort demonstrates the importance of
50 assessing the two fibre types separately, and raises the question as to why fast myofibres are
51 not able to compensate for dysfunctional slow myofibres. Inherent differences exist between
52 the two fibre types. Slow myofibres are less fatigable than fast myofibres, probably due at
53 least in part to larger numbers of mitochondria and a greater capacity for oxidative
54
55
56
57
58
59
60

1
2
3 metabolism (60, 61). Additionally, fast myofibres have a higher ATP consumption. Particular
4
5 muscle groups, such as respiratory muscles, rely on slow fibres to produce sustained, low
6
7 intensity contractions. Substantial weakness of respiratory muscles is common in *TPM3*
8
9 patients, and effective treatments that specifically target slow muscle fibre dysfunction may
10
11 ameliorate respiratory insufficiency.
12
13

14
15 In summary, contractile function was commonly impaired in *TPM3*-myopathy patients. In
16
17 particular, we showed reduced force generation caused by altered cross-bridge cycling
18
19 kinetics and reduced Ca^{2+} -sensitivity of muscle contraction. The identification of abnormal
20
21 Ca^{2+} -sensitivity suggests the use of Ca^{2+} -sensitisers may present a viable therapeutic
22
23 approach for TPM-related myopathies. To date, a number of agents are known to be effective
24
25 at improving Ca^{2+} -sensitivity in isolated skeletal myofibres from various species including
26
27 bovine, human, mouse and rabbit (21, 62-65). Additionally, Ca^{2+} -sensitisers were able to
28
29 ameliorate muscle dysfunction in a rat model of myasthenia gravis (62) and isolated skeletal
30
31 myofibres from congenital myopathy patients with mutations in *TPM3*, *TPM2* and *NEB* (21,
32
33 63). This therapeutic approach appears to be promising; however, most of these agents target
34
35 the fast troponin isoforms and are unlikely to ameliorate slow fibre dysfunction. A Ca^{2+} -
36
37 sensitiser acting on slow skeletal/cardiac troponin-C did not improve Ca^{2+} -sensitivity in
38
39 skeletal myofibres in a recent study, suggesting that new compounds targeting slow myofibre
40
41 dysfunction have yet to be developed (66). Also, it appears that *TPM2* and *TPM3* mutations
42
43 can either increase or decrease Ca^{2+} -sensitivity in a patient and mutation-specific manner
44
45 (overview in Supplementary Tab. 4), thus Ca^{2+} -sensitisers will only be useful in a subset of
46
47 patients. Patients with increased Ca^{2+} -sensitivity display a hyper-contractile clinical
48
49 phenotype (21, 54), suggesting treatment with Ca^{2+} -sensitisers must be tightly regulated to
50
51 ensure appropriate muscle function and avoid side effects.
52
53
54
55
56
57
58
59
60

Materials and Methods

Study approval

This study was approved by the human ethics committees of the Stollery Children's Hospital, Edmonton, Canada (ID: 5856), Royal Children's Hospital, Melbourne, Australia (ID: 21102A), Children's Hospital at Westmead, Sydney, Australia (ID: 2000/068, 10.CHW.45), University of Sydney, Australia (ID: 01/11/50) and Boston Children's Hospital Institutional Review Board (03-08-128R). Informed consent was obtained from all individuals.

Molecular modelling

Molecular modelling was based on the 7 Ångstroms resolution crystal structure of an α -TPM_{fast} dimer isolated from adult porcine ventricles (RCSB Protein Data Bank 1C1G, Whitby and Phillips (23)). Molecular graphics were created with Swiss-PDB Viewer v4.1.0 (67).

Antibodies

Mouse anti-sarcomeric actin (**5C5**, 1:100 for immunohistochemistry [IHC] and 1:10000 for Western blot), fast myosin [**MY32**, 1:800 for IHC, tropomyosin (**TM311**, 1:20,000 for Western blot and 1:800 for IHC), troponin-T_{fast} (**TNNT3**, 1:30 for IHC and 1:1000 for Western blot) were obtained from Sigma Aldrich. S283-phosphorylated tropomyosin was detected using the rabbit **anti-Tm-pS283-050** (1:500 for Western blot and 1:30 for IHC, 21st Century Biochemicals) and slow myosin antibodies were obtained from Chemicon (1:800 for IHC and 1:7000 for Western blot). Polyclonal α -actinin-3 antibodies were produced in-house (antibody **5B3** diluted 1:50 for IHC and antibody **5A2** 1:1500 for Western blot) (68). Troponin-I_{slow} (**MYNT-S**, diluted 1:10 for IHC) and fast (**MYNT-F**, diluted 1:150) antibodies were kindly supplied by Takeshi Nakamura, Japan. Troponin-T_{slow} antibodies (**CT3**) were obtained from the Developmental Studies Hybridoma Bank, University of Iowa

1
2
3 (diluted 1:50 for IHC). Cardiac actin and neonatal myosin heavy chain (MHC) antibodies
4
5 were obtained from American Research Products Inc, USA and Novocastra Laboratories Ltd,
6
7 UK, respectively.
8
9

10 11 ***IHC and Zenon labelling*** 12

13
14 IHC was performed as described previously (69). Sections were either fixed as described in
15
16 (37) (MYNT-S) or for 10 min in 3% PFA (MYNT-F, CT3 and TNNT3) or used unfixed
17
18 (other antibodies). A Zenon mouse IgG labelling kit (Molecular Probes) was used to directly
19
20 label primary antibodies with different fluorophores for co-staining with two mouse
21
22 antibodies as per manufacturer's instructions (either MHC type-2A and type-1 [Fig. 5] or
23
24 neonatal MHC and cardiac actin [Supplementary Fig. 2C]). Staining was imaged using
25
26 standard fluorescence microscopy.
27
28
29
30
31

32 ***Fibre morphometry*** 33

34 Fibre morphometry was performed on cryo-sections stained for myosin ATPase (70)] or
35
36 following IHC for MHC isoforms. At least 200 fibres, visible in two distant fields of the same
37
38 section were analysed using ImagePro Plus 4 software (Media Cybernetics). The greatest
39
40 distance between opposite sides of the narrowest aspect, the MinFerret diameter, was
41
42 measured to obtain the fibre diameter from a cross sectional cut. The percentage fibre-size
43
44 disproportion (%FSD) was calculated as described in (1) and slow fibre area was calculated
45
46 assuming circular shape of myofibres.
47
48
49
50
51

52 ***Western blot and 2D-polyacrylamide gel electrophoresis (2D-SDS-PAGE)*** 53

54 Western blot methods were based on (71) and tropomyosin isoforms were resolved as
55
56 described in (54). Extraction of the filamentous protein pool from skeletal muscle sections
57
58
59
60

1
2
3 and 2D-SDS-PAGE to determine mutant tropomyosin expression were performed as
4
5 described previously (14, 72).
6
7

8 9 ***Protein sources and actin-tropomyosin co-sedimentation***

10
11 We employed site-directed mutagenesis to produce wild-type and mutant (R168C, K169E) α -
12
13 TPM_{slow} baculoviruses to infect *Sf9* insect cells using the baculovirus expression method as
14
15 described previously (73, 74).
16
17

18
19 Filamentous actin was prepared from actin-acetone powder isolated from rabbit muscle (75)
20
21 and a 1 μ M stock with 1 μ M phalloidin and 0.1 mM ATP was used for experiments.
22
23

24
25 All protein stocks were prepared in and dialyzed against a buffer containing 100 mM KCl, 50
26
27 mM Imidazole, 8 mM MgCl₂, 2 mM EDTA, 10 mM DTT and 0.5 mg/mL ultrapure bovine
28
29 serum albumin (BSA, Sigma). Ten μ M tropomyosin stocks were cleared of aggregates by
30
31 ultracentrifugation at 603,180 x g (Sorvall M120-SE centrifuge, S100AT6-0199 rotor) for 20
32
33 min at 4 °C. Ten nM actin were co-sedimented with incremental amounts of tropomyosin
34
35 (50-1000 nM) in 1 mL reaction volume at 51,427 x g for 1.5 hr at 25 °C (Sorvall Evolution
36
37 RC centrifuge, F20-Micro rotor) in siliconised polypropylene tubes. The pelleted fractions
38
39 were solubilised in loading buffer and loaded on 4-15 % Criterion TGX gels (Biorad).
40
41 Densitometry analysis on actin and tropomyosin bands was performed using GeneTools 4.0
42
43 software (Synoptics Ltd). Values were corrected for sedimentation in the absence of actin and
44
45 plotted as the ratio tropomyosin/actin vs. total [tropomyosin] added. Data were fitted to a Hill
46
47 equation to determine the binding constant K_d and Hill's coefficient h using GraphPad, Prism
48
49 (Version 5.01).
50
51
52

53 54 ***Contractile measurement of myofibres isolated from frozen human muscle biopsies***

55
56
57
58
59
60

1
2
3 Small fractions of frozen muscle biopsies were thawed as described previously (63) in a
4 solution containing 50 % glycerol and 50 % Ca^{2+} -free relaxing-solution (100 mM BES, 6.97
5 mM EGTA, 6.48 mM MgCl_2 , 6 mM Na_2ATP , 1 mM DTT, 40.76 mM K-propionate, 14.5 mM
6 creatine phosphate, 0.5 mM PMSF, 10 μM E64, 40 μM leupeptin, pH 7.1 and pCa 9 at 15
7 $^\circ\text{C}$).
8
9

10
11
12 For contractile measurements, single fibres or small fibre bundles [$\sim 0.07 \text{ mm}^2$ cross sectional
13 area (CSA) and $\sim 0.5 \text{ mm}$ length] were dissected in glycerinating solution at 4 $^\circ\text{C}$. Fibre
14 bundles were prepared if the fibre CSA was too small for reliable force measurements.
15 Aluminium T-clips were attached to both ends of the preparation followed by chemical
16 skinning in glycerinating solution containing 1 % TritonX-100 for 10 min (single fibres) or
17 30 min (bundles) at 4 $^\circ\text{C}$. The preparations were then stored at 4 $^\circ\text{C}$ in glycerinating solution
18 until mounting onto a permeabilised fibre apparatus between a length motor and a force
19 transducer (ASI 802D, ASI 403A, ASI 315C-I, respectively, Aurora Scientific Inc., Canada)
20 in relaxing-solution. All force measurements were performed at sarcomere lengths of 2.5 μm
21 [optimal myofilament overlap, (76)] and at a temperature of 20 $^\circ\text{C}$ (bath temperature
22 controller ASI 825A, Aurora Scientific). The sarcomere length was set and the CSA was
23 measured as described in (63).
24
25
26
27
28
29
30
31
32
33
34
35
36
37
38
39
40
41
42

43
44 Prior to $[\text{Ca}^{2+}]$ -induced activations preparations were pre-activated for 1 min in 100 mM
45 BES, 0.1mM EGTA, 6.42 mM MgCl_2 , 6 mM Na_2ATP , 41.14 mM K-propionate, 14.5 mM
46 creatine phosphate, 6.9 mM HDTA (pH 7.1 and pCa 9 at 15 $^\circ\text{C}$). Maximal isometric
47 contraction (F_{max}) was measured by bathing fibres in saturating $[\text{Ca}^{2+}]$ buffer (100 mM BES,
48 7 mM CaEGTA, 6.28 mM MgCl_2 , 6 mM Na_2ATP , 40.64 mM K-propionate, 14.5 mM
49 creatine phosphate, pH 7.1 and pCa 4.5 at 15 $^\circ\text{C}$) until a force plateau was achieved. The
50 maximal specific force (F_{max} at pCa 4.5 normalised to the CSA) is presented in this study.
51
52
53
54
55
56
57
58
59
60

1
2
3 Force/pCa curves and pCa 50 were measured as described in (20). The rate constant of
4
5 tension re-development (K_{tr}) was measured by allowing the preparations to shorten to 70 % of
6
7 the initial length for 30 ms followed by re-stretch to 100 % and fitting the data to a mono-
8
9 exponential function using Labview (National Instruments, USA) as described in (20). Active
10
11 stiffness was measured immediately after the K_{tr} protocol as described previously (32, 77). In
12
13 brief, we measured the force response (FI) to six 2 s length changes (ΔL : +0.3 %, +0.6 %,
14
15 +0.9 %, -0.3 %, -0.6 %, -0.9 %; Supplementary Fig. 4). ΔL was plotted against the force
16
17 changes (ΔF) and a linear regression was fitted to obtain the slope using Graph Pad, Prism
18
19 (Version 5.01).
20
21
22
23

24
25 The MHC content of measured fibres was determined as described previously (63) and the
26
27 proportion of each MHC was determined by densitometry. Single myofibres/fibre bundles
28
29 containing exclusively slow MHC (>90 % type-1), exclusively fast MHC (>90 % type-2A or
30
31 2X) or a mixture of both (11–90 % type-1 or type-2A/2X) were grouped for analysis. The
32
33 contractile properties of bundles and hybrid fibres containing a mix of type-1 and type-2A/2X
34
35 MHC represent the average properties of both fibre types. The K_{tr} in bundles/hybrid fibres is
36
37 highly variable due to the physiologically difference in type-1 or type-2A/2X fibres and was
38
39 therefore not presented. Preparations were excluded from the analysis if the Fmax decreased
40
41 >15 % during the protocol. Single myofibres from eight control biopsies (age 6-54 y) and
42
43 bundles from two control biopsies (aged 0.6 and 6 y) were pooled for statistical analysis.
44
45
46
47
48
49
50
51
52
53
54
55
56
57
58
59
60

Acknowledgements

The authors would like to thank the study patients and their families for their participation. Additionally, we are thankful to Dr. Nicole Monnier and Dr. Isabelle Pennison-Besnier (CHU Angers, Département de Neurologie, Angers, France) for supply patient tissue for this study. This work was supported by the National Health and Medical Research Council of Australia [APP571287 to N.F.C., K.N.N. and B.I.; APP1022707 to N.F.C. and K.N.N.; APP1048816 to S.T.C.; APP1035955 to G.R.] and by the National Institutes of Health (USA) [R01 HD075802 from the National Institute of Child Health and Human Development to A.H.B.]. M.Y. is supported by a University of Sydney Australian Postgraduate Award, an International Postgraduate Research Scholarship and a Boehringer Ingelheim Fonds Travel Grant. K.J.N. is supported by an Australian Resource Council Future Fellowship [FT100100734].

Conflict of Interest Statement

The authors declare that they have no conflict of interest.

References

- 1 Clarke, N.F., Kolski, H., Dye, D.E., Lim, E., Smith, R.L., Patel, R., Fahey, M.C.,
2 Bellance, R., Romero, N.B., Johnson, E.S. *et al.* (2008) Mutations in TPM3 are a common
3 cause of congenital fiber type disproportion. *Ann. Neurol.*, **63**, 329-337.
- 4 Lawlor, M.W., Dechene, E.T., Roumm, E., Geggel, A.S., Moghadaszadeh, B. and
5 Beggs, A.H. (2009) Mutations of tropomyosin 3 (TPM3) are common and associated with
6 type 1 myofiber hypotrophy in congenital fiber type disproportion. *Hum Mutat.*, **31**, 176-183.
- 7 Marttila, M., Lehtokari, V.L., Marston, S., Nyman, T.A., Barnerias, C., Beggs, A.H.,
8 Bertini, E., Ceyhan-Birsoy, O., Cintas, P., Gerard, M. *et al.* (2014) Mutation update and
9 genotype-phenotype correlations of novel and previously described mutations in TPM2 and
10 TPM3 causing congenital myopathies. *Hum. Mutat.*, **35**, 779-790.
- 11 Tan, P., Briner, J., Boltshauser, E., Davis, M.R., Wilton, S.D., North, K., Wallgren-
12 Pettersson, C. and Laing, N.G. (1999) Homozygosity for a nonsense mutation in the alpha-
13 tropomyosin slow gene TPM3 in a patient with severe infantile nemaline myopathy.
14 *Neuromuscul. Disord.*, **9**, 573-579.
- 15 Wattanasirichaigoon, D., Swoboda, K.J., Takada, F., Tong, H.Q., Lip, V., Iannaccone,
16 S.T., Wallgren-Pettersson, C., Laing, N.G. and Beggs, A.H. (2002) Mutations of the slow
17 muscle alpha-tropomyosin gene, TPM3, are a rare cause of nemaline myopathy. *Neurology*,
18 **59**, 613-617.
- 19 Lehtokari, V.-L., Pelin, K., Donner, K., Voit, T., Rudnik-Schöneborn, S., Stoetter, M.,
20 Talim, B., Topaloglu, H., Laing, N.G. and Wallgren-Pettersson, C. (2008) Identification of a
21 founder mutation in TPM3 in nemaline myopathy patients of Turkish origin. *Eur. J. Hum.*
22 *Genet.*, **16**, 1055-1061.

- 1
2
3 7 Lawlor, M.W., Dechene, E.T., Roumm, E., Geggel, A.S., Moghadaszadeh, B. and
4
5 Beggs, A.H. (2010) Mutations of tropomyosin 3 (TPM3) are common and associated with
6
7 type 1 myofiber hypotrophy in congenital fiber type disproportion. *Hum. Mutat.*, **31**, 176-183.
8
9
10 8 Laing, N.G., Wilton, S.D., Akkari, P.A., Dorosz, S., Boundy, K., Kneebone, C.,
11
12 Blumbergs, P., White, S., Watkins, H., Love, D.R. *et al.* (1995) A mutation in the alpha
13
14 tropomyosin gene TPM3 associated with autosomal dominant nemaline myopathy. *Nat.*
15
16 *Genet.*, **9**, 75-79.
17
18 9 Schreckenbach, T., Schroder, J.M., Voit, T., Abicht, A., Neuen-Jacob, E., Roos, A.,
19
20 Bulst, S., Kuhl, C., Schulz, J.B., Weis, J. *et al.* (2014) Novel TPM3 mutation in a family with
21
22 cap myopathy and review of the literature. *Neuromuscul. Disord.*, **24**, 117-124.
23
24
25 10 Kiphuth, I.C., Krause, S., Huttner, H.B., Dekomien, G., Struffert, T. and Schroder, R.
26
27 (2010) Autosomal dominant nemaline myopathy caused by a novel alpha-tropomyosin 3
28
29 mutation. *J. Neurol.*, **257**, 658-660.
30
31
32 11 Ohlsson, M., Fidzianska, A., Tajsharghi, H. and Oldfors, A. (2009) TPM3 mutation in
33
34 one of the original cases of cap disease. *Neurology*, **72**, 1961-1963.
35
36
37 12 De Paula, A.M., Franques, J., Fernandez, C., Monnier, N., Lunardi, J., Pellissier, J.F.,
38
39 Figarella-Branger, D. and Pouget, J. (2009) A TPM3 mutation causing cap myopathy.
40
41 *Neuromuscul. Disord.*, **19**, 685-688.
42
43
44 13 Penisson-Besnier, I., Monnier, N., Toutain, A., Dubas, F. and Laing, N. (2007) A
45
46 second pedigree with autosomal dominant nemaline myopathy caused by TPM3 mutation: a
47
48 clinical and pathological study. *Neuromuscul. Disord.*, **17**, 330-337.
49
50
51 14 Waddell, L.B., Kreissl, M., Kornberg, A., Kennedy, P., McLean, C., Labarre-Vila, A.,
52
53 Monnier, N., North, K.N. and Clarke, N.F. (2010) Evidence for a dominant negative disease
54
55 mechanism in cap myopathy due to TPM3. *Neuromuscul. Disord.*, **20**, 464-466.
56
57
58
59
60

- 1
2
3 15 Geeves, M.A., Hitchcock-DeGregori, S.E. and Gunning, P.W. (2015) A systematic
4 nomenclature for mammalian tropomyosin isoforms. *J. Muscle Res. Cell Motil.*, **36**, 147-153.
5
6
7 16 Billeter, R., Heizmann, C.W., Reist, U., Howald, H. and Jenny, E. (1981) alpha- and
8 beta-tropomyosin in typed single fibers of human skeletal muscle. *FEBS Lett.*, **132**, 133-136.
9
10
11 17 Pieples, K. and Wieczorek, D.F. (2000) Tropomyosin 3 increases striated muscle
12 isoform diversity. *Biochemistry (Mosc)*. **39**, 8291-8297.
13
14
15 18 McLachlan, A.D. and Stewart, M. (1975) Tropomyosin coiled-coil interactions:
16 evidence for an unstaggered structure. *J. Mol. Biol.*, **98**, 293-304.
17
18
19 19 McLachlan, A.D. and Stewart, M. (1976) The 14-fold periodicity in alpha-
20 tropomyosin and the interaction with actin. *J. Mol. Biol.*, **103**, 271-298.
21
22
23 20 Ottenheijm, C.A., Lawlor, M.W., Stienen, G.J., Granzier, H. and Beggs, A.H. (2011)
24 Changes in cross-bridge cycling underlie muscle weakness in patients with tropomyosin 3-
25 based myopathy. *Hum. Mol. Genet.*, **20**, 2015-2025.
26
27
28 21 Ochala, J., Gokhin, D.S., Penisson-Besnier, I., Quijano-Roy, S., Monnier, N.,
29 Lunardi, J., Romero, N.B. and Fowler, V.M. (2012) Congenital myopathy-causing
30 tropomyosin mutations induce thin filament dysfunction via distinct physiological
31 mechanisms. *Hum. Mol. Genet.*, **21**, 4473-4485.
32
33
34 22 Johnson, M.A., Polgar, J., Weightman, D. and Appleton, D. (1973) Data on the
35 distribution of fibre types in thirty-six human muscles. An autopsy study. *J. Neurol. Sci.*, **18**,
36 111-129.
37
38
39 23 Polgar, J., Johnson, M.A., Weightman, D. and Appleton, D. (1973) Data on fibre size
40 in thirty-six human muscles. An autopsy study. *J. Neurol. Sci.*, **19**, 307-318.
41
42
43 24 Billeter, R., Heizmann, C.W., Reist, U., Howald, H. and Jenny, E. (1982) Two-
44 dimensional peptide analysis of myosin heavy chains and actin from single-typed human
45 skeletal muscle fibers. *FEBS Lett.*, **139**, 45-48.
46
47
48
49
50
51
52
53
54
55
56
57
58
59
60

- 1
2
3 25 Corbett, M.A., Akkari, P.A., Domazetovska, A., Cooper, S.T., North, K.N., Laing,
4 N.G., Gunning, P.W. and Hardeman, E.C. (2005) An alphaTropomyosin mutation alters
5 dimer preference in nemaline myopathy. *Ann. Neurol.*, **57**, 42-49.
6
7
8
9
10 26 Clarkson, P.M., Devaney, J.M., Gordish-Dressman, H., Thompson, P.D., Hubal, M.J.,
11 Urso, M., Price, T.B., Angelopoulos, T.J., Gordon, P.M., Moyna, N.M. *et al.* (2005) ACTN3
12 genotype is associated with increases in muscle strength in response to resistance training in
13 women. *J. Appl. Physiol.*, **99**, 154-163.
14
15
16
17
18 27 Eynon, N., Hanson, E.D., Lucia, A., Houweling, P.J., Garton, F., North, K.N. and
19 Bishop, D.J. (2013) Genes for elite power and sprint performance: ACTN3 leads the way.
20 *Sports Med.*, **43**, 803-817.
21
22
23
24
25 28 Mak, A., Smillie, L.B. and Barany, M. (1978) Specific phosphorylation at serine-283
26 of alpha tropomyosin from frog skeletal and rabbit skeletal and cardiac muscle. *Proc. Natl.*
27 *Acad. Sci. U. S. A.*, **75**, 3588-3592.
28
29
30
31 29 Montarras, D., Fiszman, M.Y. and Gros, F. (1981) Characterization of the
32 tropomyosin present in various chick embryo muscle types and in muscle cells differentiated
33 in vitro. *J. Biol. Chem.*, **256**, 4081-4086.
34
35
36
37
38 30 Rao, V.S., Marongelli, E.N. and Guilford, W.H. (2009) Phosphorylation of
39 tropomyosin extends cooperative binding of myosin beyond a single regulatory unit. *Cell*
40 *Motil. Cytoskeleton*, **66**, 10-23.
41
42
43
44
45 31 Linari, M., Caremani, M., Piperio, C., Brandt, P. and Lombardi, V. (2007) Stiffness
46 and fraction of Myosin motors responsible for active force in permeabilized muscle fibers
47 from rabbit psoas. *Biophys. J.*, **92**, 2476-2490.
48
49
50
51 32 Chandra, M., Mamidi, R., Ford, S., Hidalgo, C., Witt, C., Ottenheijm, C., Labeit, S.
52 and Granzier, H. (2009) Nebulin alters cross-bridge cycling kinetics and increases thin
53
54
55
56
57
58
59
60

1
2
3 filament activation: a novel mechanism for increasing tension and reducing tension cost. *J.*
4
5 *Biol. Chem.*, **284**, 30889-30896.
6

7 33 Baylor, S.M. and Hollingworth, S. (2012) Intracellular calcium movements during
8
9 excitation-contraction coupling in mammalian slow-twitch and fast-twitch muscle fibers. *J.*
10
11 *Gen. Physiol.*, **139**, 261-272.
12

13 34 Westerblad, H. and Allen, D.G. (1991) Changes of myoplasmic calcium concentration
14
15 during fatigue in single mouse muscle fibers. *J. Gen. Physiol.*, **98**, 615-635.
16

17 35 Allen, D.G., Lamb, G.D. and Westerblad, H. (2008) Skeletal muscle fatigue: cellular
18
19 mechanisms. *Physiol. Rev.*, **88**, 287-332.
20

21 36 Launikonis, B.S., Stephenson, D.G. and Friedrich, O. (2009) Rapid Ca²⁺ flux through
22
23 the transverse tubular membrane, activated by individual action potentials in mammalian
24
25 skeletal muscle. *J. Physiol.*, **587**, 2299-2312.
26
27

28 37 Ilkovski, B., Mokbel, N., Lewis, R.A., Walker, K., Nowak, K.J., Domazetovska, A.,
29
30 Laing, N.G., Fowler, V.M., North, K.N. and Cooper, S.T. (2008) Disease severity and thin
31
32 filament regulation in M9R TPM3 nemaline myopathy. *J. Neuropathol. Exp. Neurol.*, **67**,
33
34 867-877.
35
36

37 38 Ilkovski, B., Cooper, S.T., Nowak, K., Ryan, M.M., Yang, N., Schnell, C., Durling,
38
39 H.J., Roddick, L.G., Wilkinson, I., Kornberg, A.J. *et al.* (2001) Nemaline myopathy caused
40
41 by mutations in the muscle alpha-skeletal-actin gene. *Am J Hum Genet*, **68**, 1333-1343.
42
43

44 39 Marston, S.B., Copeland, O., Messer, A.E., MacNamara, E., Nowak, K., Zampronio,
45
46 C.G. and Ward, D.G. (2013) Tropomyosin isoform expression and phosphorylation in the
47
48 human heart in health and disease. *J. Muscle Res. Cell Motil.*, **34**, 189-197.
49

50 40 Schulz, E.M., Wilder, T., Chowdhury, S.A., Sheikh, H.N., Wolska, B.M., Solaro, R.J.
51
52 and Wieczorek, D.F. (2013) Decreasing tropomyosin phosphorylation rescues tropomyosin-
53
54 induced familial hypertrophic cardiomyopathy. *J. Biol. Chem.*, **288**, 28925-28935.
55
56
57
58
59
60

- 1
2
3 41 Schulz, E.M. and Wieczorek, D.F. (2013) Tropomyosin de-phosphorylation in the
4 heart: what are the consequences? *J. Muscle Res. Cell Motil.*, **34**, 239-246.
5
6
7 42 Warren, C.M., Arteaga, G.M., Rajan, S., Ahmed, R.P., Wieczorek, D.F. and Solaro,
8 R.J. (2008) Use of 2-D DIGE analysis reveals altered phosphorylation in a tropomyosin
9 mutant (Glu54Lys) linked to dilated cardiomyopathy. *Proteomics*, **8**, 100-105.
10
11
12 43 Heeley, D.H. (2013) Phosphorylation of tropomyosin in striated muscle. *J. Muscle*
13 *Res. Cell Motil.*, **34**, 233-237.
14
15
16 44 Lehman, W., Medlock, G., Li, X.E., Suphamungmee, W., Tu, A.Y., Schmidtman,
17 A., Ujfalusi, Z., Fischer, S., Moore, J.R., Geeves, M.A. *et al.* (2015) Phosphorylation of
18 Ser283 enhances the stiffness of the tropomyosin head-to-tail overlap domain. *Arch.*
19 *Biochem. Biophys.*, **571**, 10-15.
20
21
22 45 Vahebi, S., Ota, A., Li, M., Warren, C.M., de Tombe, P.P., Wang, Y. and Solaro, R.J.
23 (2007) p38-MAPK induced dephosphorylation of alpha-tropomyosin is associated with
24 depression of myocardial sarcomeric tension and ATPase activity. *Circ. Res.*, **100**, 408-415.
25
26
27 46 Houle, F., Poirier, A., Dumaresq, J. and Huot, J. (2007) DAP kinase mediates the
28 phosphorylation of tropomyosin-1 downstream of the ERK pathway, which regulates the
29 formation of stress fibers in response to oxidative stress. *J. Cell Sci.*, **120**, 3666-3677.
30
31
32 47 Houle, F., Rousseau, S., Morrice, N., Luc, M., Mongrain, S., Turner, C.E., Tanaka, S.,
33 Moreau, P. and Huot, J. (2003) Extracellular signal-regulated kinase mediates
34 phosphorylation of tropomyosin-1 to promote cytoskeleton remodeling in response to
35 oxidative stress: impact on membrane blebbing. *Mol. Biol. Cell*, **14**, 1418-1432.
36
37
38 48 Widegren, U., Ryder, J.W. and Zierath, J.R. (2001) Mitogen-activated protein kinase
39 signal transduction in skeletal muscle: effects of exercise and muscle contraction. *Acta*
40 *Physiol. Scand.*, **172**, 227-238.
41
42
43
44
45
46
47
48
49
50
51
52
53
54
55
56
57
58
59
60

- 1
2
3 49 Li, X.E., Tobacman, L.S., Mun, J.Y., Craig, R., Fischer, S. and Lehman, W. (2011)
4
5 Tropomyosin position on F-actin revealed by EM reconstruction and computational
6
7 chemistry. *Biophys. J.*, **100**, 1005-1013.
8
- 9
10 50 Marston, S., Memo, M., Messer, A., Papadaki, M., Nowak, K., McNamara, E., Ong,
11
12 R., El-Mezgueldi, M., Li, X. and Lehman, W. (2013) Mutations in repeating structural motifs
13
14 of tropomyosin cause gain of function in skeletal muscle myopathy patients. *Hum. Mol.*
15
16 *Genet.*, **22**, 4978-4987.
17
- 18
19 51 Orzechowski, M., Moore, J.R., Fischer, S. and Lehman, W. (2014) Tropomyosin
20
21 movement on F-actin during muscle activation explained by energy landscapes. *Arch.*
22
23 *Biochem. Biophys.*, **545**, 63-68.
24
- 25
26 52 Robaszkiewicz, K., Dudek, E., Kasprzak, A.A. and Moraczewska, J. (2012)
27
28 Functional effects of congenital myopathy-related mutations in gamma-tropomyosin gene.
29
30 *Biochim. Biophys. Acta*, **1822**, 1562-1569.
31
- 32
33 53 Moraczewska, J., Greenfield, N.J., Liu, Y. and Hitchcock-DeGregori, S.E. (2000)
34
35 Alteration of tropomyosin function and folding by a nemaline myopathy-causing mutation.
36
37 *Biophys. J.*, **79**, 3217-3225.
38
- 39
40 54 Mokbel, N., Ilkovski, B., Kreissl, M., Memo, M., Jeffries, C.M., Marttila, M.,
41
42 Lehtokari, V.L., Lemola, E., Gronholm, M., Yang, N. *et al.* (2013) K7del is a common TPM2
43
44 gene mutation associated with nemaline myopathy and raised myofibre calcium sensitivity.
45
46 *Brain*, **136**, 494-507.
47
- 48
49 55 Akkari, P.A., Song, Y., Hitchcock-DeGregori, S., Blechynden, L. and Laing, N.
50
51 (2002) Expression and biological activity of Baculovirus generated wild-type human slow
52
53 alpha tropomyosin and the Met9Arg mutant responsible for a dominant form of nemaline
54
55 myopathy. *Biochem. Biophys. Res. Commun.*, **296**, 300-304.
56
57
58
59
60

- 1
2
3 56 Ochala, J. (2008) Thin filament proteins mutations associated with skeletal
4 myopathies: Defective regulation of muscle contraction. *J. Mol. Med.*, **86**, 1197-1204.
5
6
7 57 Memo, M. and Marston, S. (2013) Skeletal muscle myopathy mutations at the actin
8 tropomyosin interface that cause gain- or loss-of-function. *J. Muscle Res. Cell Motil.*, **34**,
9 165-169.
10
11
12
13 58 Orzechowski, M., Fischer, S., Moore, J.R., Lehman, W. and Farman, G.P. (2014)
14 Energy landscapes reveal the myopathic effects of tropomyosin mutations. *Arch. Biochem.*
15 *Biophys.*, **564**, 89-99.
16
17
18
19
20 59 Robaszkiewicz, K., Ostrowska, Z., Cyranka-Czaja, A. and Moraczewska, J. (2015)
21 Impaired tropomyosin-troponin interactions reduce activation of the actin thin filament.
22 *Biochim. Biophys. Acta*, **1854**, 381-390.
23
24
25
26
27 60 Schwerzmann, K., Hoppeler, H., Kayar, S.R. and Weibel, E.R. (1989) Oxidative
28 capacity of muscle and mitochondria: correlation of physiological, biochemical, and
29 morphometric characteristics. *Proc. Natl. Acad. Sci. U. S. A.*, **86**, 1583-1587.
30
31
32
33 61 Jackman, M.R. and Willis, W.T. (1996) Characteristics of mitochondria isolated from
34 type I and type IIb skeletal muscle. *Am. J. Physiol.*, **270**, C673-678.
35
36
37
38 62 Russell, A.J., Hartman, J.J., Hinken, A.C., Muci, A.R., Kawas, R., Driscoll, L.,
39 Godinez, G., Lee, K.H., Marquez, D., Browne, W.F.t. *et al.* (2012) Activation of fast skeletal
40 muscle troponin as a potential therapeutic approach for treating neuromuscular diseases. *Nat.*
41 *Med.*, **18**, 452-455.
42
43
44
45
46
47 63 de Winter, J.M., Buck, D., Hidalgo, C., Jasper, J.R., Malik, F.I., Clarke, N.F., Stienen,
48 G.J., Lawlor, M.W., Beggs, A.H., Ottenheijm, C.A. *et al.* (2013) Troponin activator
49 augments muscle force in nemaline myopathy patients with nebulin mutations. *J. Med.*
50 *Genet.*, **50**, 383-392.
51
52
53
54
55
56
57
58
59
60

- 1
2
3 64 Lee, E.J., De Winter, J.M., Buck, D., Jasper, J.R., Malik, F.I., Labeit, S., Ottenheijm,
4
5 C.A. and Granzier, H. (2013) Fast skeletal muscle troponin activation increases force of
6
7 mouse fast skeletal muscle and ameliorates weakness due to nebulin-deficiency. *PLoS One*,
8
9 **8**, e55861.
10
11
12 65 Hooijman, P.E., Beishuizen, A., de Waard, M.C., de Man, F.S., Vermeijden, J.W.,
13
14 Steenvoorde, P., Bouwman, R.A., Lommen, W., van Hees, H.W., Heunks, L.M. *et al.* (2014)
15
16 Diaphragm fiber strength is reduced in critically ill patients and restored by a troponin
17
18 activator. *Am. J. Respir. Crit. Care Med.*, **189**, 863-865.
19
20
21 66 de Winter, J.M., Joureau, B., Sequeira, V., Clarke, N.F., van der Velden, J., Stienen,
22
23 G.J., Granzier, H., Beggs, A.H. and Ottenheijm, C.A. (2015) Effect of levosimendan on the
24
25 contractility of muscle fibers from nemaline myopathy patients with mutations in the nebulin
26
27 gene. *Skelet. Muscle*, **5**, 12.
28
29
30 67 Guex, N. and Peitsch, M.C. (1997) SWISS-MODEL and the Swiss-PdbViewer: an
31
32 environment for comparative protein modeling. *Electrophoresis*, **18**, 2714-2723.
33
34
35 68 Chan, Y., Tong, H.Q., Beggs, A.H. and Kunkel, L.M. (1998) Human skeletal muscle-
36
37 specific alpha-actinin-2 and -3 isoforms form homodimers and heterodimers in vitro and in
38
39 vivo. *Biochem. Biophys. Res. Commun.*, **248**, 134-139.
40
41
42 69 Lo, H.P., Cooper, S.T., Evesson, F.J., Seto, J.T., Chiotis, M., Tay, V., Compton, A.G.,
43
44 Cairns, A.G., Corbett, A., MacArthur, D.G. *et al.* (2008) Limb-girdle muscular dystrophy:
45
46 diagnostic evaluation, frequency and clues to pathogenesis. *Neuromuscul. Disord.*, **18**, 34-44.
47
48
49 70 Brooke, M.H. and Kaiser, K.K. (1970) Muscle fiber types: how many and what kind?
50
51 *Arch. Neurol.*, **23**, 369-379.
52
53
54 71 Cooper, S.T., Lo, H.P. and North, K.N. (2003) Single section Western blot: improving
55
56 the molecular diagnosis of the muscular dystrophies. *Neurology*, **61**, 93-97.
57
58
59
60

- 1
2
3 72 Ilkovski, B., Nowak, K.J., Domazetovska, A., Maxwell, A.L., Clement, S., Davies,
4 K.E., Laing, N.G., North, K.N. and Cooper, S.T. (2004) Evidence for a dominant-negative
5 effect in ACTA1 nemaline myopathy caused by abnormal folding, aggregation and altered
6 polymerization of mutant actin isoforms. *Hum. Mol. Genet.*, **13**, 1727-1743.
7
8
9
10
11 73 Akkari, P.A., Song, Y., Hitchcock-DeGregori, S., Blechynden, L. and Laing, N.
12 (2002) Expression and biological activity of Baculovirus generated wild-type human slow
13 alpha tropomyosin and the Met9Arg mutant responsible for a dominant form of nemaline
14 myopathy. *Biochem. Biophys. Res. Commun.*, **296**, 300-304.
15
16
17
18 74 Marttila, M., Lemola, E., Wallefeld, W., Memo, M., Donner, K., Laing, N.G.,
19 Marston, S., Gronholm, M. and Wallgren-Pettersson, C. (2012) Abnormal actin binding of
20 aberrant beta-tropomyosins is a molecular cause of muscle weakness in TPM2-related
21 nemaline and cap myopathy. *Biochem. J.*, **442**, 231-239.
22
23
24
25 75 Bing, W., Fraser, I.D. and Marston, S.B. (1997) Troponin I and troponin T interact
26 with troponin C to produce different Ca²⁺-dependent effects on actin-tropomyosin filament
27 motility. *Biochem. J.*, **327**, 335-340.
28
29
30
31 76 Ottenheijm, C.A., Witt, C.C., Stienen, G.J., Labeit, S., Beggs, A.H. and Granzier, H.
32 (2009) Thin filament length dysregulation contributes to muscle weakness in nemaline
33 myopathy patients with nebulin deficiency. *Hum. Mol. Genet.*, **18**, 2359-2369.
34
35
36
37 77 Manders, E., Bogaard, H.J., Handoko, M.L., van de Veerdonk, M.C., Keogh, A.,
38 Westerhof, N., Stienen, G.J., Dos Remedios, C.G., Humbert, M., Dorfmueller, P. *et al.* (2014)
39 Contractile dysfunction of left ventricular cardiomyocytes in patients with pulmonary arterial
40 hypertension. *J. Am. Coll. Cardiol.*, **64**, 28-37.
41
42
43
44
45
46
47
48
49
50
51
52
53
54
55
56
57
58
59
60

Legends to Figures

Fig. 1: Dominant mutations in *TPM3* affect amino acids located within or close to actin binding domains

Tropomyosins form α -helical coiled-coil dimers via a seven residue repeat motive in their amino acid sequence [*a-b-c-d-e-f-g*] as illustrated in (A-B). Positions *a* and *d* (blue) are usually hydrophobic and create a hydrophobic pocket between two tropomyosin chains facilitating dimerisation in a “knobs-into-holes” fashion. Positions *g* and *e* (green) are occupied by charged amino acids that further stabilise the dimer through inter-helical salt bridges. Positions *b*, *c* and *f* (yellow) localise to the surface of the TM dimer and likely modulate interactions with protein binding partners such as actin and troponin. (C) A ribbon model of a whole tropomyosin dimer with the actin binding domains marked in pink on one strand. The residues affected by dominant mutations in *TPM3* are shown. All affected residues are located in or close to actin binding domains. Eight mutations affect residues in the *b*, *c* or *f* positions of the repeat (yellow). Three mutations affect residues in the *a* and *d* position (blue) and two affect residues in the *g* and *e* position (green). RCSB Protein Data Bank access code for protein structure model is 1C1G [tropomyosin dimer, Whitby and Phillips (23)]. Swiss-PDB Viewer v4.1.0 was used to create molecular graphics (67).

Fig. 2: *TPM3*-myopathy patients have slow fibre hypotrophy and a deregulation of slow and fast muscle fibre proportions

(A) ATPase pH 4.6 stained muscle cross section of one control and four patients with mutations at residue R168, of α -TPM_{slow} demonstrating a selective hypotrophy of slow type-1 myofibres. Fast type-2 fibres are between 1.7 and 5.2 times larger in size than type-1 fibres, whereas age-matched controls (age between 0.8 -57 y) showed roughly equally sized fibres (B). This corresponds to a fibre-size disproportion (FSD) between 41 % and 78.3 % (C).

1
2
3 Patients with *TPM3* mutations show an abnormal fibre type distribution ranging from
4
5 complete type-1 fibre predominance (A: Patient 10) to type-2 fibre predominance (A: Patient
6
7 8). (D) In the majority of control biopsies between 40-60 % of the CSA is composed of type-
8
9 1 fibres. *TPM3*-myopathy patients have either below 40 % or above 60 % type-1 fibre area.
10
11 Fibre type measurements were performed twice at different times from the same biopsy in
12
13 Patients 2, 3c, 6b and 8 (also see Supplementary Tab. 2) and the plotted values represent the
14
15 average of both measurements. All images were taken at 100x magnification. Fibre size
16
17 measurements and further information on patient and control biopsies are summarised in
18
19 Supplementary Tab. 2.
20
21
22
23
24
25

26 **Fig. 3: Tropomyosin isoform ratios are not commonly altered and mutant α -TPM_{slow} is**
27 **expressed in *TPM3*-myopathy patient muscle**
28
29

30 (Ai) A representative Western blot of *TPM3*-myopathy patient and control muscle tissue
31
32 showing the three skeletal muscle tropomyosin isoforms (β -TPM, α -TM_{fast} and α -TPM_{slow}). In
33
34 normal muscle, type-1 fibres contain about 50:50 α -TPM_{slow}/ β -TPM and type-2 fibres contain
35
36 about 50:50 α -TPM_{fast}/ β -TPM. Most sample had β -TPM and α -TPM_{fast/slow} levels consistent
37
38 with the relative proportion of type-1 and type-2 fibres present in the sample (% type-1 fibre
39
40 area was determined from ATPase staining, see Supplementary Tab. 2). Only one patient
41
42 (*TPM3* M9R mutation, lane 5) had reduced β -TPM levels and increased expression of α -
43
44 TPM_{slow} relative to other tropomyosin isoforms and the fibre type proportion in the biopsy as
45
46 described previously (25). (Aii-iiiii) Densitometry analysis of Western blots from 10 patients
47
48 with mutations L100M (n=3), R168C (n=1), R168G (n=1), R168H (n=3), K169E (n=1),
49
50 R245G (n=1) was performed to quantify the proportion of each tropomyosin isoform as a
51
52 percentage of total TPM. The relative abundance of each isoform was plotted against the %
53
54 type-1 fibre area (measurements from *TPM3* M9R patient are not included). (Aii) β -TPM
55
56
57
58
59
60

1
2
3 levels are about 50 % of total tropomyosin in patients and controls. (Aiii-iiii) About 50 % of
4
5 tropomyosin is α -TPM_{fast/slow}, but the amount of these fibre-type specific isoforms correlates
6
7 closely with the % type-1 fibre area in both patients and controls (positive correlation for α -
8
9 TPM_{slow}, negative correlation for α -TPM_{fast}). Linear regression analysis showed that slopes of
10
11 patient and controls were not significantly different for any of the three isoforms ($p=0.4997$,
12
13 0.9538 and 0.4595 for α -TPM_{slow}, α -TPM_{fast} and β -TPM, respectively). (B) Isoelectric
14
15 focusing of patient and control muscle lysates shows three spots (corresponding to β -TPM, α -
16
17 TPM_{fast}, α -TPM_{slow}). An additional spot (marked by an arrow) consistent with the predicted
18
19 isoelectric point (pI) of each mutation (as annotated, wild-type α -TPM_{slow} is 4.69) is present
20
21 in patient biopsies. Mutant α -TPM_{slow} accounted for 27-45% of total α -TPM_{slow} in different
22
23 patient biopsies (annotated in the blot, the proportion of each tropomyosin in patient slow
24
25 fibres is given in Supplementary Tab. 3). Note the ratio of expression of α -TPM_{fast/slow}
26
27 depends on the percentage of slow and fast myofibres in the biopsy (e.g. Patient 8 (R168C)
28
29 mainly contains fast myofibres). Picture 3 from the left in (B) is reprinted from Neuromuscul
30
31 Disord, 20/7 Waddell et al., Evidence for a dominant negative disease mechanism in cap
32
33 myopathy due to TPM3, 464-466, Copyright (2010), with permission from Elsevier.
34
35
36
37
38
39
40

41 **Fig. 4: Mutant α -TPM_{slow} R168C proteins has a reduced affinity to filamentous actin**

42 Phalloidin stabilised actin filaments were co-sedimented with incremental amounts of
43
44 tropomyosin and the pelleted fractions were analysed by SDS-PAGE. (A) A representative
45
46 SDS-PAGE of wild-type α -TPM_{slow} protein as was used for densitometry analysis. (B) The
47
48 ratio of TPM/actin was plotted vs. total [TPM] added and a Hill's equation was fitted. The K_d
49
50 was increased in α -TPM_{slow} R168C compared to α -TPM_{slow} wild-type and K169E suggesting
51
52 weaker binding affinity to actin (771.4 ± 188.6 nM, 180.2 ± 37.6 nM, 164.0 ± 110.6 nM for α -
53
54 TPM_{slow} R168C, wild-type and K169E, respectively). The Hill's coefficient h and maximal
55
56
57
58
59
60

1
2
3 binding (B_{max}) was similar in all three proteins (h = wild-type 4.471 ± 3.0 , R168C 3.308 ± 2.4 ,
4
5 K169E 1.602 ± 1.3 ; B_{max} wild-type 0.489 ± 0.055 , R168C 0.431 ± 0.078 and K169E
6
7 0.443 ± 0.156). Values are best-fit values \pm 95% confidence interval.
8
9

10
11
12 **Fig. 5: *TPM3* patients show increased phosphorylation of tropomyosin and ectopic**
13 **expression of fast fibre specific α -actinin-3 in slow myofibres**
14

15
16 (A) Consecutive sections were labelled with type-1 and type-2a MHC (blue and green, co-
17
18 labelled respectively), type-2 MHC (red), α -actinin-3 (green) and troponin- T_{fast} (green) (the
19
20 same fibre in multiple stains is indicated by a white arrow). Troponin- T_{fast} is only expressed
21
22 in fast fibres as expected. Abnormal expression of α -actinin-3, a fast fibre specific Z-disc
23
24 protein, was observed in type-1 myofibres of Patients 10, 4 and 6a (yellow stars). The biopsy
25
26 of Patient 6b showed similar abnormalities but is not shown in this panel. Other patients had
27
28 normal expression of α -actinin-3. Staining of Patient 1 and 8 are representative for these
29
30 patients. (Bi) S283 is conserved and can be phosphorylated in all three sarcomeric
31
32 tropomyosin proteins. (Bii) We assessed the level of S283 phosphorylation (pTPM) and total
33
34 tropomyosin protein levels by duplicate Western blot and equal loading was confirmed by
35
36 using sarcomeric actin (s Actin) (representative Western blot shown). The phosphorylation
37
38 status of all three tropomyosin isoforms was determined by densitometry and normalised to
39
40 the total tropomyosin levels. The graph shows phosphorylation levels normalised to the
41
42 control average in (Biii) *TPM3* patients and (Biiii) patients with congenital myopathies and
43
44 muscular dystrophies due to mutations in *TPM3*, *TPM2*, *ACTA1*, *DNM2*, *DMD* and *DYSF*.
45
46 Horizontal lines and error bars represent mean and standard deviation. Phosphorylation was
47
48 commonly increased in both *TPM3* patients and patients with other genetic causes of muscle
49
50 disease. Statistical analysis was only performed on patients with the R168H mutation due to
51
52
53
54
55
56
57
58
59
60

1
2
3 insufficient data points for other groups. Phosphorylation was significantly higher in patients
4
5 with the R168H mutation compared to controls (* $p < 0.05$, Mann-Whitney U test).
6
7

8
9
10 **Fig. 6: The force generation at saturating $[Ca^{2+}]$ is decreased in *TPM3*-myopathy**
11 **patients**

12
13 Maximal force generation (F_{max}) measured at pCa 4.5 and sarcomere length of 2.5 μm ,
14
15 normalised to fibre CSA. (A) A typical force trace from a patient (Patient 6) and control type-
16
17 1 fibre. Most *TPM3* patients showed a significant force deficit in type-1 myofibres (C)
18
19 whereas type-2 fibres produced similar maximal force compared to controls (B). In hybrid
20
21 fibres and fibre bundles all patients had a slightly lower force average, however only Patient
22
23 1 showed a significant force deficit (D). C_{slow} = Control type-1 fibres (pooled from eight
24
25 biopsies aged: 11-54 y), C_{fast} = Control type-2 fibres (pooled from eight biopsies aged: 6-54
26
27 y), $C_{h/b}$ = Control hybrid fibres (contain a mix of type-1 and type-2 MHC, age 11-54 y) and
28
29 small fibre bundles (bundles were taken from two biopsies of 0.9 y and 6 y old controls). $P =$
30
31 Patient. The black line in (B-D) indicates the average. *** $p < 0.0001$, * $p < 0.01$, one-way
32
33 ANOVA.
34
35
36
37
38
39
40
41
42

43 **Fig. 7: The force deficit in *TPM3*-myopathy patients is likely due to abnormal cross-**
44 **bridge cycling**

45
46 We assessed the rate of tension re-development (K_{tr}) (A) and active stiffness (B) in *TPM3*-
47
48 myopathy patients to investigate if the force deficit in patient type-1 fibres was due to altered
49
50 cross-bridge cycling. A typical K_{tr} trace of a patient (Patient 6) and a control are shown in
51
52 (Ai). The K_{tr} in single myofibres from *TPM3* patient biopsies and control biopsies are shown
53
54 in (Aii) (type-1) and (Aiii) (type-2). Note that due to different MHC-ATPase properties the
55
56 K_{tr} is physiologically higher in type-2 than in type-1 fibres. (Aii) The type-1 fibres of most
57
58
59
60

1
2
3 *TPM3* patients showed a significant decrease in K_{tr} compared to control type-1 fibres
4 (exceptions: Patient 1, 2 and 3a (***) $p < 0.0001$, * $p < 0.01$, one-way ANOVA) (**Aiii**) The type-
5 2 fibres were not different to control type-2 fibres, with the exception of Patient 6 which
6 showed a small decrease in K_{tr} . (**B**) Active stiffness was analysed by plotting the length
7 changes (ΔL) against the force changes (ΔF) and fitting a linear regression to the data. A
8 representative graph of type-1 fibres from Patient 4 and from controls is shown in (**Bi**:
9 absolute length change) and (**Bii**: length change/ F_{max}). Graphs from other all other samples
10 are presented in Supplementary Fig. 6. Error bars represent standard deviation. (**Biii-v**) The
11 slope of the linear regression was not significantly different from controls in all fibre-types in
12 most patients with the exception of type-1 fibres or bundles/hybrid fibres of Patient 1, 2 and 7
13 where stiffness was reduced (* $p < 0.01$, ** $p < 0.001$, *** $p < 0.0001$, one-way ANOVA).
14 However, a trend towards a small reduction was present in type-1 fibres and bundles/hybrid
15 fibres of most patients (**Biii-iiii**). (**vi-vii**) When ΔF was normalised to F_{max} the slope was not
16 significantly different from controls with the exception of P3c, which showed an increase in
17 the slope (I, *** $p < 0.0001$, one-way ANOVA). Error bars represent standard deviation. C_{slow}
18 and C_{fast} = Control type-1 and type-2 fibres (pooled from eight biopsies aged: 11 - 54 y), $C_{h/b}$
19 = Control hybrid fibres (contain a mix of type-1 and type-2 MHC, age 6 - 54 y) and small
20 fibre bundles (bundles were taken from two biopsies of 0.9 y and 6 y old controls). The black
21 line in all scatter plots indicates the average.
22
23
24
25
26
27
28
29
30
31
32
33
34
35
36
37
38
39
40
41
42
43
44
45
46
47

48 **Fig. 8: Ca^{2+} -sensitivity is decreased in *TPM3*-myopathy patients resulting in reduced**
49 **specific force generation at physiological $[Ca^{2+}]$**
50

51 (**A**) Specific force generation at incremental $[Ca^{2+}]$ in skinned type-1 fibres (**i**), hybrid fibres
52 or bundles (**ii**) and type-2 fibres (**C**) shown as percent of F_{max} fitted to a variable slope log
53 (dose) response curve. Note the rightward shift of the force/pCa curve in type-1 fibres, hybrid
54
55
56
57
58
59
60

1
2
3 fibres/bundles in *TPM3* patients, whereas type-2 fibres were not different to controls. The
4
5 dotted lines indicate the pCa50 ($[Ca^{2+}]$ required to achieve 50 % of maximal force) and the
6
7 yellow area indicates physiological cytoplasmic $[Ca^{2+}]$ during muscle contraction (between 1
8
9 - 5 μ M) (B) The pCa 50 was significantly higher in type-1 fibres, hybrid fibres/ bundles of
10
11 *TPM3* patients compared to controls and type-2 fibres of *TPM3* patients. (C) Specific force
12
13 generation measured at pCa 6.0 (1 μ M, physiological calcium). The force was significantly
14
15 lower in (i) type-1 fibres and (ii) hybrid fibres/bundles of all *TPM3* patients, but was not
16
17 different from controls in (iii) type-2 fibres. C_{slow} and C_{fast} = Control type-1 and type-2 fibres
18
19 (pooled from eight biopsies aged: 11-54 y), $C_{h/b}$ = Control hybrid fibres (contain a mix of
20
21 type-1 and type-2 MHC, age 6-54 y) and small fibre bundles (bundles were taken from two
22
23 biopsies of 0.9 y and 6 y old controls). The black line in the scatter plot indicates the average
24
25 and error bars in force/pCa curves are standard deviations. *** $p < 0.0001$, * $p < 0.01$, one-way
26
27 ANOVA. P=Patient, C= control.
28
29
30
31
32
33
34
35
36

37 Tables

38 **Table 1: Patient cohort with dominant TPM3 mutations**

39 P	40 Mutation	41 Disease	42 Muscle	43 Sex	44 Age at	45 Clinical	46 Publication	47 Contractile
	48 in <i>TPM3</i>		49 type		50 biopsy	51 classification		52 studies
43 1	44 K169E	45 CFTD	46 Q	47 M	48 16 m	49 moderate	50 (1): P 2	51 Y
52 2	53 R245G	54 CFTD	55 Q	56 M	57 20 m	58 moderate	59 (1): P 1	60 Y
61 3a	62 L100M	63 CFTD	64 Q	65 F	66 3 y	67 mild	68 (1): P 5	69 Y
70 3b	71 L100M	72 CFTD	73 B	74 M	75 30 y	76 mild	77 (1): P 7	78 Y
79 3c	80 L100M	81 CFTD	82 B	83 M	84 36 y	85 mild	86 (1): P 8	87 Y
88 4	89 R168G	90 CFTD	91 Q	92 M	93 10 y	94 mild	95 (1): P 3	96 Y
97 5	98 R168H	99 CFTD	100 Q	101 F	102 40 y	103 mild	104 unpublished	105 Y
106 6a	107 R168H	108 NM	109 D	110 F	111 20 y	112 mild	113 (1): P 10	114 N

6b	R168H	CFTD	?	M	56 y	mild	(1): P 11	Y
7	R168C	Cap	?	M	3 y	mild	(14): P 1	Y
8	R168C	CFTD	Q	F	19 y	moderate	(1): P 9	Y
9	M9R	NM	Q	F	21 y	mild	(8); (37): P 1	N
10	R168H	NM	D	M	53 y	mild	(13): P III-4	N
11	E241K	CFTD	Q	F	0.5y	moderate	(2): P 311-1	N
12	R91P	CFTD	Q	F	0.5y	severe	(2): P 913-1	N

Q=Quadriceps, B = Biceps, D = Deltoid, P = Patient

Abbreviations

α -tropomyosin _{slow}	α -TPM _{slow}
α -tropomyosin _{fast}	α -TPM _{fast}
bovine serum albumin	BSA
β -tropomyosin	β -TPM
congenital fibre-type disproportion	CFTD
cross sectional area	CSA
immunohistochemistry	IHC
$-\log$ of molar free $[Ca^{2+}]$	pCa
maximal isometric contraction	Fmax
myosin heavy chain	MHC
percentage fibre-size disproportion	% FSD
phosphate buffered saline	PBS
two-dimensional SDS polyacrylamide gel electrophoresis	2D-SDS-PAGE

1
2
3
4
5 Michaela Yuen, PhD
6 Postdoctoral Fellow
7 Institute for Neuroscience and Muscle Research
8 The Children's Hospital at Westmead
9 Level 3, Kids Research Institute
10 Phone: +61 2 9845 1495
11 Fax: +61 2 9845 3489
12 Email: michaela.kreissl@sydney.edu.au
13

14 20 July 2015
15

16
17 Dear Editor,
18
19

20 **Re: Manuscript number: HMG-2015-W-00595: Yuen *et al.*, 'Muscle weakness in *TPM3*-myopathy is due to reduced Ca^{2+} -**
21 **sensitivity and impaired acto-myosin cross-bridge cycling in slow fibres.'**
22

23 Thank you for the timely review of our manuscript. Below I have addressed your queries and those of the reviewer's
24 below.
25

26 Kind regards,
27

28 Michaela Yuen
29
30
31
32
33
34
35
36
37
38
39
40
41
42
43
44
45
46
47
48
49
50
51
52
53
54
55
56
57
58
59
60

1. FORMATTING ERRORS

I have corrected the following formatting errors:

TITLE PAGE

The corresponding author was designated with an asterisk (*) and address, telephone, FAX, and email address were listed.

MANUSCRIPT

TIMES NEW ROMAN font was used for all text and text was double-spaced.

REFERENCES

References were edited to comply with the Human Molecular Genetics format (specifically, all abbreviated words in journal titles were punctuated, i.e. Hum. Mol. Genet. NOT Hum Mol Genet.)

2. REVIEWERS' COMMENTS

Reviewer: 1

Question 1: I am intrigued by the mutant/wt expression data. I would have predicted (a) that mutant protein is produced and (b) that its levels would correspond to phenotype. The latter point does not seem to come out in the experimentation, as the samples with the most severe clinical phenotype have the lowest mutant protein levels. (c) Were the overall levels of TPM3 reduced in those samples?

Redress to 1(a) and (b): Yes, one might reasonably expect mutant protein levels to correlate with clinical disease severity. However, many additional factors likely determine the overall weakness observed in a TPM3-myopathy patient.

For instance, TPM3 is specifically expressed in slow muscle fibres. The area occupied by slow fibres and thus the number of fibres expressing the mutant protein may vary in different parts of each patients biopsy (see **Table 1** below) and in different muscles in the same patient (Ilkovski et al, 2008). Thus in addition to taking into account the amount of mutant protein, one has to consider the number of slow fibres in the affected muscle groups to correlate clinical severity with the presence of mutant protein. This is further complicated by the specific defects exerted by each mutation.

Interestingly, a shift towards slow fibre predominance is commonly observed in our cohort and in other congenital myopathies. This would result in more fibres expressing mutant protein, however, high numbers of slow fibres did not correlate with more severe disease (see **Table 1**). On the contrary, more severely affected patients were among the patients with the lowest slow fibre area (marked in yellow in **Table 1**). We believe this suggests fast fibre predominance is unable to compensate for slow fibre dysfunction and may confer a more severe presentation.

We inserted the following comment in the manuscript to address this question (paragraph 2 of the discussion):

"Interestingly, the amount of α -TPM_{slow} mutant protein did not correlate well with disease severity in our patient cohort. This may be explained by a number of factors influencing disease severity, such as a mutation-specific effect and varying proportions of slow fibres in different parts of the same muscle or different muscle groups."

Redress to 1(c): Concerning potentially reduced levels of α -TPM_{slow}: We observed a strict correlation of α -TPM_{slow} relative to slow fibre cross sectional area in our entire cohort, with the exception of patient 12 where poor muscle quality did not allow fibre typing of the muscle.

Question (2): Is there any way to examine the ratio of WT/mut in the remaining samples? Perhaps by proteomics?

Redress to (2): We agree, knowing mutant and wild type protein ratios for the remaining samples would be useful but technical limitations of mass spectrometry (MS) preclude these studies. We determined the mutant/wild type ratio in all samples that expressed α -TPM_{slow} (presence of sufficient number of slow fibres) and resulted in a charge change as required for separation from wild type protein via 2D-PAGE (see **Table 1**). We inquired in our proteomics facility about the use of mass spectrometry for analysis of mutations without a charge change, but were advised tropomyosin presents a poor candidate for MS due to the abundance of trypsin sites. But also, there is no guarantee (for any protein) that the particular subset of fragments ionized and detected by MS will include a fragment bearing a missense mutation of interest. Therefore, we were unable to pursue any missense mutations without a charge change.

Table 1: Mutant α -TPM_{slow} expression and slow fibre area do not correlate with clinical severity

P	Mutation in TPM3	Age at biopsy	Clinical classification	IEF result	Type 1 fiber area*
1	K169E	16 m	moderate	38% mutant	23.3
2	R245G	20 m	moderate	no/very low levels of TPM3 due to fiber typing (6.4% type 1 fiber area in biopsy available)	20.5 6.4
3a	L100M	3 y	mild	no charge change	61.8
3b	L100M	30 y	mild	no charge change	73.4
3c	L100M	36 y	mild	no charge change	37.3
					25.9
4	R168G	10 y	mild	39% mutant	74.6
5	R168H	40 y	mild	no charge change	N/D
6a	R168H	20 y	mild	no charge change	62.8
6b	R168H	56 y	mild	no charge change	16.3
					39.6
7	R168C	3 y	mild	published in Waddell et al 2010 ~50% mutant	100
8	R168C	19 y	moderate	37% mutant	13.7 5.1
9	M9R	21 y	mild	published in Ilkovski et al 2008 ~50% mutant	N/D
10	R168H	53 y	mild	no charge change	100
11	E241K	0.5y	moderate	90% mutant	27.9
12	R91P	0.5y	severe	23% mutant	N/D due to insufficient sample quality

*two values are stated for a patient when fibre typing was performed twice, at different times and on different parts of the biopsy

1
2
3 **Question (3):** Can one evaluate the amount of mut/WT protein in the non filamentous fractions? Perhaps much of the
4 mutant protein is not being incorporated.

5 **Redress to (3):** This is a good suggestion. Unfortunately, we did not determine mutant/wild type levels in the soluble
6 fraction at the time these experiments were performed and due to limited amount of biopsy material we are unable to
7 perform these experiments retrospectively. We sincerely hope this will not detract from the overall quality of the paper.
8

9
10 **Question (4):** In terms of the actin co-sedimentation assay, given that this is a dominant disease and that the mutant and
11 WT proteins co-exist, it seems like the most accurate way to do this experiment would be to look at the data using
12 equimolar (and skewed) ratios of WT/mut and then measuring actin co-sedimentation. It is known for some other
13 dominant diseases that the effect of mut protein can be quite different when all polymers are composed of mutant protein
14 vs combo polymers of WT/mut proteins.

15 **Redress to (4):** Actin-TPM co-sedimentation assays are a useful tool in evaluating the interaction of actin and mutant TPM
16 in an isolated system and can provide important insights into specific actin-binding defects. Mutant α -TPM_{slow} wild type α -
17 TPM_{slow} and wild type β -TPM protein indeed co-exist in skeletal muscle (predicted ratios are presented in supplementary
18 table 3) where they interact with a range of other proteins to form the thin filament. Rather than exhaustively study
19 different ratios of the tropomyosins, which in itself also present technical caveats due to an absence of troponins and other
20 thin filament proteins specific to slow fibres, we chose to instead pursue single fibre contractility testing. In this setting, the
21 exact ratio of tropomyosin isoforms present in the patient fibres are studied in the setting of an intact contractile
22 apparatus. We felt this was a better approach to study how the mutant α -TPM_{slow} impacted the contractile properties in
23 the muscle fibres of affected patients.
24

25 **Minor comment (1):** Have similar studies been performed for TPM2? Do they provide any parallel insight or corroboration
26 with the current data?

27 **Redress to minor comment (1):** To our knowledge, no study has been performed for a large cohort of TPM2 patients
28 studied collectively by one group using the same methodology. However, contractile mechanics have previously been
29 assessed in TPM2 patients in a number of smaller studies yielding variable results:

- 30 • TPM2 null and TPM2 E181K (Ochala et al, 2012): normal specific force in TPM2 null and E181K. TPM2 null showed
31 decreased calcium sensitivity and normal Ktr while TPM2 E181K showed increased calcium sensitivity and reduced
32 Ktr
- 33 • TPM2 K7del (Mokbel et al, 2013): normal specific force, increased calcium sensitivity, reduced actin affinity.
- 34 • TPM2 E41K (Ochala et al, 2008): normal specific force, lower Ktr and lower calcium sensitivity
- 35 • TPM2 R133W (Ochala et al, 2007): found lower specific force and lower Ktr but no difference in calcium sensitivity

36
37 Based on these studies the contractile phenotype of TPM2-myopathy related mutations appears variable and is likely
38 mutation specific. This is paralleled by TPM2 causing muscle weakness in some patients and a hypercontractile phenotype
39 in others (Mokbel et al, 2013). In contrast, TPM3 has been associated only with muscle weakness to date and we observed a
40 consistent reduction of force, Ktr and calcium sensitivity in our TPM3 cohort. I believe further studies of larger cohorts with
41 all patients subject to the same testing regimes are needed to confirm if reduced Ca^{2+} -sensitivity is a unifying feature of all
42 TPM3 mutations, as this may be amenable to targeted therapy. However, we concede it remains plausible and possible
43 that specific mutations may either sensitise or desensitise the thin filament to Ca^{2+} , or affect other thin filament properties
44 that may similarly manifest as weakness in patients.

45 **Minor comment (2):** Have the authors looks at α -actinin-3 expression in other forms of NM? Is this a specific or non-
46 specific observation.
47

48 **Redress to minor comment (2):** Our group has previously observed ectopic α -actinin-3 expression in ACTA1 nemaline
49 myopathy patients. This finding has been published in (Ilkovski et al, 2001). Patients with ACTA1 mutations I357L, G268C,
50 and I136M had 90 %–100 % slow fibre predominance and abnormal expression of α -actinin-3 in a subset of slow fibres
51 and/or fibres expressing both slow- and fast-myosin heavy chain. Below is a small panel showing ectopic α -actinin 3
52 expression in a patient with an ACTA1 I136M mutation (**Figure 1**). Ectopic expression of α -actinin-3 is therefore not specific
53 to disease caused by α -TPM_{slow} mutations. Please note due to loss of α -actinin-3 resulting from a homozygous null mutation
54 in 20 % of normal individuals (North et al, 1999) α -actinin-3 expression cannot be studied in all patients.
55
56
57
58
59
60

We added the following comment to paragraph 3 of the discussion in the manuscript:

"Interestingly, similar ectopic expression of α -actinin-3 was previously observed in some patients with ACTA1 mutations (Ilkovski et al, 2001) and is thus not specific to TPM3-associated disease but could potentially be due to incomplete or abnormal fibre type conversion present in some myopathy patients."

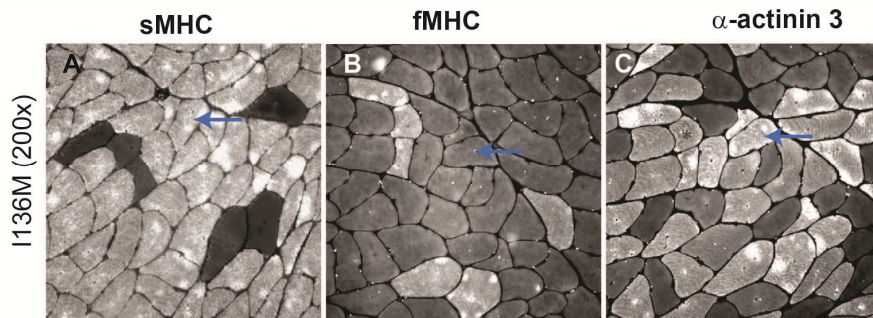


Figure 1: Ectopic expression of fast fibre specific α -actinin-3 in slow fibres in a patient with the ACTA1 I136M mutation
Consecutive muscle section stained with slow and fast myosin heavy chain (sMHC and fMHC, respectively) and α -actinin-3 showing ectopic expression of α -actinin-3 in sMHC positive fibres (blue arrow).

Minor comment (3): What do the authors make of their data vis-a-vis a strong contracture phenotype? One hypothesis about this has been some element of hypercontractility exists (at least for TPM2). Do you feel your data now "puts to rest" the idea that some TPM3 mutations are associated with hypercontraction? And how does this compare to TPM2, where data (I believe from the authors group) has shown some mutations (TPM2del7K) do in fact cause hypercontractility under certain circumstances.

Redress to minor comment (3): We believe our data conclusively shows that none of the mutations we investigated cause a hypercontractile phenotype. This topic is thoroughly discussed in the 6th paragraph of the discussion. A hypercontractile phenotype has been associated with the TPM2 K7del mutation (Mokbel et al, 2013) and it is likely that the effect on thin filament activation is highly dependent on the nature of the amino acid substitution, so mutation to mutation variability is expected.

Reviewer: 2

Comment (1): Please consider adapting or cross-referencing the new tropomyosin nomenclature.

Redress to comment (1): We support adapting a universal nomenclature in order to allow clear distinction between the large number of tropomyosin proteins, so we cross referenced to the new nomenclature in the second paragraph of the introduction and have now also added a citation (Geeves et al, 2015). However, we believe for skeletal muscle the old nomenclature better reflects the expression patterns and properties of the three skeletal muscle tropomyosin isoforms and is thus easier to follow. We would prefer to maintain the old nomenclature for this manuscript but hope that cross-referencing the new nomenclature at the start provides sufficient clarity.

Comment (2): Was there any emerging correlation between the in vitro force measurements and the relative severities of the clinical phenotype?

Redress to comment (2): Two out of three patients rated to have a moderate clinical presentation displayed the lowest specific forces measured in our cohort so there appears to be a correlation (see **Table 2**). However, unfortunately our cohort is not large enough to draw scientifically valid conclusions. Additionally, other factors may influence clinical severity as discussed above (**Question 1, Reviewer 1**) such as fibre typing in various muscle groups and slow fibre atrophy (e.g. smaller slow fibres will produce less force than bigger slow fibres; our force measurements do not reflect this as we normalise to cross sectional area).

Comment (3): Was there any evidence that the state of S283 phosphorylation affected the measurements (I may have missed that)?

Redress to comment (3): Phosphorylation at S283 is physiologically higher during development and decreases drastically in the first years of life (data not shown). Thus we were unable to interpret phosphorylation in young patients due to high

variability among patients and controls (N/D in **Table 2**). Most adult patients have a mild clinical phenotype. Low phosphorylation was detected in two patients, one was classified as mild and the other as moderate suggesting there is no correlation with clinical severity. As the cohort is not big enough to draw scientifically valid conclusions, and given phosphorylation at S283 is also altered and elevated in other forms of muscle disease, we do not think these data should be discussed further within manuscript.

Table 2: Correlate clinical severity with contractile force and phosphorylation

P	Mutation in <i>TPM3</i>	Age at biopsy	Clinical classification	Average force in slow fibres (mN/mm ³)	S283 p
1	K169E	16 m	moderate	77.24±12.48 (type 1, n=2) 52.17±13.74 (h/b, n=8)	N/D
2	R245G	20 m	moderate	79.51±8.345 (type 1, n=2) 105.5±25.16 (hybrid, n=6)	N/D
3a	L100M	3 y	mild	116.0±43 (type 1, n=9)	N/D
3b	L100M	30 y	mild	82.27±35.31 (type 1, n=16)	+++
3c	L100M	36 y	mild	98.6±36.56 (type 1, n=15)	+++
4	R168G	10 y	mild	87.83±21.1 (type 1, n=12)	N/D
5	R168H	40 y	mild	100.6±27.00 (type 1, n=14)	N/D
6a	R168H	20 y	mild	N/D	+++
6b	R168H	56 y	mild	105.8±49.51 (type 1, n=17)	++
7	R168C	3 y	mild	89.37±27.18 (type 1, n=15)	N/D
8	R168C	19 y	moderate	96.48±27.61 (type 1, n=4)	+
9	M9R	21 y	mild	N/D	+
10	R168H	53 y	mild	N/D	++
11	E241K	0.5y	moderate	N/D	N/D
12	R91P	0.5y	severe	N/D	N/D

References

Geeves MA, Hitchcock-DeGregori SE, Gunning PW (2015) A systematic nomenclature for mammalian tropomyosin isoforms. *J Muscle Res Cell Motil* **36**: 147-153

Ilkovski B, Cooper ST, Nowak K, Ryan MM, Yang N, Schnell C, Durling HJ, Roddick LG, Wilkinson I, Kornberg AJ, Collins KJ, Wallace G, Gunning P, Hardeman EC, Laing NG, North KN (2001) Nemaline myopathy caused by mutations in the muscle alpha-skeletal-actin gene. *Am J Hum Genet* **68**: 1333-1343

Ilkovski B, Mokbel N, Lewis RA, Walker K, Nowak KJ, Domazetovska A, Laing NG, Fowler VM, North KN, Cooper ST (2008) Disease severity and thin filament regulation in M9R TPM3 nemaline myopathy. *J Neuropathol Exp Neurol* **67**: 867-877

Mokbel N, Ilkovski B, Kreissl M, Memo M, Jeffries CM, Marttila M, Lehtokari VL, Lemola E, Gronholm M, Yang N, Menard D, Marcorelles P, Echaniz-Laguna A, Reimann J, Vainzof M, Monnier N, Ravenscroft G, McNamara E, Nowak KJ, Laing NG, Wallgren-Pettersson C, Trehwella J, Marston S, Ottenheijm C, North KN, Clarke NF (2013) K7del is a common TPM2 gene mutation associated with nemaline myopathy and raised myofibre calcium sensitivity. *Brain* **136**: 494-507

North KN, Yang N, Wattanasirichaigoon D, Mills M, Easteal S, Beggs AH (1999) A common nonsense mutation results in alpha-actinin-3 deficiency in the general population. *Nat Genet* **21**: 353-354

Ochala J, Gokhin DS, Penisson-Besnier I, Quijano-Roy S, Monnier N, Lunardi J, Romero NB, Fowler VM (2012) Congenital myopathy-causing tropomyosin mutations induce thin filament dysfunction via distinct physiological mechanisms. *Hum Mol Genet* **21**: 4473-4485

Ochala J, Li M, Ohlsson M, Oldfors A, Larsson L (2008) Defective regulation of contractile function in muscle fibres carrying an E41K -tropomyosin mutation. *The Journal of Physiology* **586**: 2993-3004

Ochala J, Li M, Tajsharghi H, Kimber E, Tulinius M, Oldfors A, Larsson L (2007) Effects of a R133W beta-tropomyosin mutation on regulation of muscle contraction in single human muscle fibres. *The Journal of Physiology* **581**: 1283-1292

Pre-Review